Heavy Metal Root Efflux of *Mesembryanthemum crystallinum* and *Nicotiana tabacum*

by

Anthony S. Cieri

A thesis submitted in partial fulfillment
of the requirements for the degree of
Master of Science
(Environmental Science)
in the University of Michigan-Dearborn
2023

Master Thesis Committee:

Professor John C. Thomas, Chair
Professor Emeritus Kent Murray
Assistant Professor Thomas Bianchette, Oakland University

Acknowledgements

I wish to acknowledge the help of Corey Lambert, Chemistry Lab Manager, Natural Sciences Department, University of Michigan-Dearborn. I also acknowledge Dr. Johnna Birbeck, Analytical Chemistry Core Facility, Wayne State, University, Detroit MI for their help analyzing efflux and plant matter extracts for heavy metals with ICP/MS. I also thank my family for supporting throughout the years I worked on this project.

Table of Contents

List of Tables

List of Figures

Abstract

Heavy metal pollution is increasing globally due to anthropogenic activities which create health risks not only for societies, but also native plant species. Plants have shown various methods for metal detoxification within plants, including root efflux which is proposed to flush out excessive and toxic ions from the rhizosphere. Root heavy metal efflux is largely unstudied, particularly comparing glycophyte and halophyte plants for phytoremediation purposes. For this reason, studies with the glycophyte *Nicotiana tabacum* (SR1 strain tobacco), and a halophyte plant (salt-tolerant) represented by *Mesembryanthemum crystallinum* (common ice plant) following nickel stress were performed. When nickel-stressed plants were allowed to recover and efflux into water (non-stress conditions), both species demonstrated nearly identical Ni^{+2} efflux patterns. Besides other trace metals responding in a nickel-independent pattern, several nickel specific responses differed greatly between the *M. crystallinum* and *N. tabacum*. The *M. crystallinum* responded to nickel stress with efflux of Zn^{+}, while in *N. tabacum*, Mg^{+} was the most significant metal passed into the surrounding water. Differential metal efflux, when recovering from nickel stress, may suggest differing strategies for metal sequestration and release in these two plant species. In summary, root efflux may present temporary relief of nickel metal stress in higher plants, and these two plant species differ in their nickel-specific efflux of other metals. These results suggest *N. tabacum* and the *M. crystallinum* may use differing strategies for promoting plant resilience after exposure to a metallotoxic environment.

Chapter 1 Introduction

1.1 Heavy Metal Toxicity and Protection

Heavy metal ions interact with the earth with soil-dependent factors including pH, soil structure, and particle composition. At sub-mM levels, metals such as nickel and copper are considered important micronutrients, but they become toxic to plants at higher concentrations. Likewise, heavy metals are utilized by organisms for redox state maintenance, and they are often bound to organic compounds containing oxygen, nitrogen, and sulfur (Callahan et al., 2006). At high levels, metals instead bind to high affinity thiol groups and inhibit key metabolic steps (Seregin & Ivanov, 2000). Such significant sources of heavy metal pollution include electroplating, smelting, chemical manufacturing, and waste from batteries, incinerators, and motor vehicle fuel combustion (Mohammed et al., 2011). Toxic mercury and cadmium displace other metal ions or disable functional groups. Redox-active Metals (Figure 1) like nickel and cadmium generate ROS (Reactive Oxygen Species) indirectly by interfering with metabolism (Jalmi et al., 2018).

Transition metals can lead to excessive oxidative stress through Fenton Reactions, named after the scientist who discovered that iron salt catalyzes the conversion of hydrogen peroxide into a hydroxide and a hydroxide radical (Meyerstein, 2021). While Fenton's Reagent uses an iron salt, other transition metals including copper and cobalt in their lowest oxidation states can also perform a Fenton reaction with the same result (Goldstein et al., 1993). The most damaging free radical to organisms is the hydroperoxide. It is known to damage DNA, reduce DNA and

RNA polymerase activity, catalyze protein disfunction, interfere with chlorophyll production, and contribute to several diseases (Halliwell and Gutteridge, 1984; Frankel et al., 1987; Kholodova et al., 2005). Copper II is the most catalytic Fenton metal, while nickel is most active in generating free radicals at pH 7.5 or higher (Kolar et al., 2003). Magnesium, best thought of as an ROS counterbalance, lowers the attractive interactions of oxidized lipids, preventing lipid bilayer pore formation normally seen in oxidized membranes (Fernández et al., 2021).

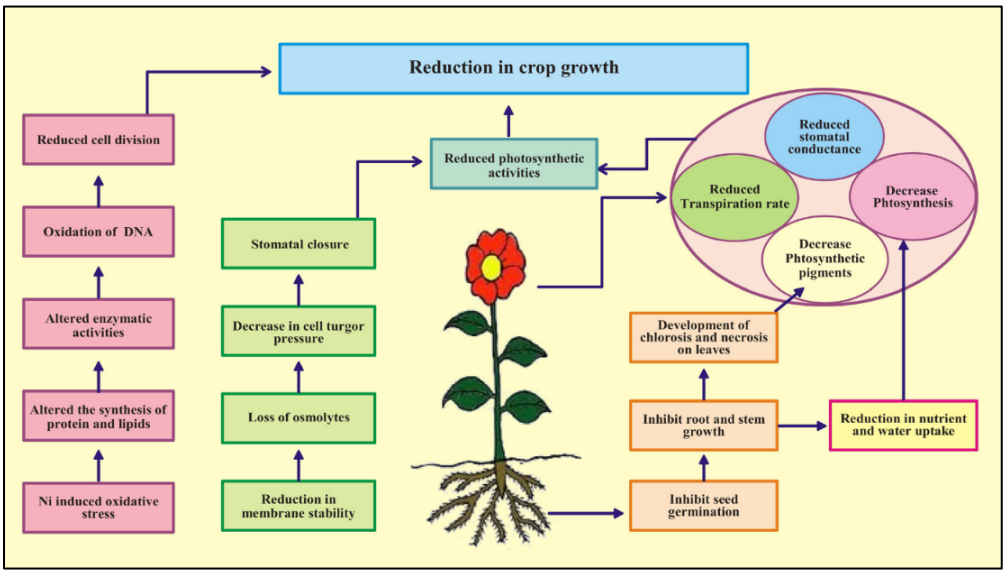

Figure 1: Effects of metal toxicity (Hassan et al., 2019).

1.2 Metal Tolerance in Plants

Unlike resistance, metal tolerance is a complex trait that includes physiological parameters such as metal dose, length of exposure, uptake rate, transport, and sequestration (Antonio et al., 2016). Physical parameters that can damage DNA such as temperature and light intensity at certain wavelengths can also hamper the metal tolerance of a plant (Dutta et al., 2018). Some organisms are specially adapted to the excessive presence of heavy metals in their habitat. In the case of serpentine-based soils, plants have developed a finely controlled accumulation of certain elements according to their soil's contents which varies between

locations (Arnold, et. al., 2016). It is believed such adaptations are necessary for surviving in the extreme environment resulted from gene drift between neighboring plant populations (Arnold, et. al., 2016).

Common strategies for plants excluding metals include ion uptake shifts between the rhizosphere and its symbiotic mycorrhiza fungi, pH modification of surrounding medium to precipitate metal ions, the generation of redox barriers at the roots, along with the release of metal-laden leaves (Javedet al., 2018). Guttation through small pores (hydathodes) in leaves, followed by exterior precipitation limits internal metal levels and provides tolerance (Javed et al., 2018). Metal micronutrient availability and tolerance/resistance is dependent on the movement of metal cations from root to shoot; movement is limited by the high cation exchange capacity of xylem cell walls (Yusuf et al., 2011). When presented with appropriate doses of heavy metal ions, the organism transports them from the rhizosphere to photosynthetic tissue via the xylem using specific transporter pathways (Page & Feller, 2015).

A basic plant-initiated protective measure against heavy metals are ligand molecules (including amino acids, and organic acids) with a high affinity for those ions (Callahan, 2006). Additionally, phytochelatins (Figure 2) are produced de novo, very small peptides rich in cysteine that effectively complexes with cadmium (Cobbett, 2000), likely transported it from the cytosol into the vacuole (Liu et al., 2015). Sequestering of metal ions is performed by a family of ATP-binding proteins known as ABC proteins, found in both plants and mammals (Choudhuri, & Klaassen, 2006). Metallothionein (MT) proteins are another class of chelating proteins that normally and safely transports metal ions within plants, often using tissue specific MT family members such as MT1 family members (root associated), and MT2 class (leaf associated), often toggling from an apometalloproteins (no metal bound) to a metalloprotein (metal bound)

(Thomas, 2005). Ions such as calcium signal heavy metal stress in plants by initiating stress signaling cascades, that increase the levels of stress defense gene expression, which produce more antioxidants and metal-binding chelators (Jalmi, 2018).

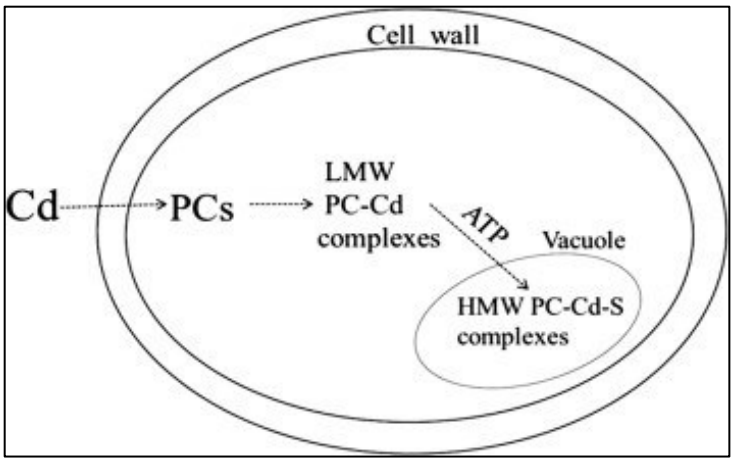

Figure 2: Cd and Phytochelatins (PCs) (Liu et al., 2015).

One unique class of plant species, often found exclusively on metalliferous soils are generically known as "hyperaccumulators." They accumulate and detoxify metal ions within the shoots (Baker, 1981), and have greater than 1% dry weight of a particular metal element. It is hypothesized that these abnormally high metal ion concentrations serve as a defense mechanism against predation (Callen, 2006). Hyperaccumulator plant species employ several strategies to accommodate the resulting abiotic stress; *T. caerulescens* have their highest metal concentration in the leaf petioles and blades, and their lowest in their younger parts (Seregin, 2007). *Arabidopsis helleri* accommodates excess zinc by secreting nicotianamine (Munkhtsetseg, 2014). These pathways are found to benefit non-hyperaccumulating plants too as experiments featuring nicotinamide-overexpressing plants demonstrate that they perform better than controls in a metal-rich environment (Pianelli, 2005). Nicotinamide is thought to represent one chelating compound in *N. tabacum*, as it provides metal binding sites that allow great accumulation of zinc

and cadmium. Despite this, *N. tabacum* is classified as non-tolerant of metals, as it actively prevents the build-up of excess heavy metals, which are markers for an excluder strategy.

1.2.1 Root Efflux Mechanics

One simple, yet largely unstudied mechanism of metal tolerance and exclusion is the ability to sequester toxic metal levels, which can quickly and efficiently be flushed into water during infrequent water undulations, such as excess rain, or flood events. Water soaking may temporarily relieve metal stressed plants, permitting vegetative and/or reproductive development post-metal efflux, insuring a potential next generation of plants within the metal rich environment. This efflux-based survival strategy is largely dependent on a variety of biological mechanisms including K^+ and Na^+ antiporters (Britto & Kronzucker, 2015). Several known genetic resources may contribute to such a passive water soaking strategy for plant survival. In a brief examination, more than 200 Na or K/H exchanger genes (Na/H exchanges or NHEs) are present in public databases (Britto et al., 2002). The *Arabidopsis* SOS1 gene was identified by screening for salt sensitivity in the genus (Shi et al., 2003). The SOS1 gene encodes a plasma membrane electroneutral Li^+ or Na^+/H^+ antiporter that moves and relies on a calcium-binding protein (SOS3) that regulates the SOS2 protein kinase, phosphorylating and thereby activating SOS1 (Moffat, 2002; Shi et al., 2003).

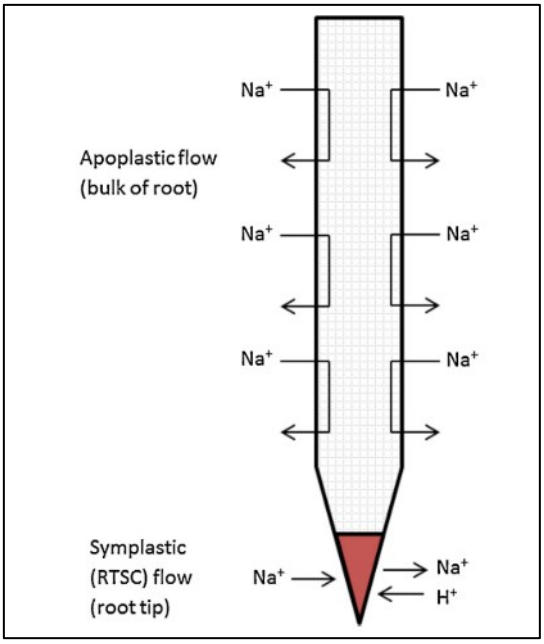

Figure 3: A model of Na+/H+ (Britto, & Kronzucker, 2015).

Many eukaryotic plant species remove excess cytoplasmic H^+ with plasma membrane (PM) H^+-ATPase efflux pump protein coordinated with the NHE exchangers to regulate cytosolic pH and maintain a proton electrochemical gradient, which encourages uptake and efflux of other ion species across the cell membrane (Figure 3, Sze et. al., 1999; Britto & Kronzucker, 2006). This system also has a role in nutrient uptake; mammalian cells are well-known to rely on the Na+-driven glucose symport which moves the sugar molecules from the outside of the cell membrane of low concentration (1 μM), to high (intestinal epithelium cells) (Alberts et al., 2015). To maintain membrane potential, there are minimal Na^+ ions inside the cytoplasm, while K^+ leak channels release K^+ ions outside to reach a near-equilibrium (Alberts et al., 2015). The resulting potential gradient is constantly maintained unless the Na^+K^+/H^+ exchangers are disabled (Alberts et al., 2015). The genetics of ion passage throughout eukaryotic cells is indeed complex.

Efflux transporters in roots have been attributed to adsorption of micronutrients. Membrane-localized and high affinity ion channels can respond to changes in membrane potential, which then releases a subset of anions specific to that ion channel including Cl^-, nitrate, and sulfate, while lower affinity transporters likely impact import/export of a variety ion species (Britto, 2006). Among the low affinity transporters is the superfamily of proteins, ABC transporters utilized by bacteria, plants, and mammals (Alberts et al., 2015). Each ABC transporter tends to be designed for a specific class of molecules, but at least 78 genes are found in genomes of prokaryotes, with even more in those of eukaryotes, which allows for the efflux of a broad collection of particles, including inorganic ions such as heavy metals (Alberts et al., 2015). Ion acquisition allows some degree of ion efflux from the cell to the environment due to its low affinity nature (Britto, 2006). While channel proteins can allow multiple different elements to pass, they have a lower affinity for a single micronutrient metal (Britto and Kronzucker, 2006). Some nickel hyperaccumulators demonstrate Ni:Co selectivity from 100–5,000:1 even though both metals present similar chemical attributes (Callahan, 2006). After a significant metal stress, it is hypothesized that these low affinity transporters may play an important role in metal efflux responses. Low and high affinity ion transporters and channels likely play intersecting roles in different ion's membrane permeability.

1.2.2 Root Efflux and Evolution

Most efflux transporters are thought to have originated from ancient microorganisms (Britto et al., 2005). A variety of P-type ATPases found in prokaryotes allowed metal ion tolerance by pumping different heavy metals outside the cell (Rensing et al., 1999). Eukaryotes have also developed analogs of prokaryotes' reductases and transporters for heavy metals such as arsenic (Rosen, 1999). One subfamily of these P-type ATPases in *A. thaliana*, the HMA2 and

HMA4 proteins, were found to control zinc homeostasis (Hussain et al., 2004). Heterologous over-expression of HMA4 in yeast enhanced tolerance to zinc, cadmium, and lead while forming an increased sensitivity towards cobalt was observed (Verret, 2005). It is hypothesized that the efflux channels for heavy metals are also analogous with those from microorganisms. Both low-affinity transporters for magnesium/nickel and high-affinity nickel transport systems were identified in species of bacteria (Watt & Ludden, 1999).

1.2 Nickel Toxicity

There is little literature on nickel's toxicity on plants due to its complex chemistry (Yusef et al., 2011). In the soil environment, nickel exists as a cation as Ni^{2+}, and as a hydrated complex as Ni $(H2O)_6^{2+}$ in soil solution (Yusuf et al., 2011). Accumulated nickel at low biomass concentrations of 0.1 mg/g dry weight is essential for plant growth but is toxic at levels greater than 20–30 mg/g dry weight (White & Brown, 2010). The minimal amount of nickel required for optimized plant development is usually between 4 and 80 ppm (ATSDR, 1998). Nickel toxicity can result from natural factors influencing the environment's local geology such as glacial advance or retreat as shown in Aberdeenshire serpentine soils rich in mafic metals (Crooke, & Inkson, 1955). These serpentine soils formed from volcanic ultramafic bedrock containing high concentrations of heavy metals including nickel, iron, and magnesium (Brearley, 2005), which pose a risk to most wildlife. Anthropogenic pollution sources are often the byproduct from mining, and ally production of alloys, after which nickel-containing particles settle from the atmosphere onto the soil or water (ATSDR, 1988). The most common exposure to nickel for humans is through food intake, and while metallic nickel is poorly absorbed in humans, it can accumulate in plants (ATSDR, 1988), which allows nickel-laden crops to be consumed by humans, making nickel a pollutant of concern (Figure 4).

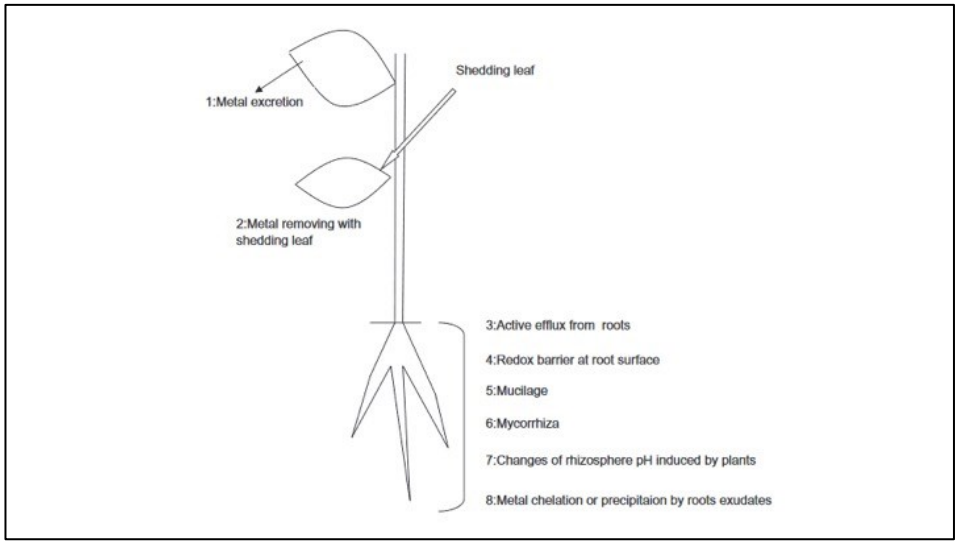

Figure 4: Summary of nickel management in plants. (Javid et al., 2018).

Nickel plays an important role within non-phytotoxic amounts, increasing the yield of several crop plants by regulating the mineral metabolism, enzyme activity, and several other metabolic processes (Meshra & Kar, 1974). One of the first formulations for Hoagland's nutrient solution contained nickel (Schropp & Arenz, 1942), but was removed in later publications (Hoagland & Arnon, 1950). Modified Hoagland's solution salts containing nickel as a recognized micronutrient are commercially available today. A similar case is found with Murashige and Skoog medium which originally did not contain nickel (Murashige & Skoog, 1962), but proposals for adding nickel were made after the recognition of nickel as a true micronutrient (Witte et al., 2002), and has been reported to be more effective with the addition of trace levels of nickel (Witte et al., 2007).

Nickel is utilized in metalloenzymes including urease, an enzyme responsible for the hydrolysis of urea, superoxide dismutase, a key enzyme in lowering oxidative stress in plants, and acetyl coenzyme-A synthase, a key feedstock biochemical for fat and carbohydrate metabolism in plants (Ahmad, & Ashraf, 2011). Nickel has a role in a plant's defense as a cofactor for glyoxalases and as a possible regulator in glutathione production (Fabiano et al.

2015). It's otherwise rare for nickel to be an enzyme's center due to its complex-forming capabilities which lowers its potential for catalytic performance (Munakata et al., 1970). The transport of magnesium, as a low affinity solute, is thought to also be the pathway for nickel and zinc cellular import, described as metal "hitchhikers" (Webb, 1970). Small metallothioneins specific for divalent metals are thought to modulate zinc and copper levels in enzyme and nucleic acid biochemistry are associated with imported nickel (Blanchard & Cousings, 1997). Likewise, the NikR protein is a nickel-dependent DNA-binding transcription regulating protein, that stimulated the production of an ABC protein specifically for nickel transport (Chivers, & Sauer, 1999). There is conflicting data that metallothioneins function to promote nickel transport and toxicity in animals (Homa, et. al., 2016).

1.2.1 Nickel Toxicity Mechanics

Nickel is both a needed micronutrient, and a toxic compound which has little known about its storage and efflux within higher plants. Nickel does accumulate in the sink leaves (Figure 7; Page & Feller, 2015) and as a result nickel pollution in soils decreases farmland productivity (Nishida, 2011). Uncovering the mysteries of plant nickel storage and transport of nickel is necessary to also appreciate nickel contamination of watersheds.

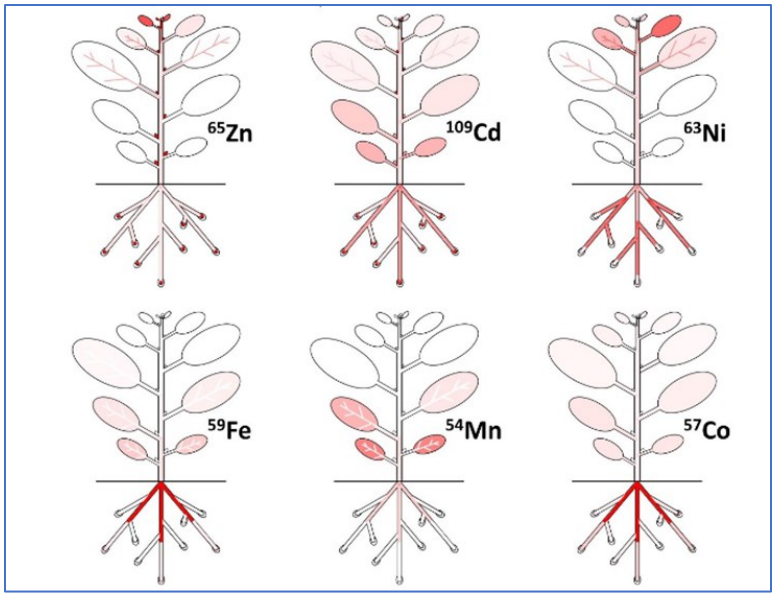

Figure 5: Micronutrient distribution on plants (red color representing higher concentrations). (Page & Feller, 2015).

Plants have means of protection by metal exclusion, chelation, and vacuole sequestration, making nickel toxic only at higher concentrations of mM at which the defenses are overwhelmed (Yusuf et al., 2011). Nickel owes its toxicity to the interference with other micronutrient uptake (K, Ca, Mg, Fe) in different plant parts (Rubio et al. 1994) (Crooke & Inkson, 1955). Thus, nickel is considered a generalized disruptor of micronutrient transport (Coogan et al. 1989), with detrimental effects on mammals including cardiovascular diseases, lung fibrosis, gene mutations, and cancer (ATSDR, 1988; Valko & Cronin, 2005). Additionally at pH 7.5 or greater, nickel can generate reactive oxygen species (ROS) and free radicals via the Fenton Reaction, thereby damaging membrane integrity, protein, and DNA (Frankel et al., 1984; Mittler, 2002; Kolar et al., 2003). In excess, nickel can cause mitotic disturbances in the root tips of plants (Meshra, & Kar, 1974), resulting in reduced root growth (Pandey, & Sharma, 2002), glutathione depletion, and sulfhydryl protein group interference (Valko et al. 2005). Common symptom of nickel toxicity includes progressive chlorosis (along with increased red pigment content) and necrosis on young leaves, and shoot apex (Pandey, & Sharma, 2002), visible as early as the third day of

stress, due to a 2.5-fold increase in ROS (Gajweska & Skłodowska, 2007). Depending on the species, dry matter is also reduced by nickel, and more so if potassium is low or phosphorus is high (Crooke & Inkson, 1955).

A contributing factor for nickel tolerance is a plant's ability to release sequestered nickel which reestablishes normal metabolism; nickel likely competes with other metal ions absorbed by roots (Yusuf et al., 2011). In a competition kinetic study, nickel and copper were absorbed by soybean seedlings with the same metal carrier site (Cataldo et al. 1978). The biosynthesis of the iron trafficking protein IRT1, the main entry for divalent heavy metals such as Fe^{2+}, was observed in nickel and copper in iron-deficient plants (Barberon et al., 2014). An experiment by Nishida showed that in iron-deficient conditions, AtIRT1-defective mutants of *A. thaliana* accumulated far less nickel over the wild type (2011). Excess nickel exposure with or without the presence of iron in the growing medium causes the expression of AtIRT1 to exponentially increase, leaving iron-starved plants vulnerable to nickel outcompeting iron (Nishida, 2011). Nickel and iron ions also interact with the efflux membrane-bound protein FPN2, which transports nickel, cobalt, and iron from cytoplasm to vacuole (Conte & Walker, 2011). There are some complex interactions between heavy metal tolerance and genetics that lead to both gaps and overlaps in a plant's defense. Nickel tolerance was found to be heritable and not correlated with genes that confer copper tolerance (Tilstone, & Macnair, 1997), but rather with magnesium and cobalt (Watt, & Ludden, 1999).

1.3 Copper Toxicity

Copper was also selected as a second focus in this study due to its documented nature in plants and distribution pathways. Copper and nickel are located adjacent to one another in the Periodic Chart and have similar in chemistry and biological terms. *M. crystallinum* is also shown

to be more tolerant towards copper than *A. thaliana* (Thomas, et. al., 1998). The antioxidant pathways *M. crystallinum* developed to protect itself from salt stress is argued to also be used against copper stress given its tolerance (Thomas et al., 1998). Nickel is unique amongst many trace metals, as it demonstrates high mobility in phloem and is directed to the growing parts of the plant, while other heavy metals such as iron and manganese accumulate in older leaves (Page & Feller, 2015). Copper by contrast is an immobile nutrient that does not go through redistribution within the plant after incorporation (Page & Feller, 2015).

The copper concentration in field soil is dependent on labile copper, the soil's adsorbing capacity, and soluble copper complexes (Nielsen, 1976). Copper naturally forms complexes with organic and inorganic materials within soil components, while easily binding to the surface of root cells (Yruela, 2005; Nielsen, 1976). Cu^{+} ions are valuable cofactors in oxidases due to their high affinity for oxygen molecules (Yruela, 2005). Cu-amino oxidases (Cu-AOs) function as a catalyst for the conversion of amino groups to their corresponding amino aldehydes by the addition of O_2 (Medda et al., 1995). Plastocyanin and Cu/Zn SOD (superoxide dismutase) are the most plentiful proteins containing copper in the aerial portion of plants alongside copper-blue binding proteins (Yruela, 2005). Another important protein, the Cu/Zn SOD enzymes is found in the cell cytosol, chloroplast, and peroxisome devoted to detoxifying H_2O_2 radicals (Pilon et al., 2011). However excess copper is the most powerful ROS generating divalent cation in physiological conditions. The resultant free radicals are deleterious to biological health (Halliwell and Gutteridge, 1984).

The COP (copper transporter) family of genes is responsible for copper homeostasis; COPT1 in root cells accumulates Cu^{+} ions under copper-limiting conditions and is expressed less as copper enters the plant (Yruela, 2005). COPT transporters are stimulated by extracellular

potassium cations (Yruela, 2005). Chloroplasts also have their own group of copper transporters: PAA2 encodes a P-type ATPase which delivers copper to the thylakoid membrane's inside, while PAA1 has a similar function at the chloroplast peripheral (Abdel-Ghany S., et. al., 2005). Their relative importance was shown when disabling both genes led to plant death (Abdel-Ghany, et. al., 2005).

Copper contamination of the environment is more likely to be anthropogenic in origin compared to nickel. Copper sulfate is used as a pesticide ingredient for pathogens of various crops in the Mediterranean, leading to excess copper released into the local environment (Pietrini et al., 2019). The examination of the soil profile of a Cu-Mo mine in Wunugetushan, China found that nickel had non-point source pollution while copper spread out from the mine to the surrounding environment by human activity (Wang, 2018). Plants in such an environment are found to develop mutations in which they overexpress CUP1-1, a copper metallothionein, along with genes encoding vacuolar transporters, an H^+-ATPase, and a mitochondrial morphology stabilizer (Gerstein, 2015). This finding implies that multiple genes are responsible for copper homeostasis during metal stress.

1.3.1 Copper Toxicity Mechanics

Copper toxicity results from cellular oxidative damage, ions outmatching the intake of other micronutrients, and interfering with enzymes' sulfhydryl groups (Yruela, 2005). Gene expression is also hindered by copper resulting in increased osmotic potential, metal-specific mechanisms, free radical generation, and lipid peroxidation contributing to cell death (Thomas et al. 2004). Ionic copper can also induce cell death by binding with lipoylated proteins in the Krebs cycle, which disables the respiration stages within mitochondria (Tsvetkov et al., 2022). It is hypothesized that as older leaves of a copper-stressed plant accumulate copper, the plant

overproduces cytokine to preserve the younger tissues of the plant (Thomas, et. al., 2005). Excess copper has been documented to interfere with the uptake of iron and zinc during the first week of stress of giant reed (Pietrini, 2019). With excess copper exposure of 0.3 mM, nitrate intake was reduced by 20% in *C. reinhardti* (Mosulén et al., 2003), and at 0.5 mM. decreases of both iron intake, and the activity of iron-dependent enzymes, and chlorophyll content was observed in *B. oleracea* (Pandey, & Sharma, 2002). Cu^{+2} ions can also displace the Mg^{+2} center of chlorophyll which deactivates photosynthesis (Yruela, 2005).

1.4 *M. crystallinum* Adaptations

M. crystallinum is a unique facultative halophyte, a plant tolerant of environments of high salinity, compared to the non-tolerant glycophyte *N. tabacum*. *M. crystallinum* can switch from C3-photosynthesis to CAM during stress conditions of drought, low temperature, high soil salinity (Adams et al., 1992), and low ratios of red light to far-red light absorbed by phytochrome (Cockburn et al., 1996). CAM is initiated by the de novo synthesis of the mRNA and protein production of phosphoenolpyruvate carboxylase (PEPcase) (Höfner et al., 1987), encoded from the gene *Ppc1* (Thomas et al., 2004). During the night, PEPcase creates oxaloacetate from PEP and bicarbonate which is then reduced to malic acid, which triggers CAM (Höfner et al., 1987). Linked with this change in gene expression, a cysteine protease (*Sep7)* also accumulates during water and salt stress (Forsthoefel 1998). It's hypothesized that SEP7 takes part in proteolysis to provide the biological materials necessary for both short- and long-term metabolic changes associated with CAM (Forsthoefel 1998). The CAM pathway is reversible when salt stress is removed, which has PEPcase activity and concentration decrease (Vernon, 1988). Confirmatory studies in the *M. crystallinum* affirmed at the gene transcriptional level, CAM can reverse course back to C3 (Cushman et al., 1990). However, PEPcase mRNA transcription gradually increases

with the age of the *M. crystallinum* (Vernon, 1988). Four distinct phases of CAM demonstrate this plasticity is mediated by both environmental conditions and molecular signaling, and by structural constraints conferred within different succulent tissues (Dodd et al., 2002).

The antioxidant pathways *M. crystallinum* likely evolved to protect itself from salt stress and some protective strategies may be used against copper stress given its tolerance (Thomas et al., 1998). *M crystallinum* as a halophile, produces compatible solutes, a group of small organic metabolic-inert molecules which provide osmotic pressure to the cells to retain water and nutrients (Antón, 2011). In a comparison between *M. crystallinum* and *B. juncea* by Amari et al. (2014), roots were the preferred sites for nickel storage in both plants, with *B. juncea* having a higher shot from root translocation factor than *M. crystallinum*. Both plants acted as excluders (below a threshold value) (Baker, 1981). Despite *M. crystallinum* not hyperaccumulating, it has a higher threshold for nickel, and accumulates more inside the leaves and stem than *B. juncea* (Amari et al., 2014).

1.4.1 M. crystallinum Bladder Cell Biology

The unique epidermal bladder cells, which generate high osmotic pressure to serve water and ion storage (Adams et al., 1992). Compatible solutes such as pinitol, a sugar alcohol solute, are present in bladder cells and are capable of scavenging hydroxyl radical groups (Smirnoff & Cumbes, 1989). Cyclic polyol retains water within leaves, accumulates in the bladder cells of salt-stressed plants to build up osmatic pressure in the leaves and flowers (Adams et al., 1992). Analysis of the bladder cells via ICP-MS determined that there are twenty-seven major and micro elements present including cadmium, chromium, and mercury (Barkla, 2016). *M. crystallinum* was deemed to tolerant nickel treatments, as the metal accumulated in the aerial portions (Amari et al., 2016). This study focused on a comparison of heavy metal efflux

following nickel stress in both *N. tabacum* and *M. crystaillinum,* and whether nickel tolerance in *M. crystallinum* was seen.

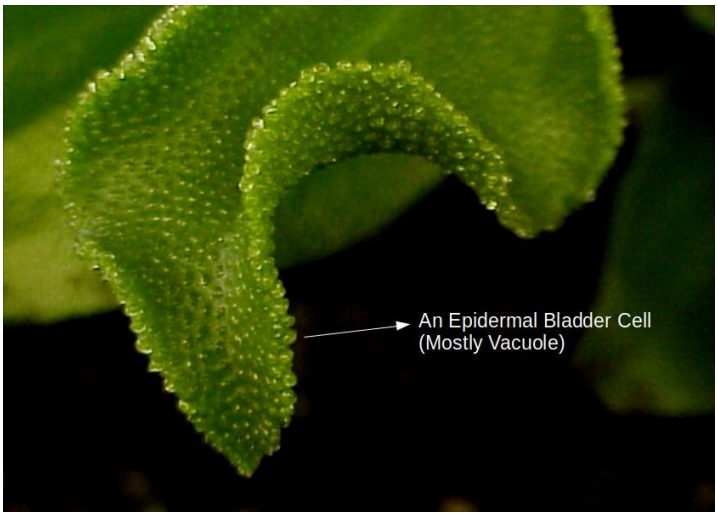

Figure 6: M. crystallinum bladder cells (500 µm in diameter), store water, ions, and solutes.

Chapter 2 Methods

2.1 Goals of Experiment

While there is plentiful research on plant heavy metal uptake and incorporation, literature on plant efflux releasing metal was scarce. The minimal studies of nickel treatment on plant toxicity help justify the primary focus of metal efflux after nickel stress in this project (Muhammad et al., 2013; Yusef et al., 2011). The fundamental goal of this project is to compare how nickel and copper stress may influence metal root efflux, and to explore whether water inundation may provide plant resilience in the environment. Besides metal sequestration and efflux, their toxic effects on plants and how they may impact leaf and root morphology were recorded. These observations will highlight any differences between a halophyte (a CAM plant) and a glycophyte (with a C3 pathway) represented by a tobacco species. The experiment will also observe how root efflux impacts the nutrient distribution as the default distribution of plants' nutrients mobile and immobile is known. This experiment should reveal whether nutrient distribution between leaves and roots remain constant after efflux or not. If the halophytes tolerate metal excess better than glycophytes, this should reveal whether they perform efflux differently from glycophytes or if they are identical. If metal detoxification via efflux is viable, this experiment can also serve as a model for flooding/ponding the crops to remove excess metal content from the plants.

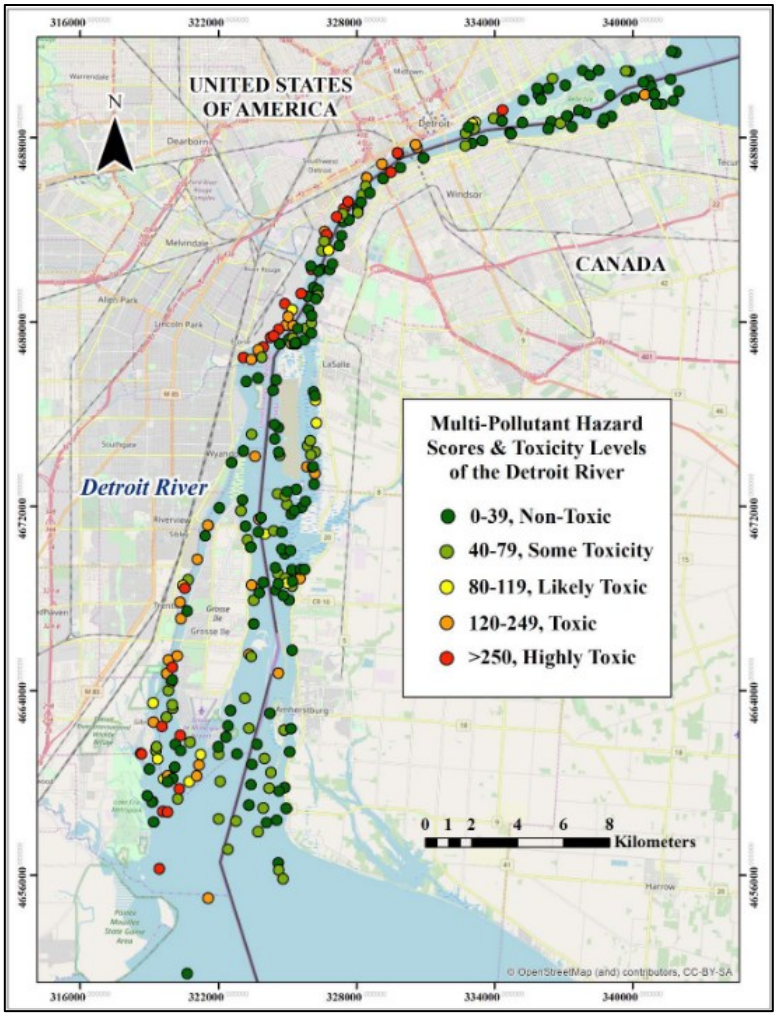

Figure 7: Detroit River nickel pollution (Ellison, 2022).

Another potential application for the results is in environmental remediation. In a spatial and temporal sediment study of the Huron-Erie Corridor, probable effect concentrations (PEC) were found to have a wide diversity of pollutants including microelements like nickel (Drouillard et al., 2020). The contaminated sediments' gradient is highest near the shoreline and decreases towards the deepest parts of the river, meaning the nickel is generally immobile (Ellison et al., 2022). The nickel found in river sediment has likely originated from the nickel-plating facilities neighboring the Detroit River still in use today (Figure 6; Ellison et al., 2022). It may be possible for nickel-tolerant halophytes within the plots of nickel pollution to clean them up. The Detroit River is native to wetland plants tolerant of salt such as *Phragmites australis* (common reed),

and *Pontederia cordata* (pickerelweed) (Fennessey, 2021). It's possible such plants can be utilized in the remediation of the Detroit River.

2.2 Independent Key Variable

The independent key variables in this study are the heavy metal concentrations in the different groups of hydroponics growing in defined sets of nutrient hydroponic concentrations. Dependent variables are heavy metal cations in both plant matter and efflux solution. It's hypothesized that nickel and other heavy metals are more biologically available in hydroponics than soil due to the latter's components that restrict nutrient mobility (Amari, et. al., 2016). Hydroponics also bypasses the need for root washing of soil.

2.3 Selected Criteria

2.3.1 Plant Species Selection

N. tabacum was selected for the experiment as it is a user-friendly model organism (sufficiently studied species with broadly applicable genetic findings). The SR1 strain was chosen for its small leaves that are easier to work with compared to the commercial plant's very large leaves. There is no documentation of *N. tabacum* being significantly tolerant to nickel or copper, but it possesses metal-chelating proteins that allow the plant to hyperaccumulate zinc into the leaves while tolerating excess cadmium (Vera-Estrella et al., 2017). *M. crystallinum* is chosen as a comparison for its status as a model organism with a C3 to CAM switch pathway during salt stress (Thomas, et. al., 2004). The differences between halophytes and glycophytes can be observed in this efflux experiment while the potential correlation between anti-oxidation activity and compartmentalization of heavy metal ions within the unique bladder cells of *M. crystallinum* can also be tested. Bladder cell biology has been shown to respond with large

changes in gene expression when presented with salt stress conditions, underlying the importance of these epidermal structures to stress tolerance (Barkla et al. 2016).

2.4 Procedure

2.4.1 Hydroponic Growth

Plants were grown from seeds on agar or soil at room temperature (agarose with *N. tabacum*, soil with the first ice plant run, and agarose during the second run), two to four weeks before experiment trials. The adults are then placed into hydroponic chambers constructed by wrapping 250 mL glass jars with aluminum foil to accommodate the seedlings to the medium for two to three weeks. In the first week, an agar box was covering each seedling to prevent excessive moisture loss. Hoagland's solution was prepared according to the original recipe by Hoagland, and Arnon (1934). During the growth period, hydroponic solutions were made following the same recipe as before, with a plastic box covering each of the plants to limit dehydration. Plastic gutter grating was cut into squares with a small hole cut into it to act as lids that keep the plant's roots submerged while lifting the plant.

The stress trials with heavy metals were performed with hydroponics to prevent interference with the soil's complex interactions such as cation exchange capacity and precipitation of metals in solution. The stress period for *N. tabacum* was one week, while *M. crystallinum* was two weeks. *M. crystallinum* has been documented to be very salt tolerant, copper, and nickel tolerant, so an extended time for the specimens was chosen (Thomas et al., 1998; Amari et al., 2016). During the trial period, the nutrients of the solutions were reduced to one-tenth of the original concentrations to prevent nutrient stress in conjunction with the metal stress in the experimental trail groups. Nickel was added to a stock solution by mixing reverse

osmosis (RO) water with $NiCl_2$ * 6 H_2O, and copper was added to a stock solution by $CuSO_4$ * 5 H_2O. The resulting solutions are Control (nothing added), 0.05 mM Ni, 0.5 mM Ni, 0.4 mM Cu, and 0.5 mM Ni combined with 0.4 mM Cu (Both Heavy Metals (HMs)). 10% hydroponic solution containing 0.4 M NaCl was also made exclusively for the *M. crystallinum* runs to emulate salt stress conditions. After the addition of metal, each of the solutions had their pH adjusted to 5 – 6.5.

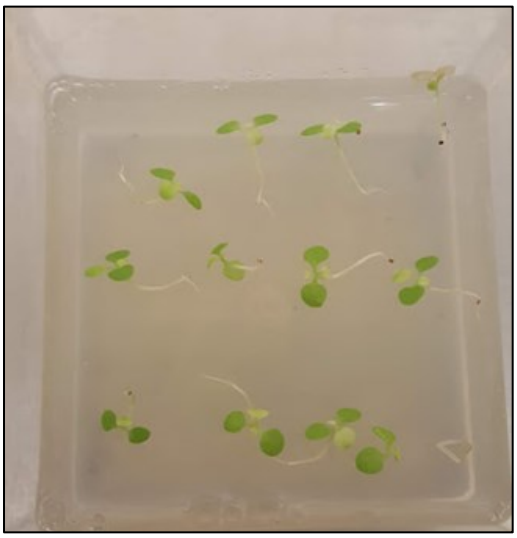

Figure 8: Seedlings growing in agarose media.

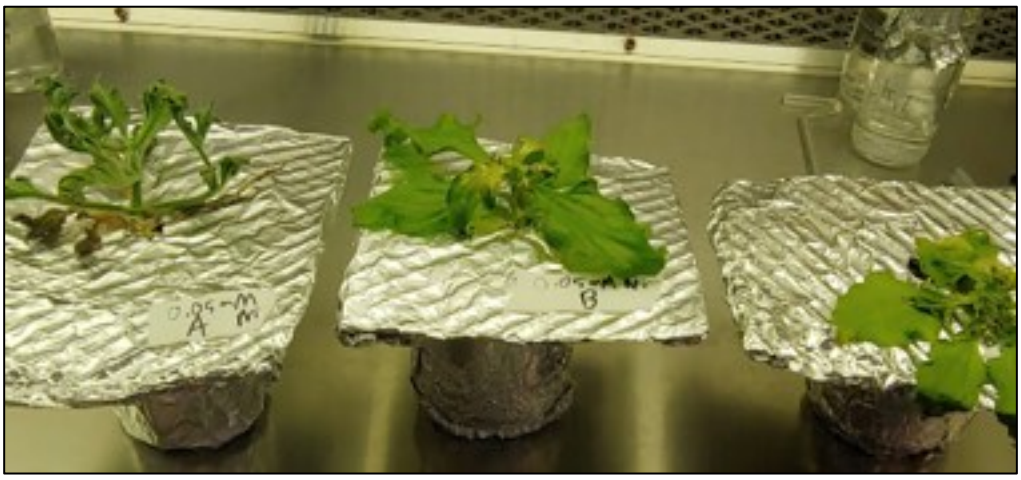

Figure 9: Hydroponic chambers with M. crystallinum.

2.4.2 Efflux Collection Procedure

The root wash procedure follows Aldrich et al. (2003) with some adjustments. Efflux preparation was done by soaking in reverse-osmosis water two times for two minutes each in 250 mL jars to remove traces of the previous hydroponic solution and non-adherent metals from the roots. The addition of acid to the wash as stated in Aldrich et al. (2003) was omitted to ensure roots are unharmed before efflux; roots are washed twice as an alternative. Efflux was performed in 100-150 mL beakers for twenty minutes with the grating holding the plants in place with RO water (pH roughly was 5.8). In literature, root efflux for Na^+ enters a slow exchange phase in distilled water between 10 and 30 minutes (Schulze, 2014). From this example, twenty minutes was chosen for the efflux transit time from the plant to the external solution.

Figure 10: Efflux Set-up with N. tabacum with two rinse containers and a 100 mL beaker for efflux collection.

2.4.3 Sample Preparation

After the efflux procedure, the leaves and roots of the plants were harvested and stored in a -80 ˚C freezer. Leaves and roots frozen with liquid nitrogen were ground with a mortar and

pestle. 50 mL of the efflux solution was acidified with 0.5 mL of concentrated nitric acid (creating a 1% nitric acid efflux solution) to break down saccharide compounds in the solution which prevents bacterial contamination. The efflux solutions were stored in a lab refrigerator for no more than a week before acidification with nitric acid. The weights of dray vials were measured, and then vials with the addition of plant material were dried in a Thermofisher oven for a week at 84 ˚C (the highest temperature of oven) and dry weight measurements made with Mettler Toledo analytical balance scale (AB204-S/FACT). Microwave digestion was performed with Synthos 3000 Rotor 64MG5 to an internal temperature minimum of 62.78 ˚C according to the manufacturer's directions, with 4 mL Wheaton vials (224802) containing a dry weight of 1-10 mg plant matter in 2 mL of concentrated nitric acid. Wheaton caps (240408) 50 µL of each of the samples are mixed with 10 mL of 1% nitric acid and RO water solution to make an analysis sample.

2.4.4 ICP MS Analysis

An ICP Mass Spectrometer (ICP MS) was used to determine the metal concentration in both the efflux solutions and plant matter samples. Metals examined in the ICP/MS includes by atomic number Al (27), Cr (52), Cr (53), Mn (55), Co (59), Ni (60), Cu (63), Cu (65), Zn (66), Zn (68), As (75), Se (77), Se (82), Sr (88), Ag (107), Cd (111), Cd (114), Ba (135), Ba (137), Pb (208), Na (23), Mg (24), K (39), Ca (44), and Fe (54). Most ICP-MS measurements were performed on an Agilent 7700x ICP-MS (Santa Clara, CA, USA) at Wayne State University. After the instrument warm-up was complete, it was tuned with a tuning solution for ICP-MS 7500cs (Agilent, part number 5185-5959) using the Online ICP-MS Mass Hunter Software in the helium (He) and high energy helium (HEHe) gas modes. Calibration standards were developed from a multi-element standard, IV-ICP-MS-71A (Inorganic Ventures, Christiansburg, VA,

USA), and diluted in a 2% HNO3/0.5% HCl solution. During sample analysis, a blank and a check standard (prepared separately from the calibration standards) were analyzed every 20 samples. The samples were analyzed (not through an EPA protocol) on an ICP MS in the Lumigen Instrument Center at Wayne State University, Detroit, MI. by Dr. Johnna Birbeck. The ICP signals for each metal analyzed were expressed as ppb/Unit of dry weight and then converted to µmol/g dry weight to standardize data.

2.4.5 MDA Procedure

Oxidation of lipids via malondialdehyde (MDA) is a direct measurement of the plant stress in both the leaves and roots with the procedure done according to Warren L. (1959). Chlorophyll loss is often cited as a symptom of oxidation within leaves. Chlorophyll is not in roots while the MDA assay can be performed in both leaves and roots (Gaweł S et al. 2004). The procedure starts with the submerging of plant matter in 600 µl of 0.1% w/v trichloroacetic acid (TCA) solution for 10 minutes, after which the capped micro flasks were centrifuged at 16.3 gravity for roughly 12-20 minutes. 500 µl of the supernatant is then mixed with 2 ml of 0.5% w/v thiobarbituric acid (TBA) in 20% w/v TCA in separate test tubes in which the solution is incubated at 90 °C for 30 minutes. After cooling, the samples were measured at 532 nm and 600 nm with a visible light spectrometer. A control factor for each of the resulting reading averages was calculated by adding together the mean value and one half of the standard deviation and dividing the value by the sum of the control group's average and half of its standard deviation.

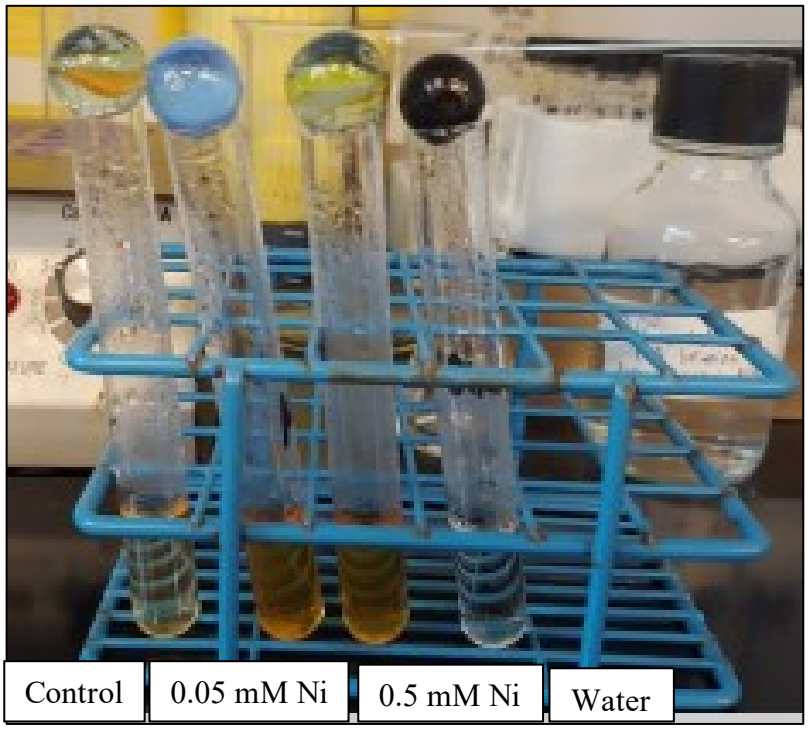

Figure 11:MDA colors after heating. Left to Right:(1) Control, (2) 0.05 mM NiCl2, (3) 0.5 mM NiCl2 and (4) water.

2.4.6 Pilot for Efflux Time and Nickel Influence

To ensure the efflux procedure is integral, validation of this approach was done in one pilot experiment, in which spare *M. crystallinum* specimens from the Control group, and the 0.05 mM Ni group effluxed for 10, 20, and 30 minutes. Tissues from the 20-minute control and 0.5 mM Ni groups were ground up for microwave digestion and ICP analysis.

2.5 Calculations

2.5.1 ICP Calculation

Equation 1: ICP Calculation

$$Element\ mol\ per\ gram\ of\ dried\ plant\ matter = \frac{ICP\ signal\left(ppb\ or\ \frac{ug\ element}{1\ L\ solution}\right) * \frac{1\ L\ fn}{1000\ ml\ fn} * \frac{10\ ml\ fn}{0.050\ ml\ og} * 4\ ml\ og\ solution * \frac{1\ g\ element}{10^6\ ug\ element} * \frac{1\ mol\ element}{Molar\ mass\ of\ element\ (g)}}{g\ of\ dried\ plant\ matter}$$

$$= \frac{ICP\ Signal * (8 * 10^{-7})}{Molar\ mass\ of\ element\ (g) * g\ of\ dried\ plant\ matter}$$

Readings converted to mol/g dry weight for plant matter and µM for efflux for data standardization.

2.5.2 MDA Formula

To calculate lipid peroxidation, the extinction coefficient of MDA and dilutions will be considered. The MDA Extinction coefficient is: 156 / mM * cm (Warren L., 1959).

Equation 2: MDA Equation

$$MDA\ nmol\ per\ gram\ of\ plant\ matter = \{\frac{\left[\frac{\Delta A}{\frac{156}{mM*cm}} * 1000\frac{nmol}{mmol}\right]}{0.2g}\} * \ 2.5\ \text{mL}$$

$$\Delta A = \ 532\ \text{nm Absorbance Reading} - 600\ \text{nm Absorbance Reading}$$

Chapter 3 Results

3.1 Plant Health

3.1.1 N. tabacum

All *N. tabacum* plants had large green leaves and white to light-brown roots during the one week-long stress period. The Control group is the healthiest out of the others, as there was minimal necrosis and leaf curling, and the roots were white and spotless. The plants of 0.05 mM Ni group had leaves which retained the green color of the control, but lost turgidity, with some necrosis areas and yellowing at the leaf margins, while the roots remained white with light brown specks. The leaves from the 0.5 mM Ni group had visible leaf veins in a patchwork-pattern not found in the other groups. The leaves have also lost their turgor and the bottom leaves gained a brown and yellow coloration, and the roots are tan with deep brown spots. The 0.4 mM Cu^{+} group had most of their leaves turgid and green, but the bottom most leaves were wrinkled with dead patches, and the roots were light tan with light brown spots. The plants from the Both HMs group had most of their leaves shriveled while being mostly green with yellow edges and necrosis spots. The stem was falling over on itself, and the roots were mostly tan with deep brown specks. 0.5 mM Nickel and Both HM group samples had severe loss of turgor; the former kept its yellow pigmentation, while the latter lost all its color, making it the least healthy out of all the stress conditions. Individual 0.4 Cu^{+} or 0.05 mM Ni^{+} groups have minimal loss of turgor but have retained a green color.

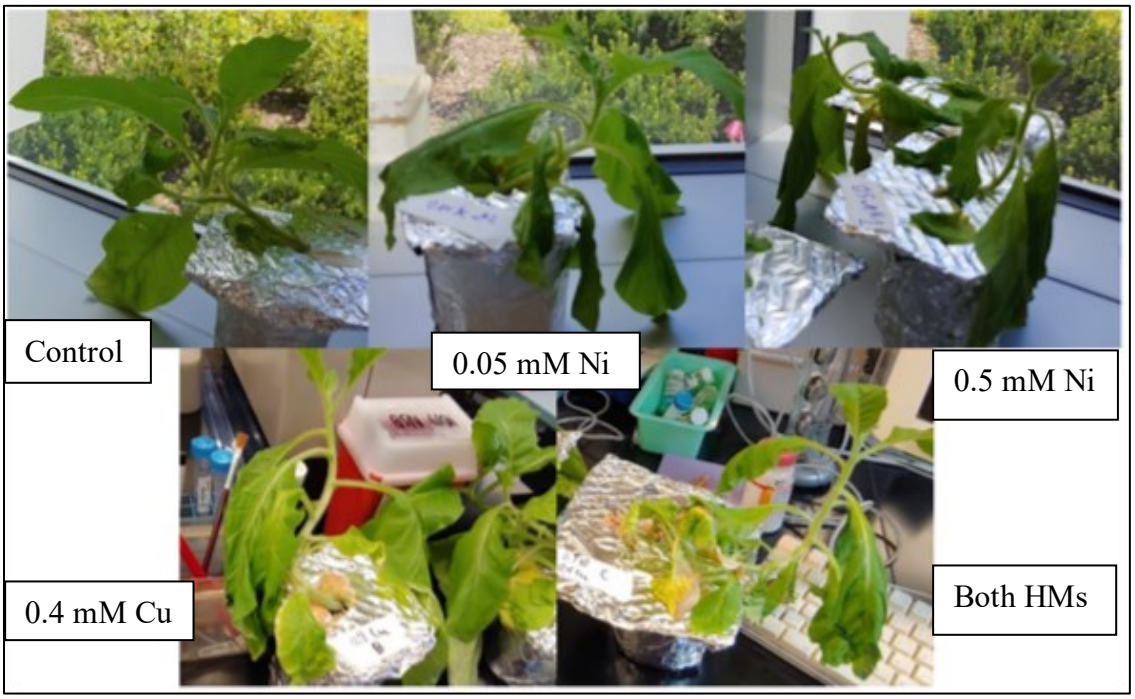

Figure 12: N. tabacum plants after stress treatments.

3.1.2 M. crystallinum

Control leaves were green and turgid while the abundant bladder cells covered the stems entirely. The roots were long and light cream in color. The 0.4 M NaCl group plants in the first week displayed curved and dying leaves due to salt signaling budding and death of the plant. There was a higher bladder cell density throughout the plants to accommodate in the salt stress treatment. Roots in the NaCl stress group are a light tan color, and darker than those of the Control group. Samples from 0.05 mM Ni plants showed some shriveled leaves with discoloration or necrosis in the first week of stress. By the second week, the plants display stunted growth, and leaves are either curled, flattened with no turgidness, or had necrosis spots; only one plant in the group was seen to have eye-visible bladder cells. Root colors ranged from cream to a darker shade of tan. 0.5 mM Ni^{+} group plants in the first week have shriveled pale yellow leaves and stem with minimal bladder cells observed. In the second week the plants are

almost entirely white with little green pigment remaining. The roots in the first and second week are light cream in color and smell like peroxidases in the second week. 0.4 Cu^{+} group plants in the first week are turgid and green with an occasional yellow leaf and a net-shaped pattern of necrosis. In the second week, most leaves retain a green color, with some yellow green, while the uppermost leaves are small. Bladder cells are present on stem, and roots are tan in color. The Both HMs leaves are similar in appearance to those in the 0.5 mM Ni group; the flattened leaves have some green coloration, but most of the plant including the steam is a pale-yellow color. No bladder cells were found to be visible as well. The roots range from a cream color to tan.

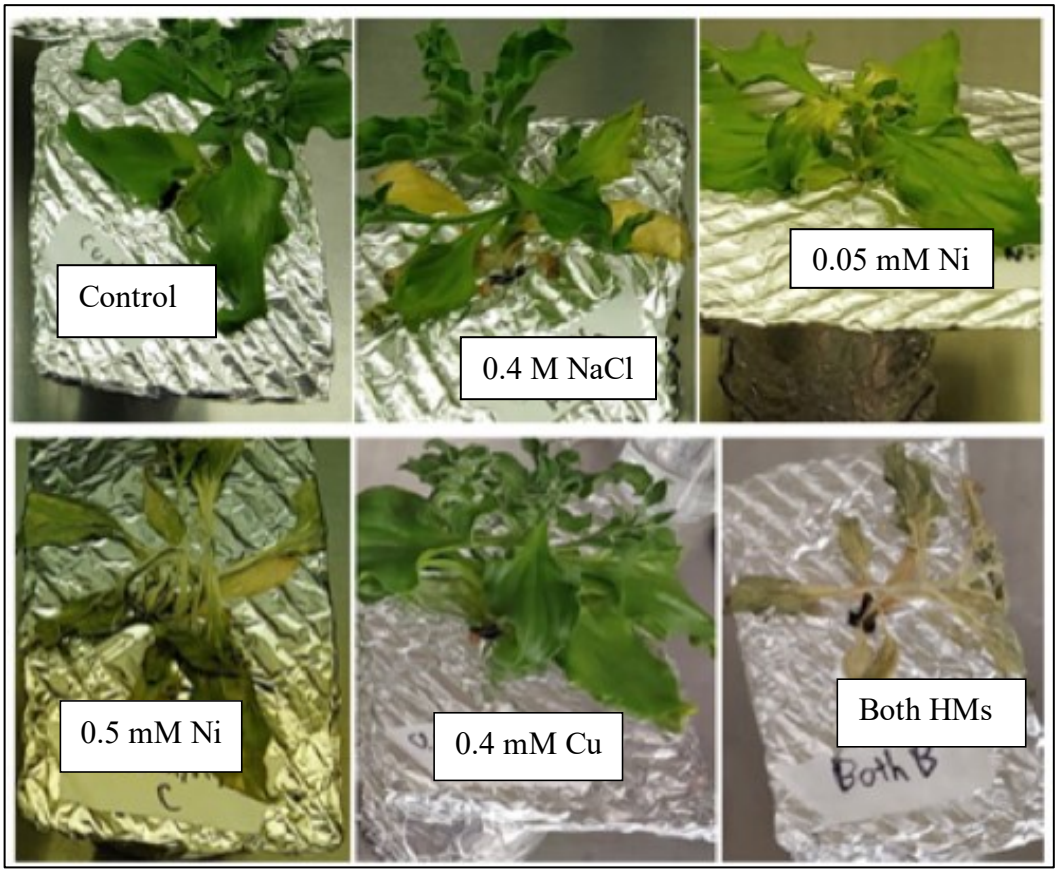

Figure 13: M. crystallinum post two-week stress period.

3.2 Plant Matter ICP Results

3.2.1 Nickel Plant Matter

N. tabacum: The average content of nickel found in the leaves was smaller than the roots in all condition trials. The maximum value of nickel in the leaves was 9.114 µmol/g at Both HMs, and the lowest at 0.5 mM Ni at roughly 1.010 µmol/g, while the control and 0.4 mM Cu^+ groups were 1.377 µmol/g and 1.0586 µmol/g respectively. Maximum Ni^+ accumulation in roots occurred following 0.5 mM Ni^+ stress at 187.486 µmol/g and the second highest is from the 0.05 mM Ni^+ group at 59.238 µmol/g. Nickel accumulation in the roots was lowest at 0.4 Cu^+ stress, determined at 1.832 µmol/g.

M. crystallinum Ni^+: 0.2858 µmol/g Leaf content and 1.126 µmol/g Root at Control, 02554 µmol/g leaf content, and 1.0130 µmol/g root content at 0.4 M NaCl, 3.451 µmol/g Leaf Content and 66.582 µmol/g at 0.05 mM Ni^+, 93.781 µmol/g leaf content, and 124.76 µmol/g content at 0.5 mM Ni^+ (max value). There was minimal content at 0.4 mM Cu^+ group that is undetectable by the ICP in use. The averages increase up to 51.285 µmol/g at leaves and 84.457 µmol/g at roots at Both HMs, which are in between the values from the 0.05 mM Ni and the 0.5 mM Ni groups.

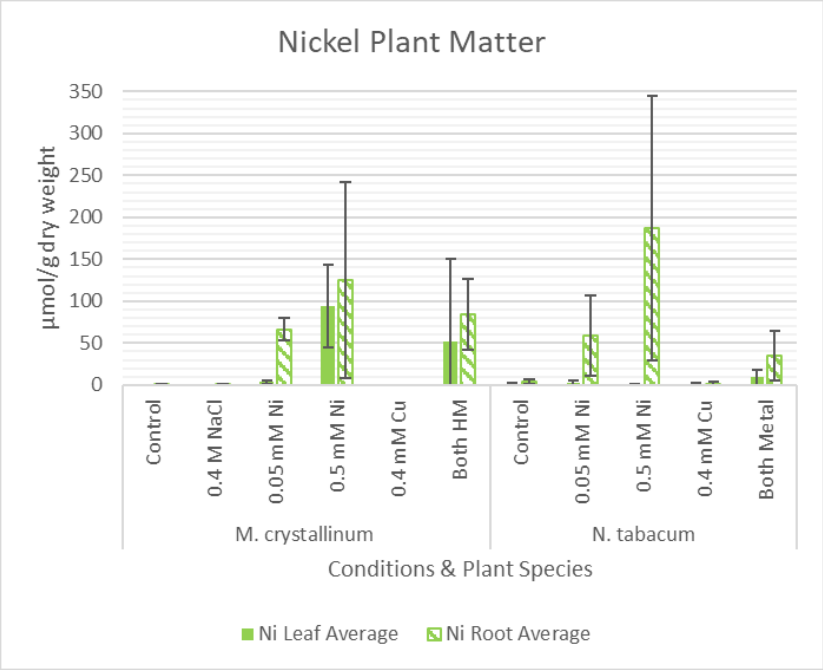

Figure 14: Nickel plant matter content (Long lines represent the standard deviation).

3.2.2 Copper Plant Matter

N. tabacum: Cu^+ content accumulation compared to unstressed samples was minimal in both leaves and roots of the 0.4 mM Cu^+ treatment media. The highest leaf concentrations were seen in the Both HMs stressed plants, at 29.674 µmol/g copper, along with 0.05 mM Ni at 29.417 µmol/g. The third highest leaf value was from 0.4 mM Cu^+ at 19.316 µmol/g. Coincidentally, the lowest copper content was following a stress of 0.5 mM Ni^+ in the roots at (7.666 µmol/g). Copper was highest in roots of both 0.4 mM Cu^+ and Both HMs at 459.522 µmol/g and 247.970 µmol/g respectively, while the lowest is at the unstressed control group (32.024 µmol/g).

M. crystallinum: Control group has 13.41 µmol/g leaf content, and 45.710 µmol/g root content, 0.4 M NaCl group has 10.154 µmol/g leaf content, and 41.962 µmol/g root content, 0.05 mM Ni^+ group has 12.763 µmol/g leaf content and 82.488 µmol/g root content, 0.5 mM Ni^+ group has 4.853 µmol/g leaf content and 50.83 µmol/g root content, 0.4 mM Cu^+ group has

7.596 µmol/g leaf content and 344.125 µmol/g root content, and Both HMs group have 4.322 µmol/g leaf content, and 152.368 µmol/g root content.

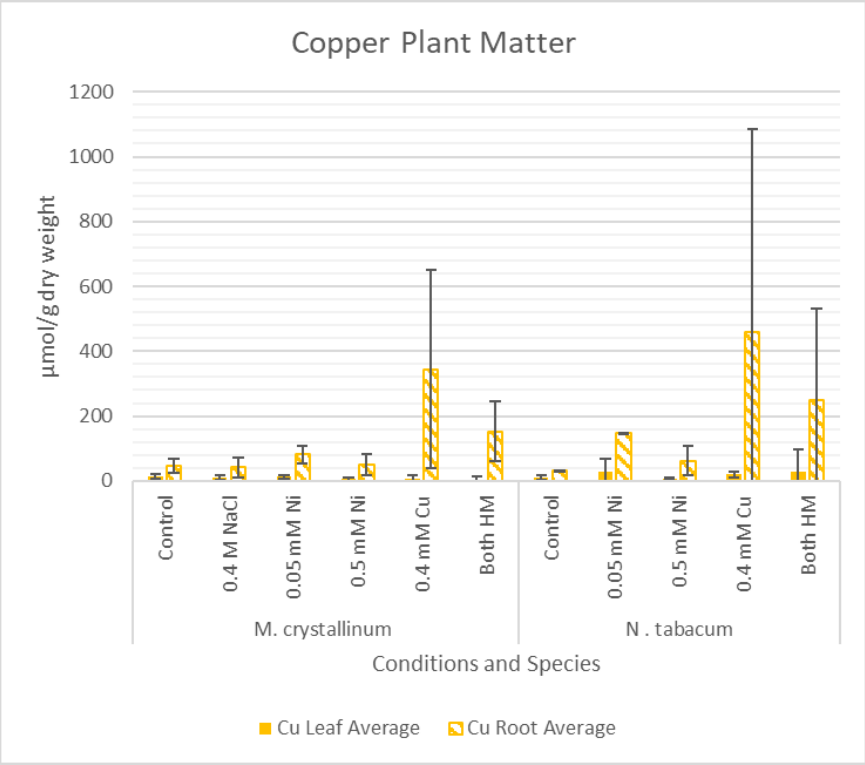

Figure 15: Copper plant matter content

3.2.3 Magnesium Plant Matter

N. tabacum leaves had the highest Mg^+ levels in the 0.05 mM Ni^+ stress at 1426.718 µmol/g with the second being Both HM at 1280.059 µmol/g. The lowest Mg^+ levels were observed at 0.5 Ni^+ at 328.61 µmol/g. For roots, the highest concentrations of Mg^+ occurred following 0.5 mM Ni^+ at 930.553 µmol/g, and the second highest was from the Control group at 844.338 µmol/g. Between the 0.05 mM - 0.5 mM Ni groups, more Mg^+ accumulated in roots from 581.905 µmol/g to 930.553 µmol/g respectively.

M. crystallinum leaf values were lower than *N. tabacum* and peaked at 550.03 µmol/g at 0.4 M NaCl. Mg^+ decreased slightly with both Ni^+ stress from 284.5 µmol/g at control, 225.1 µmol/g at 0.05 mM Ni^+, and 105.0 µmol/g at 0.5 mM Ni^+, the lowest of the averages. Control

had 402.3 µmol/g leaf, and 284.52 µmol/g root, 0.4 M NaCl group had 550.03 leaf content, and 149.95 µmol/g root, 0.05 mM Ni^{+} had 231.14 µmol/g leaf, and 225.14 µmol/g root, 0.5 mM Ni^{+} group had 55.751/g leaf and 105.04 µmol/g root, 0.4 mM Cu^{+} group had 168.696 µmol/g leaf and 212.140 µmol/g root, and Both HMs had 102.831 µmol/g leaf and 38.724 µmol/g root.

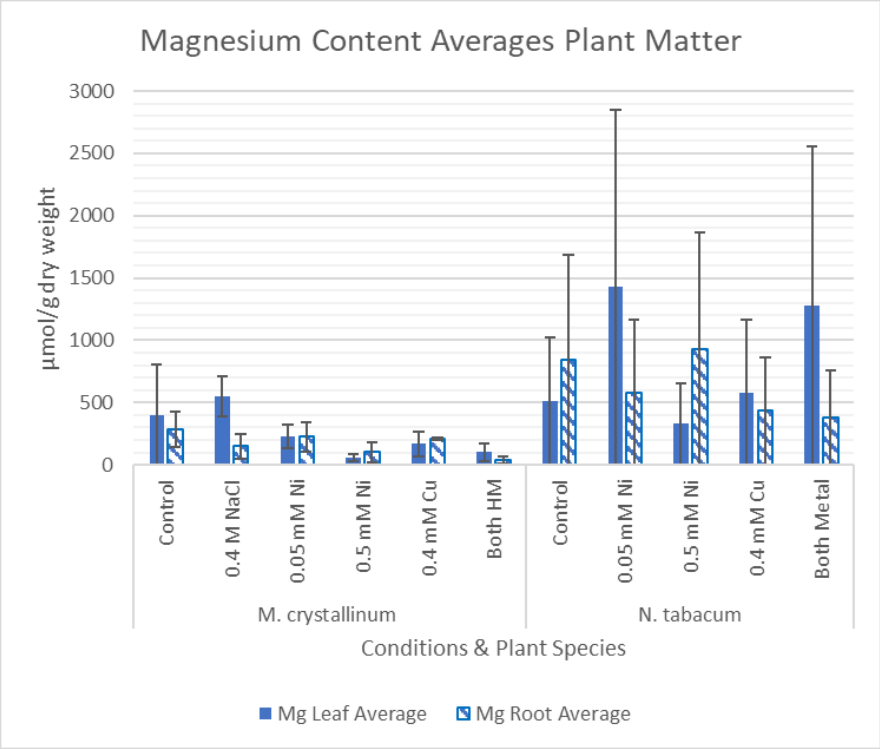

Figure 16: Magnesium plant matter content

3.2.4 Iron Plant Matter

N. tabacum: Control Leaves had 25.001 µmol/g and roots at 74.428 µmol/g of iron. Maximum levels were observed in leaves of Both HMs at 55.978 µmol/g, and the lowest levels were in 0.05 mM Ni^{+} at 6.081 µmol/g. In roots, the maximum sequestration occurred in 0.5 mM Ni^{+} stress at 154.618 µmol/g, lowest at the Control group at 74.428 µmol/g.

M. crystallinum: The control group had 57.528 µmol/g leaf content and 55.34 µmol/g root content. For the 0.05 mM Ni^{+} stress treatment, Fe^{+2} accumulation was at 35.07 µmol/g leaf content, and 92.11 µmol/g root content. In comparison the higher stressed 0.5 mM Ni^{+} group

contained 9.097 µmol/g in leaves and 86.27 µmol/g in roots. Low levels of iron were observed in the 0.4 mM Cu^+ stressed group (18.89 µmol/g leaf content, and 63.16 µmol/g root content) and both HMs group, storing 20.23 µmol/g in leaves and 15.13 µmol/g in roots.

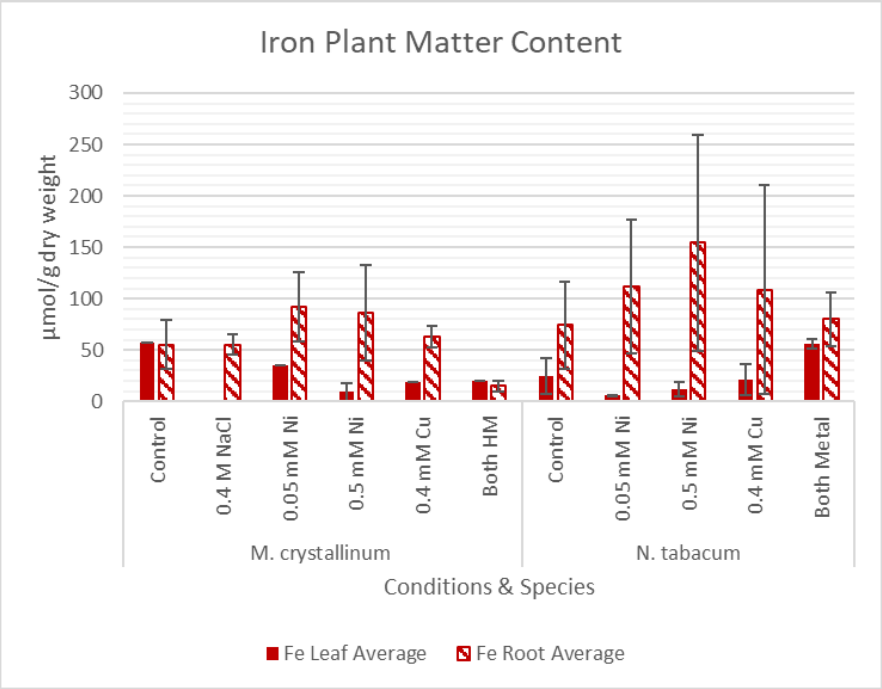

Figure 17: Iron plant matter content.

3.2.5 Manganese Plant Matter

M. crystallinum: Maximum manganese content of leaves is at Both HMs at 40.520 µmol/g, and the minimum is at 0.5 mM Ni^+ at 3.460 µmol/g. In the roots, Manganese was below detection limits at both 0.4 mM Cu^+ and Both HMs. The lowest recorded reading was from 0.4 M NaCl at 1.676 µmol/g while the maximum root reading is of 0.5 mM at 26.09 µmol/g.

In *N. tabacum* the highest reading of the leave content of manganese was at 9.705 µmol/g at 0.05 mM Ni^+, and the lowest was from 0.4 mM Cu^+ at 2.757 µmol/g. In the roots, the Control group has the highest content average of 23.297 µmol/g, while the lowest is from Both HMs at 3.136 µmol/g.

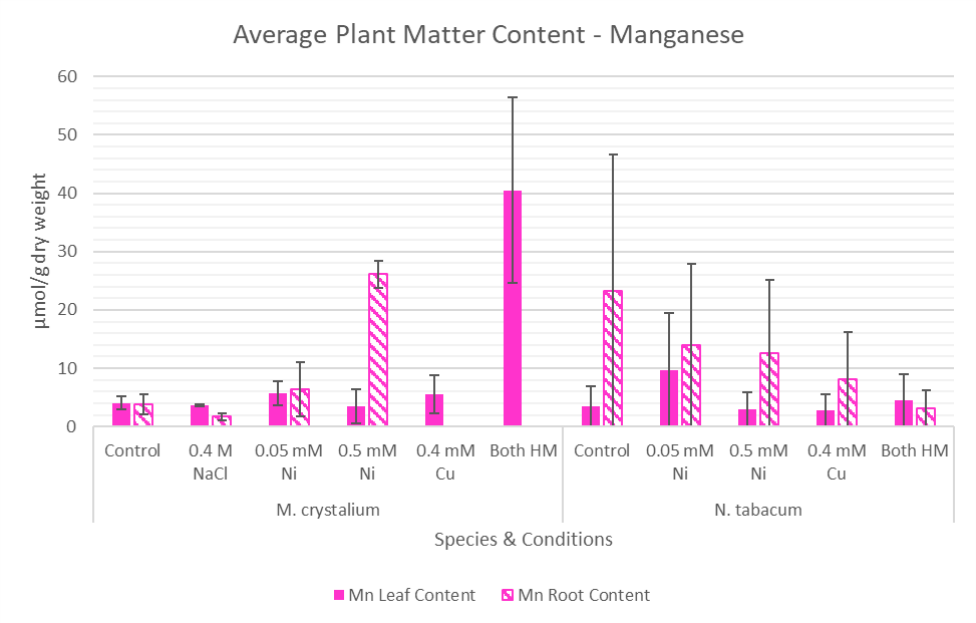

Figure 18: Manganese plant matter content.

3.2.6 Zinc Plant Matter

M. crystallinum: Content in *M. crystallinum* follows a consistent trend in the leaves. The maximum average of zinc content in the leaves is from 0.05 mM Ni at 122.817 µmol/g, while the second highest average is from 0.5 mM Ni at 59.364 µmol/g. The averages from the other groups are around the latter value average except for Both HMs at 17.047 µmol/g. In the roots the averages have a non-linear trend: The Control roots' zinc content is 204.947 µmol/g, 0.4 M NaCl at 95.152 µmol/g, the highest is of 0.05 mM Ni^+ at 297.756 µmol/g, 0.5 mM Ni at 142.724 µmol/g, 0.4 mM Cu at 90.346 µmol/g and the lowest value is from Both HMs at 65.577 µmol/g.

In *N. tabacum*, the leaves' highest zinc average is from the Both HMs group at 104.079 µmol/g, and the lowest was from 0.4 mM Cu^+ at 83.190 µmol/g, with the other conditions yielding similar values that do not exceed 60 µmol/g. The highest root average is from the 0.5 mM Ni group at 404.194 µmol/g, and the second highest is from the Both HMs group at 184.029

µmol/g. The rest of the root averages are consistent with the conditions compared to those from *M. crystaillinum,* at slightly higher values towards 100 µmol/g.

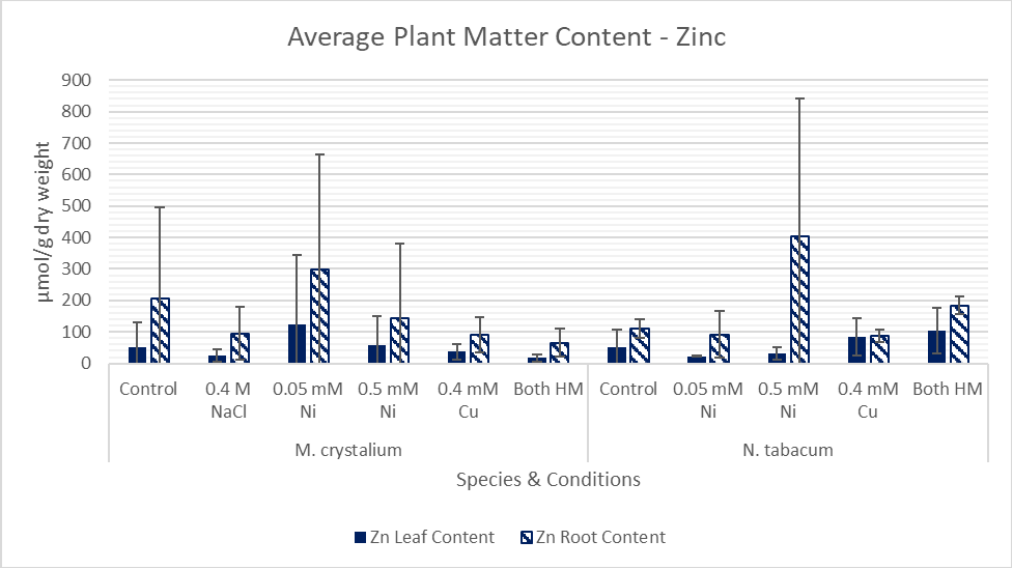

Figure 19: Zinc plant matter content.

3.2.7 Calcium Plant Matter

Calcium in the leaves and roots of *M. crystallinum* were consistently low compared to the calcium content in their *N. tabacum* counterparts. Leaves: Control: 119.62 µmol/g, 0.4 M NaCl: 108.92 µmol/g, 0.05 mM Ni: 87.508 µmol/g, 0.5 mM Ni: 3.636 µmol/g, 0.4 mM Cu: 132.57 µmol/g, Both HMs: 0.8849 µmol/g. Leaves of N. tabacum: Control: 1743.2 µmol/g, 0.05 mM Ni: 447.91 µmol/g, 0.5 mM Ni: 408.61 µmol/g, 0.4 mM Cu: 1393.64 µmol/g, and Both HMs: 3446.05 µmol/g. Roots followed a similar trend between the plant specimens. The root averages in *M. crystallinum* are 100.10 µmol/g in Control, 81.64 µmol/g in 0.4 M NaCl, 174.40 µmol/g in 0.05 mM Ni, 135.06 µmol/g at 0.5 mM Ni, 226.25 µmol/g at 0.4 mM Cu, and 6.15 µmol/g at Both HMs. The root averages of *N. tabacum* exceed the ranges of *M. crystallinum*: Control at 1734.88 µmol/g, 0.05 mM Ni at 1562.04 µmol/g, 0.5 mM Ni at 8688.86 µmol/g, 0.4 mM Cu at 1344.15 µmol/g, and Both HMs at 2032.45 µmol/g.

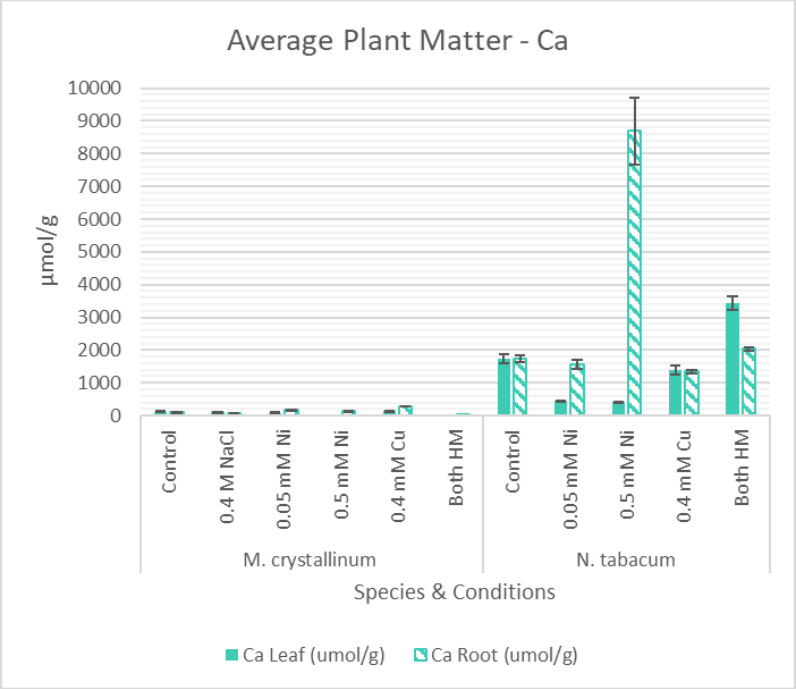

Figure 20: Calcium in plant matter.

3.3 Efflux ICP Results

3.3.1 Time Course Efflux

Non-stressed and nickel stressed plants had similar efflux rates at 20 minutes. While the efflux may not stay linear over time, the side experiment confirmed there's no bias efflux over the time of 20 minutes. While more study of the effectiveness of water dilution on sequestered heavy metal ions is required for confirmation, these experiments indicate that with the first thirty minutes, plants will efflux metal ions following nickel metal stress in a linear fashion (Figure 12).

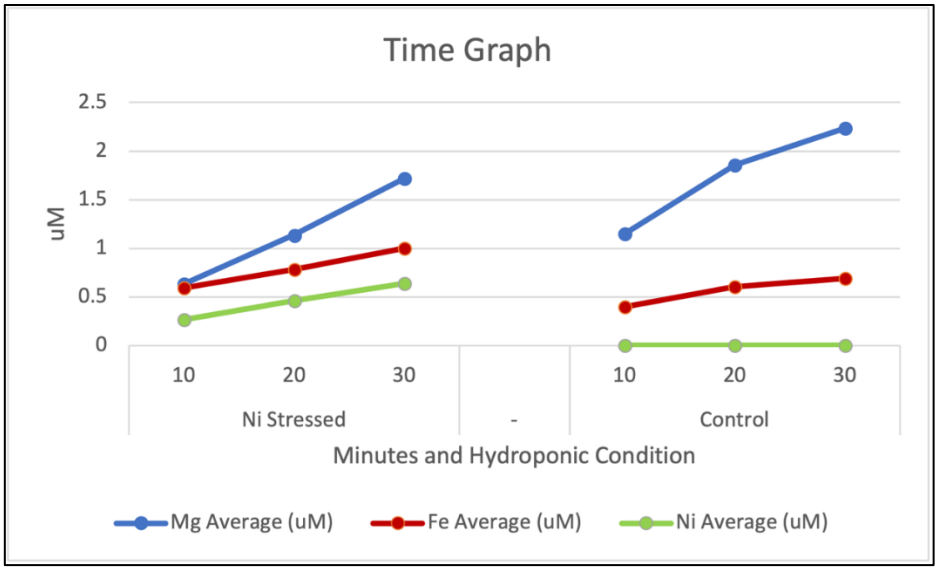

Figure 21: Mg+, Fe+, and Ni+ Efflux Time course in M. crystallinum.

3.3.2 Nickel Efflux

Nickel content in *N. tabacum* efflux was observed as: 0.007470 µM from control, 0.9172 µM from 0.05 mM Ni^+ stressed treatment (123x more than control), 4.189 µM from the 0.5 mM Ni^+ treatment (560x more than control), 0.004606 µM from 0.4 mM Cu^+ (0.6166x vs control), and 2.969 µM from both HMs (397.46x vs control).

Plants that were not stressed by nickel had trace efflux of nickel: control at 0.00861 µM, 0.4 M NaCl at 0.00293 µM, and 0.4 mM Cu^+ at 0.00444 µM. The efflux of nickel was largely seen in nickel stressed plants. In comparison to control, plants from the 0.05 mM Ni^+ treatment were 0.2416 µM (28x over control), 1.456 µM at 0.5 mM Ni^+ (169x over control), and 1.843 µM at both HMs (214x over control).

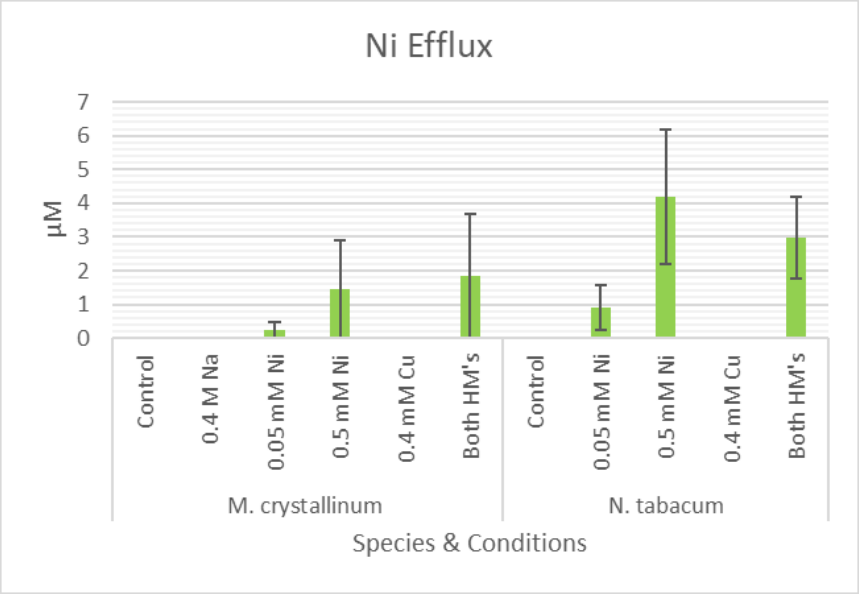

Figure 22: Nickel efflux averages.

3.3.3 Copper Efflux

Copper content in each of the treatments in *N. tabacum* plants followed an increase from control plants (0.2609 µM Cu^{+}) to 0.3809 µM at 0.05 Ni^{+} treatment (1.46 x folds control), to 0.5350 µM following 0.5 Ni^{+} stress (2.05x), 4.907 µM with 0.4 Cu^{+} mM treated plants (18.81x) and then a slight drop to 4.399 µM Cu^{+} in both HMs stress (16.86x).

M. crystallinum: Copper efflux levels were similar in plants under no copper stress. Copper efflux averages supporting this idea were Control with 0.4789 µM, 0.4 M NaCl with 0.8127 µM, 0.05 mM Ni^{+} with 0.4491 µM, and 0.5 mM Ni^{+} with 0.5848 µM. Copper levels in efflux solution increased significantly with copper stress as the 0.4 mM Cu^{+} average was at 4.152 µM (9x control), and that of both HMs were at 2.956 µM (6x control).

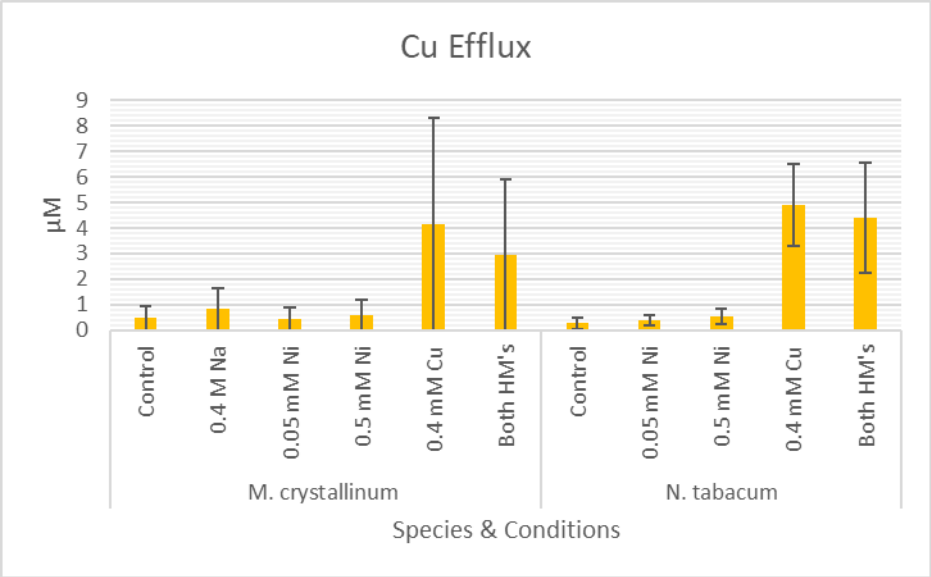

Figure 23: Copper efflux averages.

3.3.4 Magnesium Efflux

For *N. tabacum* Mg^{+} control efflux was at 1.148 µM at control, 6.102 µM at 0.05 mM Ni^{+} (5.135x), 3.825 µM at 0.5 mM (3.33x), 2.373 µM at 0.4 mM Cu^{+} (2.067x), and 2.620 µM at Both HMs (2.28x). Mg^{+} was effluxed at maximum of 6.1024 µM at 0.05 mM Ni^{+} (5.3 x), and the second highest was at 0.5 mM Ni^{+} at 3.8246 µM (3.3x).

M. crystallinum: Mg^{+} efflux was maximum at 1.395 µM at Control, 0.74229 µM at 0.4 M NaCl (x0.5321), the second highest was at 1.104 µM at 0.05 mM Ni^{+} (0.7914x). Second lowest at 0.5 mM Ni^{+} at 0.6768 µM (0.485x), and lowest at both HMs at 0.6463 µM (0.463x).

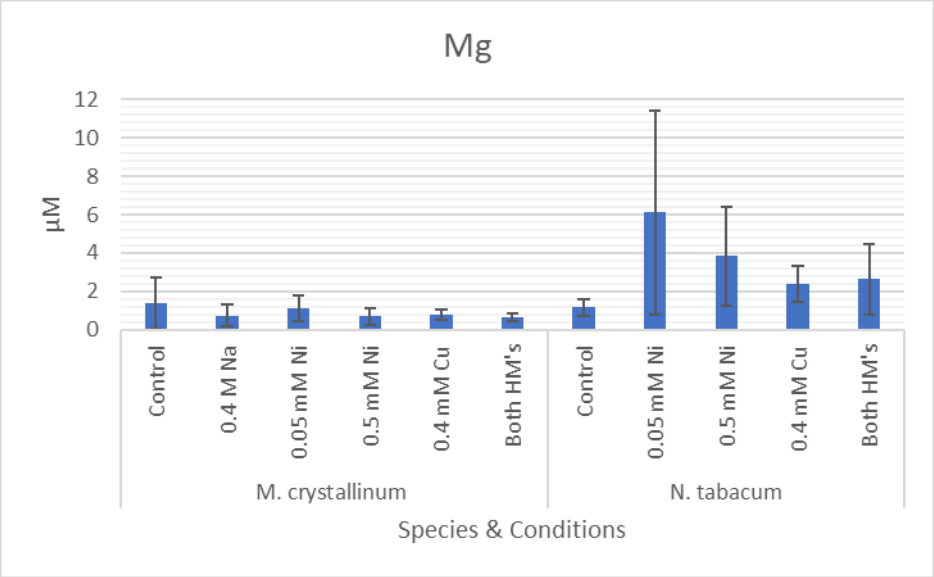

Figure 24: Magnesium efflux averages.

3.3.5 Iron Efflux

N. tabacum: Control efflux was at 0.1812 µM, 0.09413 µM at 0.05 mM Ni^+ (0.5195x), with 0.2613 µM (1.442x) at 0.5 µM Ni^+. Lowest at 0.4 mM Cu^+ at 0.04899 µM (0.27x), and both HMs at 0.06564 µM (0.3622x).

M. crystallinum Fe^+ efflux maximum was 0.0587 µM at control, 0.0688 at 0.4 M NaCl (1.172x), 0.05860 µM at 0.05 mM Ni^+ (0.998x), 0.1246 µM at 0.5 mM Ni^+ (2.123x), while a minimum found at 0.4 Cu^+ at 0.02602 µM (0.44x) and both HMs at 0.02799 µM (0.477x).

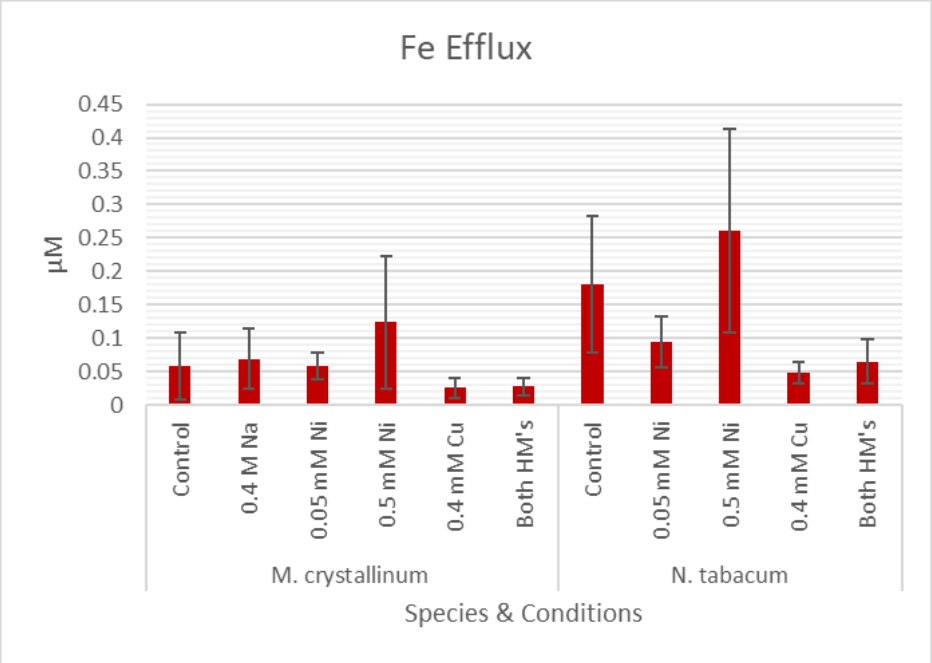

Figure 25: Iron efflux averages.

3.3.6 Manganese Efflux

The highest manganese efflux value of *M. crystallinum* is from Control group at 0.0150 µM Ni^{+}, and the lowest was from 0.5 mM Ni^{+} at 0.00485 µM. The highest of *N. tabacum* was from the 0.5 mM Ni group at 0.0805 µM, while the lowest is from the Control group at 0.0144 µM. Efflux decreased again at the 0.4 mM Cu and Both HM groups at 0.0475 µM, and 0.0367 µM respectively.

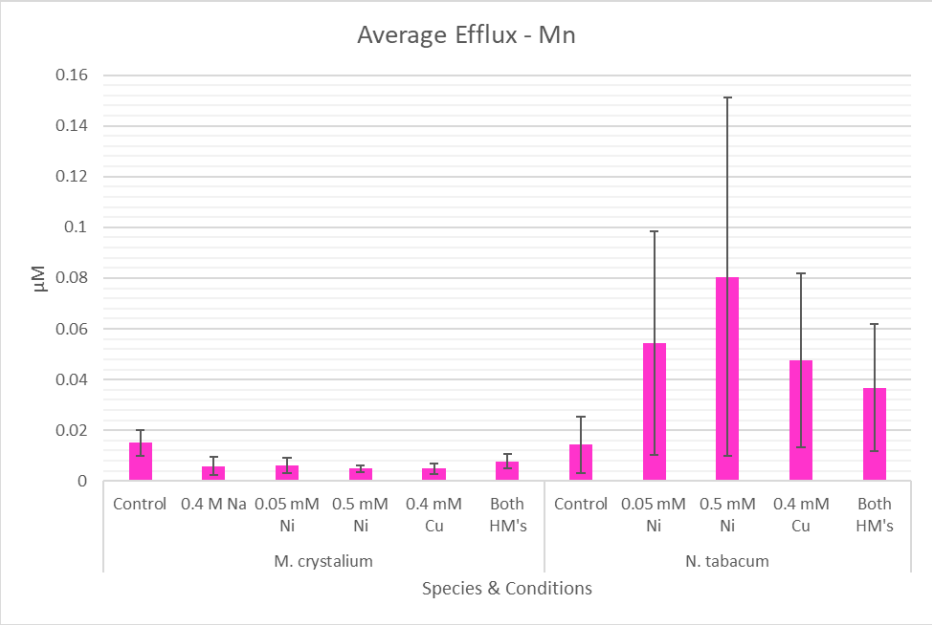

Figure 26: Manganese efflux averages.

3.3.7 Zinc Efflux

The highest of *M. crystallinum* is from the Control group at 0.05961 µM and decreases with additional stress, with the lowest value from the 0.4 mM Cu^{+} group at 0.01568 µM, and the second lowest from Both HMs at 0.01977 µM. *N. tabacum* was the inverse which had zinc efflux increase with stress. The highest average was from 0.4 Cu^{+} mM at 0.1196 µM, with 0.5 mM Ni the second highest at 0.1074 µM. The lowest is from the Control group at 0.0857 µM with the second lowest being 0.05 mM Ni at 0.08925 µM.

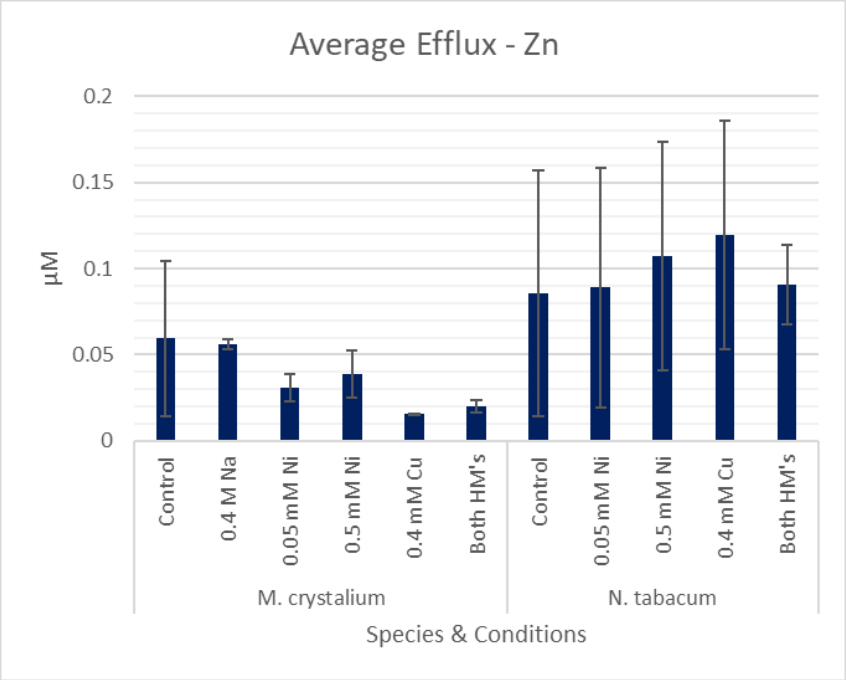

Figure 27: Zinc efflux averages

3.3.8 Na^+/K^+/ Ca^{++} Efflux

The average Na^+ efflux at 0.4 M NaCl *M. crystallinum* was 1.147 mM. The efflux of Na^+ was around below µM otherwise in *M. crystallinum*: Control was 0.9127, 0.05 mM Ni^+ at 1.659, 0.5 mM Ni^+ at 1.213, 0.4 mM Cu^+ at 1.846, and Both HMs at 1.7916. *N. tabacum* had similar low efflux readings: Control at 3.259 µM, 0.05 mM Ni^+ at 1.735 µM, 0.5 mM Ni^+ at 3.335 µM, 0.4 mM Cu^+ at 2.540 µM, and Both HMs at 1.724 µM.

The average K efflux of *M. crystallinum* was 2.943 µM at Control group, 3.992 µM at 0.4 mM Na^+, 1.879 µM at 0.05 mM Ni^+, 1.147 µM at 0.5 mM Ni^+, 1.928 µM at 0.4 mM Cu^+, and 0.8208 at both HMs. Average efflux of *N. tabacum* had higher values with Control efflux at 25.057 µM, 0.05 mM Ni^+ at 36.54 µM, 0.5 mM Ni^+ at 32.844 µM, 0.4 mM Cu^+ at 13.136 µM, and Both HMs at 15.172 µM.

Average Ca^{+2} efflux remained consistent below 1 µM throughout both species and all conditions except for *N tabacum* at 0.05 mM Ni^+ which effluxed 1.7904 µM.

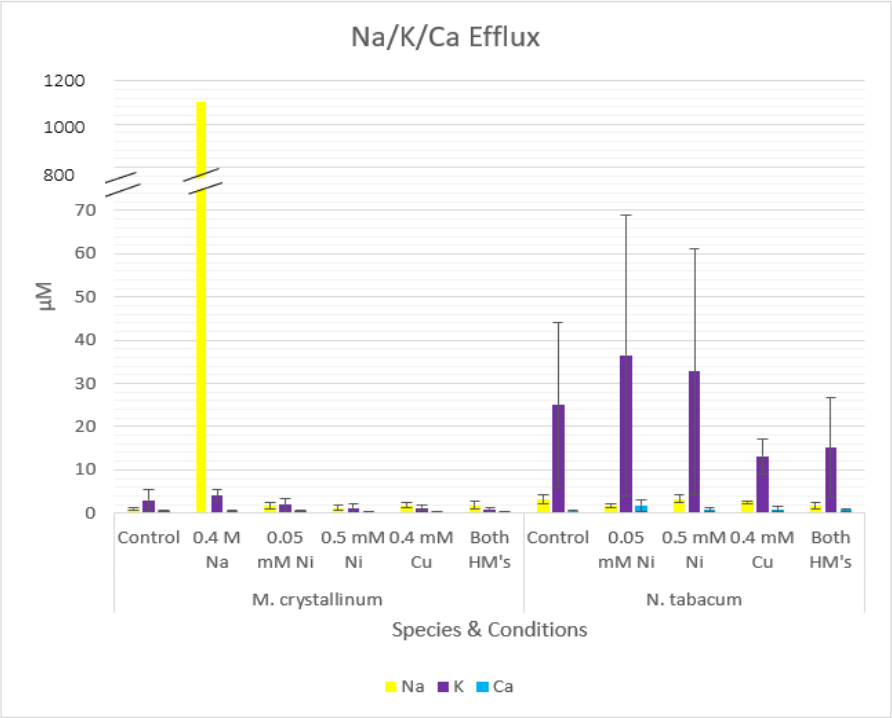

Figure 28: Efflux averages of $Na^{+}/K^{+}/Ca^{+2}$ (Dashes represents graph break).

3.4 MDA (Lipid Peroxidation) Results

3.4.1 M. crystallinum

The lowest MDA average of ice plants' leaves was 0.4 M NaCl hydroponic treatment was 6.3825. Close by, the second lowest MDA value was from the hydroponic control: 9.501 nmol/g*mL. The third lowest MDA activity was seen in the 0.05 mM Ni^{+} hydroponic treatment; 12.612 nmol/g*mL. However, the highest MDA was seen in plants in the Both HMs category at 69.459 nmol/g*mL, the second highest is 0.5 mM Ni^{+} at 66.426 nmol/g*mL and the third highest is 0.4 mM Cu^{+} at 18.192 nmol/g*mL.

Regarding roots, the MDA average of Control was the lowest, at 2.4153 nmol/g*mL. Similarly, the Both HMs treatment (2.7511 nmol/g*mL), the 0.4 mM Cu^{+} treatment (2.9113 nmol/g*mL), the 0.05 mM Ni^{+} stress (3.3653 nmol/g*mL), the 0.4 M Cu^{+} treatment at 4.2454 nmol/g*mL, and finally 0.05 mM Ni^{+} at 5.6890 nmol/g*mL.

3.4.2 N. tabacum

The lowest MDA average of all samples were found in leave of the control *N. tabacum* plants with a value of 7.4059 nmol/g*mL. The highest average of leaves is the both HM plants at 21.73 nmol/g*mL and has a control factor value of 3.18 with the others less than 2.0.

The lowest root average is 0.5 mM Ni^+ at 1.5224 nmol/g*mL The highest root average in both HMs is 19.279 nmol/g*mL, with a control factor of 7.4404 while the others are no larger than 2.0.

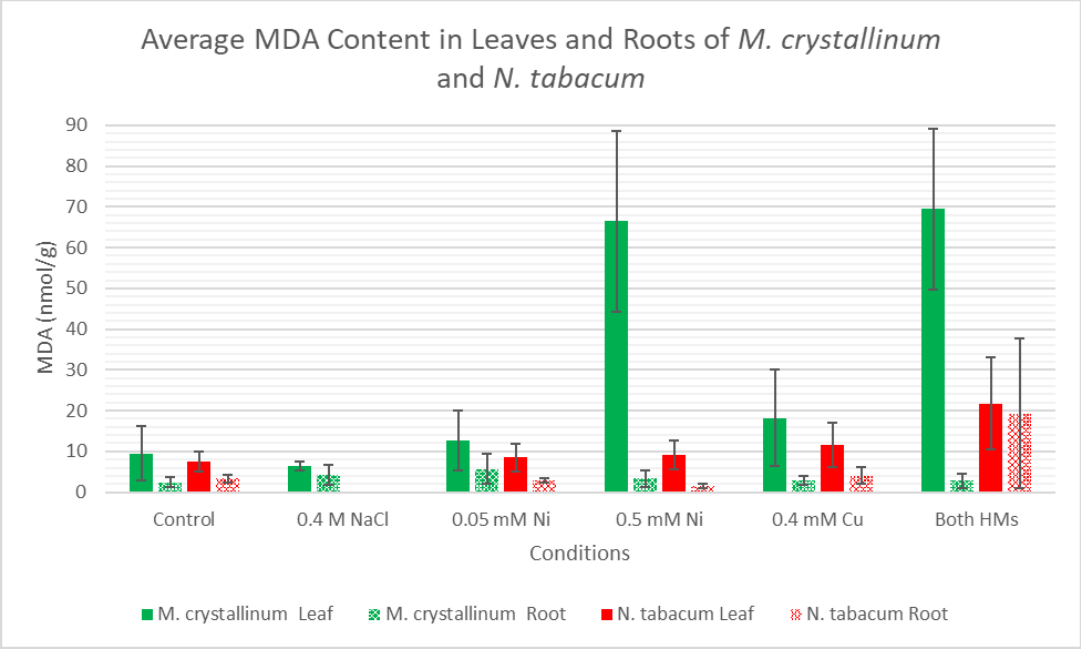

Figure 29: MDA in N. tabacum and M. crystallinum roots and leaves.

3.4.3 Leaf/Root MDA Ratio

The largest *N. tabacum* MDA Leaf/Root ratio is from the 0.5 mM Ni^+ group at 7.5637. *M. crystallinum* also has the 0.5 mM Ni^+ group yielding the highest Leaf/Root MDA ratio at 48.141. The lowest from *M. crystallinum* ratio is from 0.05 mM Ni^+ at 2.834, while the lowest ratio from *N. tabacum* is the Control group at 2.548.

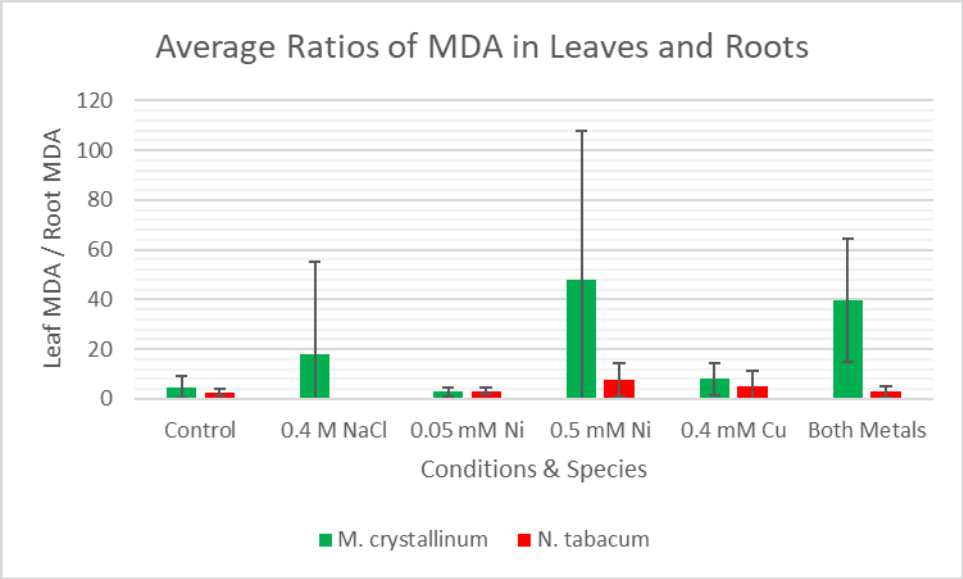

Figure 30: MDA leaf/root ratios.

Chapter 4 Discussion

4.1 Plant Health and Nickel Stress

Nickel affected both *N. tabacum* and *M. crystallinum* during each of the nickel-laden conditions. The analyses of MDA verified that the lower nickel stress condition of 0.05 mM Ni did not lead to large levels of oxidative stress in either species. 0.05 mM Ni conditions had minor effects on the *N. tabacum*, in which they had lost some turgor, as seen in Figure 12, while the *M. crystallinum* had minimal visible symptoms. However, the 0.5 mM nickel stress led to large levels of MDA produced in the *M. crystallinum* leaves but not *N. tabacum*'s leaves. At 0.5 mM Ni, the *N. tabacum* plants begun to have their leaves droop over the stems with a few dead leaves but otherwise retained their color (Figure 13), while the *M. crystallinum* at 0.5 mM Ni and Both HMs lost all turgidity and turned yellow from the loss of chlorophyll. At 0.4 mM Cu, the *N. tabacum* plants showed turgor loss like 0.05 mM Ni *N. tabacum* specimens, but also have discolored bottommost leaves, which is shared by their *M. crystallinum* counterparts in the same hydroponic condition (Figures 12 and 13). At Both HMs, the *N. tabacum* plants still have discoloration as a symptom of copper toxicity, while them leaves demonstrated significant wilting when treated with 0.5 mM Ni. The *M. crystallinum* specimens had similar chlorosis and wilting after the two-week nickel stresses.

It is not apparent that *M. crystallinum* is more resistant to nickel compared to *N. tabacum* in these experiments, but the halophyte accumulated more nickel in the leaves during stress. In the 0.5 mM Ni^{+} and Both HM groups, the nickel content within the leaves was roughly equal to

half of the nickel content stored within roots (Figure 14). This may be due to the bladder cells of *M. crystallinum* which were documented to store excess metal ions (Adams et al., 1992). The Leaf/Root MDA ratios indicate higher translocation of metal ions of leaves in *M. crystallinum* which prevented the roots from being excessively stressed at Both HMs despite the leaves' MDA levels, unlike *N. tabacum,* at which the roots' MDA readings increased. Previous studies had only used one week of stress in 0.05 mM Ni^{+} and found some decline in plant mass with higher doses inducing necrotic spots (Amari et al., 2014; 2016). While there are differences in stress duration amongst these two species used here, there was no advantage the *M. crystallinum* over *N. tabacum* when stressed with nickel. It is acknowledged that the stress duration for *M. crystallinum* was two weeks, while *N. tabacum* was only one week. This difference in stress duration was supported by a study that indicated the *M. crystallinum* was tolerant to nickel (Amari et al., 2014; 2016), and that in pilot experiments, leaf necrosis following nickel stress was observed *M. crystallinum* two weeks, while the *N. tabacum* plants displayed necrosis after one week of nickel stress.

4.2 Metal Sequestration in Unstressed and Stressed Plants

4.2.1 Unstressed Metal Accumulation in Plants

Once mineral-based metals are absorbed by roots, the metals pass in either apoplastic (extracellular) and/or symplastic (intracellular) pathways (Figure 3), later loaded into the xylem for transport to the shoot (White & Brown, 2010: Page & Feller, 2015). All cytotoxic cations are transported through the apoplast or through the symplast in a chelated form. Metals including Zn^{+}, Ni^{+}, Cu^{+}, Fe^{2+}, etc. are delivered to the apical tissues via metal complexes with asparagine, histidine, organic acids and/or nicotinamide (Guerinot 2000; Gupta 2016). Many studies focused on the subsequent distribution and levels of metals within plants, including nickel in various

plants tissues (Meshra, & Kar 1974; Ahmad, & Ashraf, 2011; Ishfa et al., 2020). To summarize, a generally accepted format for normal metal sequestration, Figure 5 represents the measurement of several metal isotopes and their relative sites of accumulation under non-stressed conditions (Page & Feller, 2015). Roots contained the largest repository of metals in *Arabidopsis* (Page & Feller, 2015). Likewise, Zn^{+} and Ni^{+} accumulated in source leaves, while Cd^{+}, Mn^{+}, Fe^{2+}, and Cd^{+} in sink leaves (Page & Feller, 2015).

Our results of metal accumulation in non-stressed plants largely verifies previous reports including Page & Feller (2018). In both *N. tabacum* and the *M. crystallinum*, root accumulation outcompeted leaf deposition for Zn^{+}, Cd^{+}, Fe^{+}, Mn^{+}, Mg^{+}, and Co^{+}. In one example, Zn^{+} was accumulated largely in root tissues with very little Zn^{+} found in leaves of either species (Figure 20). While sink and source leaves were not subdivided in this study, the two species of plants appeared quite similar for control levels of Cu^{+}, Fe^{2+}, Mn^{+}, Mg^{+}, Zn^{+} and Ca^{2+} in unstressed growing conditions (Figures 14 – 20). For comparison, Na^{+} is sequestered in high levels in the leaf bladder cells in leaves (Barkla et al., 2016), where we found rapid Na^{+} exudation from *M. crystallinum* in response to stress alleviation (Figure 29, 30).

4.2.2 Nickel Stress and Subsequent Nickel Accumulation

It has been known for some time that the uptake of many micronutrients (excluding calcium) is reduced with nickel in the growth media (Crooke & Inkson, 1955). Our studies examined this suggestion and found that upon nickel stress at low levels (0.05 mM Ni^{+}), sequestration was largely identical in both *M. crystallinum* and *N. tabacum* (Figure 14). In their comparison of nickel uptake in shoots and roots, Amari (et al., 2016) found nearly twice as much nickel in the *M. crystallinum* shoots compared to *B. juncea* after a 0.2 mM $NiCl_2$ stress for 3 months; the authors concluded that the *M. crystallinum* species are nickel "tolerant." On the

contrary, our study cannot confirm a significant degree of tolerance, as both *N. tabacum* and the *M. crystallinum* suffered widespread chlorosis at 0.05 mM and 0.5 mM $NiCl_2$ (Figure 12- *N. tabacum* 1 week stress, and Figure 13- *M. crystallinum* 2-week stress). In the 0.05 mM to 0.5 mM Ni^+ treatments, 2-4 times more nickel was accumulated in near equivalent levels in the roots of both *N. tabacum* and *M. crystallinum* (Figure 14). While tolerance may be a temporary feature of survival in a nickel inundated environment, it is likely that antioxidants, sugar alcohols like pinitol, and structural features like bladder cells and metal sequestration may simply provide some low level of tolerance to plants in soils (in which metal dosage is influenced by soil component-metal adhesion). Addressing nickel treatment, toxicity was predicted due to its ability to displace more useful nutrients such as magnesium (Webb, 1970). In contrast, Fenton reactions, and Ni-mediated free radical production also can explain the chlorosis and resulting plant tissue damage (Hong et al., 1997). This experiment used hydroponic cultures, while Amari's (et al., 2014; 2016) studies used soil in which the clays and other soil materials have an influence on metal's impact on plant biology.

4.2.3 Influence of Nickel Stress on Sequestration of Other Metals

When analyzing other metals following nickel stress, some metals had *nickel independent responses* (Fe^{2+} and Cu^+) while others triggered *species specific responses*. The latter being represented by Mn^+ and Mg^+ in *N. tabacum*, along with Zn^{+2} in the roots of *M. crystallinum*. Our study also confirms previous research in the *M. crystallinum* sequestration of Ca^{2+}. Mg^+, K^+, Fe^+, and Zn^+ in both shoots and roots were not greatly changed between control and 20 mM $NiCl_2$ stress (Amari et al., 2016). Due to the experiments being performed in hydroponic cultures, there is more assurance of the available nickel dosage control, free of occluding clays and organic materials that can make ions lose bioavailability in soils. The hydroponic conditions

have also provided the plants with a water-laden environment for soluble metals ions to be easily acquired by their roots in contrast to soil in which the analytes may remain insoluble. Both experimental designs are not incompatible, and the exact metal levels in plants may differ depending on the medium.

When comparing the *M. crystallinum* and *N. tabacum* following nickel stress, several cation levels were quite similar in the plant tissues examined (roots and leaves); such as copper (Cu^{+}) and iron (Fe^{2+}) accumulation (Figure 15, Figure 17). This result may be considered a *nickel independent response*, implying differing cellular transport pathways for Ni^{+} Fe^{2+} and Cu^{+} accumulation (with overlap such as with IRT1 transporting both Fe^{2+} and Ni^{+} (Nishida, 2011)). The existing literature indicates unique membrane-bound transporters are responsible for both iron and magnesium including IRT1 and MGT6 respectively (Vert et a., 2002; Yan et al., 2018). Noteworthy, only when 0.4 mM Cu^{+} was added was significant copper accumulation noted above the exclusive nickel treatments, again indicating little if any crosstalk in cation transport. Previous work determined that copper sequestration following copper stress occurred largely in sink (lower and older) leaves of *N. tabacum* (Thomas et al., 2002). Copper and iron ions have a competitive interaction with plant roots in media with excess copper (Yruela, 2005). This may be due to the nickel cation absorption and transfer from root to shoot being inhibited by Cu^{+} (Cataldo et al., 1978). As copper has higher priority than nickel (Cousins, 1994), copper likely outcompeted nickel in the Both HMs solution, which in turn limited iron displacement.

4.3 Species Differences of Counter Ion Efflux

4.3.1 The Influence of Magnesium Low Affinity Cotransporters

Nearly 15–35% of absorbed Mg^{+} by plants is fixed in chlorophyll pigments, with the remainder found in vacuoles or aiding in protein synthesis (at both the transcriptional and

translational levels) (Karley & White, 2009; Stitt & Zeeman, 2012; Ishfa et al., 2022). Only 15% of Mg^{+} is free within plants (Wilkinson et al., 1990). Some of the fixed Mg^{+} makes up over three hundred enzymes use Mg^{+} as a cofactor (Peng et al., 2015; Chen et al., 2018). Moreover, oxidative stress protection is also an activity linked with sufficient Mg^{+} levels (Mittler et al., 2002). Negatively impacting the effectiveness of photosynthesis, a deficiency in Mg^{+} may reflect a decline in photosynthetic activity (Tränkner & Jaghdani, 2019).

Taken together, it is plausible that a short-term response in *N. tabacum* to a Ni^{+} confrontation may be a compensatory osmotic balance response to enhance Mg^{+} uptake. Relatedly, Mg^{+} also lowers the substrate-binding of (PEPcase) and reduces CO_2 assimilation in most plants including CAM plants (Zhao et al., 2012; Yang et al., 2019). The resultant Mg^{+} enhanced uptake in response to Ni^{+} stress could be represented by a shared low affinity transporter, as predicted by Webb (1970). One family of transporters meeting this requirement are the magnesium transporters (or MGT-type transporters) which can transport diverse cations such as $Ca2^{+}$, Fe^{2+}, Mn^{+}, and Zn^{+} (Li et al., 2001; Mao et al., 2008), apart from MGT6 isoform (Yan et al., 2018).

Significantly, the Mg^{+} sequestration results in this study deviated between *N. tabacum* and *M. crystallinum*. Most notably, *N. tabacum* leaves accumulated nearly three-fold more Mg^{+} compared to controls, and nearly one-fold increase more in root tissues, unlike those of no major difference in accumulation compared to controls in the *M. crystallinum* (Figure 16). Most magnesium in higher plants is transported into the vacuole (Gao et al., 2015). When comparing the relative oxidation using MDA determination, *N. tabacum* was subjected to less oxidative stress than their *M. crystallinum* counterparts, underlying the reciprocal relationship of stress and enhanced Mg^{+} sequestration under nickel stress (Figures 16, 29 and 30). In our experiments, we

conclude *N. tabacum* used additional Mg^{+} to offset Ni^{+}-mediated stress, a significant challenge for plants under a variety of stress regiments, notably including Ni^{+} (Mittler et al., 2002; Fernández et al., 2015)

A revealing deviation in response to nickel stress may also be represented as a species-specific response to nickel by influencing Zn^{+} sequestration. The unique role of Mg^{+} import during Ni^{+} stress discussed above for *N. tabacum* is simply not applicable to the *M. crystallinum* (Figure 16). On the contrary, only the *M. crystallinum* deposited 4-fold of Zn^{+} in tissues following exposure to nickel (Figure 19). Some have proposed a low affinity Mg^{+} transporter may be shared by Zn^{+}, Ni^{+} and perhaps other metals, and their selectivity may block Ni^{+} import, which alleviates nickel–induced stress (Webb, 1970; Proctor & McGowan, 1976). Zn^{+}, and Ni^{+} share a similar place regarding plant homeostasis and toxicity as the zinc hyperaccumulator *T. caerulescens* which has been documented to also accumulate nickel and cadmium without any detrimental symptoms (Van de Mortel et al., 2006). It is true that besides the unique features of zinc hyperaccumulators, typical plant transporters for zinc include ZIP1-ZIP6, ZIP9, ZIP10, ZIP12 and IRT3 (Guerinot, 2000; Van de Mortel et al., 2006; Talke et al., 2006). Modulation of Zn^{+} uptake from rhizosphere was greatly influenced by several divalent cations including Fe^{2+}, Cd^{+}, Ni^{+}, Cu^{+}, all competing with Zn^{+} for the same ligand binding site in phytosiderophores and the transporter protein IRT1 (Vert et al., 2002; Gupta et al., 2016). Thus, to compete with Ni^{+} stress, the *M. crystallinum* imports Zn^{+} while *N. tabacum* uses Mg^{+}. One consequence of *M. crystallinum* co-sequestering of copper (versus magnesium as in *N. tabacum*) in response to nickel stress is that both copper and nickel are Fenton metals, enhancing free radical production in *M. crystallinum*; reflected in enhanced MDA results (Figure 29, 30).

M. crystallinum was found to transcribe a germin-like protein in the roots (Michalowski & Bohnert, 1992). Germin is an apoplastic manganese-containing oxalate oxidase utilized for stress defense; it's speculated to have superoxide dismutase activities which lends to the elimination of ROS (Woo et al., 2000). The mRNA expression is abundant in unstressed roots, but it decreases after three days of salt stress, which indicates either a reaction to reduced water availability, or to reduce ROS as a defensive protein (Michalowski & Bohnert, 1992). It is possible that *M. crystallinum* retains manganese during nickel stress for maintaining germin activity (Figure 18).

4.3.2 Other Cations That Accompany Mg^+ Import During Ni^+ Stress

Mn^+ only greatly accumulated in the *M. crystallinum* in response to copper stress (0.4 mM Cu^+ and Both HMs groups), and triggered leaf sequestration in the *M. crystallinum* (a 20-fold enhancement over controls). *N. tabacum*, increasing its import of Mg^+, was shown to decline in sequestered metals as nickel dosage increased. Mn^+ efflux increased in nickel stress plants while in plant matter, it decreased. (Figure 18). Zn^+ and Mn^+ efflux levels have a similar pattern with each other which was likely due to the two ions sharing the same family of Zip and Znt transporter proteins (Fukada, 2011).

Surprisingly Ca^{2+} accumulation in *N. tabacum* was quite prevalent, however no calcium changes were observed following nickel stress in the *M. crystallinum* (Figure 20). Calcium plant content decreased with nickel stress in the leaves, while calcium increased in the roots which is more apparent in *N. tabacum.* This was presumably due to the two-week stress period rather than the one-week period of *N. tabacum*. As calcium is responsible for secondary stress signals (Jalmi, 2018), when it was outcompeted by nickel, the plant was vulnerable to the unchecked heavy metal stress.

It is generally understood that high cytoplasmic Ca^{2+} levels in the cytoplasm are often rare, where most are sequestered inside the endoplasmic reticulum (Alberts et al., 2015). While links between Ca^{2+} signal transduction and metal stress have been asserted (Jalmi, 2018), specific sources of calcium elevation have implicated a germin-like protein upregulation during salt stress (Michalowski & Bohnert, 1992). Because most plant germins have oxalic acid oxidase activity, liberating free calcium from oxalic acids to permit signaling of stress events is a logical response to stress (Bernier & Berna, 2001). However, at the scale of detection in our experiments little Ca^{2+} responsiveness to nickel stress was observed in the *M. crystallinum* (Figure 20). In the case of *N. tabacum*, Ca^{2+} responsiveness to stresses such as nickel indicated a decline of sequestration of Ca^{2+}, principally in roots. It remains unclear if this is a nickel independent response, or one which in *N. tabacum* may be connected to the concurrent enhancement of Mg^{+} uptake mentioned above.

We conclude that *N. tabacum* responds to nickel stress by accumulating more Mg^{+} (in response to osmotic and or ROS), while lowering Ni^{+} uptake. In contrast, *M. crystallinum* selectively imports Zn^{+} (likely via an IRT transporter), to counterbalance Ni^{+} enhanced osmotic stress (Figures 19). This strategy synergistically triggers ROS stress, as seen in the enhanced MDA results (Figures 29 & 30), thereby influencing membrane stability integrity. The enhanced lipid peroxidation (malondialdehyde-MDA activity) observed in the *M. crystallinum* compared to those of *N. tabacum* importing Mg^{+}, and antagonizing Ni^{2+} import underlines the nickel stress response disparity between *N. tabacum* and the *M. crystallinum* species. Consideration of plant age may be an important variable to re-examine with respect to nickel stress in the future because *M. crystallinum* switches a typical C3 to CAM profile at 6-8 weeks when grown a hydroponic solution as described (Höfner et. Al., 1987).

4.4 Efflux of Sequestered Metals in Unstressed and Stressed Plants

4.4.1 Nickel Efflux Studies

To first establish the general trend of plant efflux post nickel stress, a pilot experiment (three replicated) was performed with control and 0.05 mM nickel-treated plants. As described in the Results as well as in Figure 12, efflux of nickel, iron and magnesium increased in a relatively linear fashion over 30 minutes. It was determined that a 20-minute stress duration was acceptable to compare various metal ions moving from the plant to the efflux fluid (water). Furthermore, nickel stress resulted in nickel sequestration largely partitioned in roots of both the *M. crystallinum* and *N. tabacum* (Figure 14) while only 0.5 mM nickel stress demonstrated significant nickel efflux in the *M. crystallinum* and *N. tabacum* or in Both HMs (Figure 22). As a result, we can conclude that at least within 20 minutes of nickel stress removal, significant amounts of nickel can re-enter the rhizosphere after significant dilution or inundation event. While no further conclusions regarding nickel off-loading time, or removal of nickel from aerial portions of the plant, there does seem that a water inundation event may indeed assist in plant recovery from nickel stress. The results of nickel uptake and deposition lead to variable efflux of other metals, where plant species differences were noted, as explained below.

4.4.2 Nickel Dependent Efflux

N. tabacum effluxes nickel and magnesium in nickel stress, which are dependent on nickel levels. In contrast *M. crystallinum* had a nickel independent response as the efflux of Mg^+ minimally decreased with the addition of metal stress. *N. tabacum* contained more Mg^+ in the control group than their *M. crystallinum* counterparts in both the leaves and roots, implying that the former species has larger reserves of Mg^+. This would make Mg^+ an ideal choice for the plant

to utilize as an osmatic rebalancer. In *N. tabacum,* there was less magnesium and nickel efflux in addition of copper stress into the growth medium. Copper may share a similar efflux route with magnesium in the two plant species; there was minimal change in the Mg^{+} efflux values from 0.4 Cu^{+} and Both HMs groups.

M. crystallinum had a higher retention of zinc than *N. tabacum* during the efflux procedure. In *N. tabacum* zinc efflux increased in the 0.5 mM Ni^{+} and Both HMs conditions, while *M. crystallinum* decreased with the different stress solutions. The opposite is in effect regarding plant matter, as when *M. crystallinum* was stressed in the 0.05 mM Ni^{+} condition, zinc content in the roots increased from the Control group's average, while *N. tabacum* had minimal zinc content other than the 0.5 mM Ni group. Zinc accumulation increased in *M. crystallinum* roots during 0.05 mM Ni^{+} stress, but at 0.5 mM Ni^{+}, root content of zinc decreased while the efflux became closer to the control's efflux. This indicates that nickel has an influence of zinc efflux, but it's not the deciding factor, which supports the idea of zinc being utilized as a defense against ROS within the roots. Further testing is needed to confirm whether substantial increases in zinc efflux values occur with longer efflux periods.

4.4.3 Nickel Independent Efflux

Iron is usually concentrated in the plants' roots, and considered largely immobile, and the typical leaf's concentration ranging between 50-100 µg/g dry weight (Guerinot & Yi, 1994; Page & Feller, 2015). In both species, Fe^{+2} efflux increased with nickel stress at 0.5 mM Ni in both species, while being more pronounced in *N. tabacum* (Figures 25) but decreased below the control groups' efflux values in the presence of excess copper. In contrast, *N. tabacum* iron levels were largely unchanged by nickel stress (Figure 17). Fe (III) reductase is thought to not only reduce iron chelates as they enter the plant, but also regulates cation uptake, as roots with

iron deficiency was found to have increased cation uptake (Guerinot & Yi, 1994), which likely contributed to the efflux and re-sequestration of ions. Mn^{+} efflux is dependent on Ni^{+} stress in *N. tabacum*, but independent in *M. crystallinum*. Efflux was low throughout each of the conditions in *M. crystallinum* while it accumulated in the roots at 0.5 mM nickel stress and the leaves in Both HMs group (Figure 27). In *N. tabacum,* the majority of Mn^{+} was stored in the roots which decreased with nickel and copper stress, while efflux increased.

Copper efflux was independent in both plants. It only increased substantially in the two media groups with added copper, but otherwise stayed low in the prior conditions. There was a similar pattern with the plant matter of both species. Notably the copper content and efflux were both lower in the Both HMs groups than those from the 0.4 mM Cu^{+} groups. This may be due to nickel and copper's competitive roles in metal absorption and removal. Zinc efflux trends with Ni^{+} in *N. tabacum* while dependent with plant matter content. While zinc efflux in *M. crystallinum* was independent from nickel, the root matter content of zinc was dependent on nickel stress.

Reactive oxygen species and salinity have been documented to encourage the root efflux of K^{+} and the influx of Ca^{+2} in both C4- and C3- pathway due to activating a stress response from ROS (Demidchik et al., 2003). Potassium was the highest effluent in *N. tabacum* and was the highest in the nickel stress media trails. This matches the trends of heavy metal stress inducing K efflux which is required for the inflammasome NLRP3 pathways to start (Rivers-Auty & Brough, 2015) which either causes programed cell death, or regeneration through membrane repolarization (Demidchik, 2014). *M. crystallinum* demonstrated far less efflux of K^{+} relative to *N. tabacum*, despite having higher stress responses within the leaves. *M. crystallinum* had the most efflux of potassium in the 0.4 M NaCl by a minimal margin, indicating that species

can retain sodium ions despite metal stress. Salinity and metal-derived ROS was documented to increase the efflux of K ions due to activating a stress response (Demidchik et al., 2003); in *M. crystallinum*, it was from salnity, and in *N tabacum*, it was from ROS stress.

Sodium had the largest efflux value of all elements and in all conditions at 0.4 M NaCl *M. crystallinum*. The natural life cycle of *M. crystallinum* relies on the intake of Na^+ ions, which is a signal for the metabolism switch to CAM. *M. crystallinum* is not salt tolerant early in its life in C3 as the juvenile leaves lack higher concentrations of compatible solutes compared to adult leaves (Adams et al., 1998). When they commit to flowering (usually 6-8 weeks) the CAM transition happens immediatly. Because this isn't a developmental study one "age" of the plant was used but the standard deviations are probably due to different plants on different developmental stages. The bladder cells were confirmed to accumulate sodium and metal ions even in the juvenile phase (Adams et al., 1998), which is reflected in the ICP results. Both the leaves and the roots from the 0.4 Na group of *M. crystallinum* had sodium concentrations that exceeded the ICP's detection upper limits. Root efflux in water may allow for the specimens to return from CAM to C3 if left alive as unlike other CAM plants, a reversible process in *M. crystallinum* (Vernon, 1988).

Chapter 5 Conclusions

Under the application of nickel and/or copper treatments in hydroponics, both plant species managed nickel accumulation and efflux in very similar concentrations, generally higher in roots versus leaves (Figures 14 & 22), and support the concept portrayed in Figure 1 (Hassan et al., 2019). These results contrast with nickel hyperaccumulator plants such as *Alyssum murale* and *Leptoplax emarginata*, that mostly accumulated greater than 0.4% dry weight nickel in their leaves and vegetative stems (Pardo et al., 2018). The observed nickel concentrations in that study were maximal at the mid-flowering stage, as previously reported by Bani et al. (2015). In conclusion, both non-hyperaccumulator species *N. tabacum* and the *M. crystallinum* store nickel mostly in the roots. The preferred site of nickel storage for *M. crystallinum* was confirmed to be the roots by Amari et al. (2014; 2016) which is also consistent with *N. tabacum* in this experiment (Figure 14).

M. crystallinum underwent greater ROS initiated stress in 0.5 mM Ni^{+} and both HMs than *N. tabacum.* Moreover, *M. crystallinum* has better retention of heavy metals during root efflux, and effluxed fewer macronutrients and trace metals compared to *N. tabacum*. The bladder cells in *M. crystallinum* likely factored into these results as they provide a large repository of toxic metals, spatially separated from the cytoplasm. These findings indicate that flooding plots of land may be optimal in remediating crops if they are glycophytes, as they would release the metals before human consumption. There are also implications that halophytes are viable for soil phytoremediation of abnormal heavy metal concentration; after they extract the pollutant ions,

the plants containing them can be safely disposed of. During efflux after nickel stress, the *M. crystallinum* responded to nickel stress with efflux of Zn^+, while *N. tabacum* responded using Mg^+ efflux. These differences provide the basis for greater ROS observed in the *M. crystallinum*, as Zn^+ is a much more potent Fenton metal at physiological growth conditions. Further research should investigate how salt-stressed halophytes interact with heavy metal efflux differently from non-stressed specimens during an NaCl and Ni^+ co-stress. Most of the established CAM metabolism can be redirected back to C3 at least temporarily. During this time, Na+ is significantly effluxed during this transition. Perhaps the context of *M. crystallinum* responses to nickel stress may become enhanced when coupled to NaCl stress. These questions will help underline the apparent differences between the glycophyte and halophyte efflux in response to nickel exposure and subsequent flooding and release from nickel stress. Besides using methods established here, isotope forms of nickel and other metals will precisely determine metal efflux responsiveness in glycophytes and halophytes.

Appendix

2nd Run	Sample Name	Plant Part	Growing C	Dry Weigh	23 Na (mol/g)	24 Mg (mol/g)	27 Al (mol/g)	39 K (mol/g)	44 Ca (mol/g)	52 Cr (mol/g)	53 Cr (mol/g)	55 Mn (mol/g)	56 Fe (mol/g)	59 Co (ppb)	60 Ni (mol/g)	63 Cu (mol/g)	65 Cu (mol/g)	66 Zn (mol/g)	67 Zn (mol/g)	68 Zn (mol/g)
	6x 1 E2 2	Leaf	Control	0.0111	0.0001523416	>200	ND	>200	>200	BDL	ND	0.0000044252	BDL	ND	BDL	0.0000094815	0.0000860829	BDL	BDL	BDL
	6x 1 E2 R	Root	Control	0.0034	0.0003946905	>200	0.0004492810	>200	0.0008735455	BDL	ND	0.0000427337	0.0000854496	BDL	0.0000020588	0.0000329038	0.0002855783	0.0001307201	0.0001207761	0.0001208962
	Cx2 E2L	Leaf	Control	0.0126	0.0000768282	>200	BDL	>200	>200	BDL	ND	0.0000044872	BDL	ND	0.0000009799	0.0000084475	0.0000765705	0.0000101039	BDL	BDL
	Cx2 E2R	Root	Control	0.0017	0.0009532276	0.0010482745	ND	>200	BDL	BDL	ND	0.0000511487	0.0001339328	ND	BDL	0.0000789542	0.0005788452	BDL	BDL	BDL
	Cx3 E2L	Leaf	Control	0.0106	0.0000840066	>200	BDL	>200	>200	BDL	ND	0.0000040535	BDL	ND	BDL	0.0000082060	0.0000918374	0.0000115540	BDL	BDL
	Cx3 E2R	Root	Control	0.0023	0.0005110019	0.0021198986	0.0005195105	>200	0.0007914862	BDL	ND	0.0000403605	0.0001348447	ND	0.0000088290	0.0000518371	0.0004288428	0.0000589881	0.0000544166	0.0000546752
	Cx4 E2L	Leaf	Control	0.0056	0.0001865839	0.0009520417	0.0001398307	>200	0.0005854740	BDL	ND	0.0000050779	BDL	ND	BDL	0.0000196667	0.0001716154	0.0000300866	0.0000273753	0.0000278067
	Cx4 E2R	Root	Control	0.0044	0.0002723320	0.0012691212	0.0003214545	>200	0.0008229298	BDL	ND	0.0000221488	0.0000662208	ND	BDL	0.0000357893	0.0002291413	0.0000929174	0.0000849525	0.0000857781
	0.05A Et2L	Leaf	0.05 mM Ni	0.00107	0.0012708330	0.0061281931	BDL	>200	>200	BDL	ND	0.0000483263	BDL	ND	0.0000092212	0.0001187005	0.0009143465	BDL	BDL	BDL
	0.05 A EF2 R	Root	0.05 mM Ni	0.0043	0.0002046593	0.0005394419	ND	>200	0.0007381184	BDL	ND	0.0000355958	0.0000823754	ND	0.0001292682	0.0001003972	0.0003028923	0.0000299704	0.0000277626	BDL
	.05NiB EF2 L	Leaf	0.05 mM Ni	0.0092	0.0001002457	0.0003723478	ND	>200	0.0003417984	BDL	ND	0.0000027826	BDL	ND	0.0000009594	0.0000104955	0.0001053592	BDL	BDL	BDL
	0.05 NiB EF2 R	Root	0.05 mM Ni	0.0047	0.0002118853	0.0005310922	BDL	>200	0.0005241083	BDL	ND	0.0000119892	0.0002070790	ND	0.0000408085	0.0000920797	0.0002781224	0.0000397679	0.0000363392	0.0000369912
	.05Ni C EF2 L	Leaf	0.05 mM Ni	0.0075	0.0001413843	0.0004681778	ND	>200	0.0004275661	BDL	ND	0.0000033338	BDL	ND	0.0000009369	0.0000160372	0.0001307339	BDL	BDL	BDL
	.05NiCEF2--R	Root	0.05 mM Ni	0.0024	0.0003817826	0.0007800139	BDL	BDL	0.0009071742	BDL	ND	0.0000095697	0.0001671548	ND	0.0000929278	0.0003180476	0.0006639026	0.0000563030	0.0000520846	0.0000521176
	.05 Ni D Ef2 L	Leaf	0.05 mM Ni	0.0136	0.0000710537	>200	0.0001115969	>200	>200	BDL	ND	0.0000029733	BDL	ND	0.0000006225	0.0000096611	0.0000725149	0.0000213743	0.0000196892	0.0000197232
	.05 Ni D Ef2 R	Root	0.05 mM Ni	0.0031	0.0002664797	0.0006099892	BDL	0.0008711596	0.0010845982	BDL	ND	0.0000231930	0.0001380968	ND	0.0000882495	0.0002122642	0.0004895682	0.0000848954	0.0000773770	0.0000783340
	.5 Ni A Ef2 L	Leaf	0.5 mM Ni	0.0139	0.0001025862	>200	BDL	>200	>200	BDL	ND	0.0000058663	0.0000200195	ND	0.0000014657	0.0000104465	0.0000730811	0.0000325197	0.0000299238	0.0000301405
	.5Ni A Ed2 R	Root	0.5 mM Ni	0.0038	0.0002698856	0.0005412193	BDL	BDL	0.0006984689	BDL	ND	0.0000343120	0.0001878496	0.05	0.0004184912	0.0000437327	0.0002736518	0.0000369984	0.0000344038	0.0000340805
	.5 Ni B Ef2 L	Leaf	0.5 mM Ni	0.0077	0.0001921129	0.0006589827	BDL	>200	>200	BDL	ND	0.0000051362	0.0000196994	ND	0.0000021749	0.0000126473	0.0001254330	0.0000511799	0.0000466943	0.0000474744
	.5 Ni B Ef2 R	Root	0.5 mM Ni	0.0023	0.0005485520	0.0006917536	BDL	BDL	>200	BDL	ND	0.0000091194	0.0001191304	ND	0.0002583884	0.0000391994	0.0004124468	0.0003996364	0.0003651084	0.0003700921
	.5Ni Ef2C L	Leaf	0.5 mM Ni	0.0092	0.0001204159	0.0005754457	BDL	>200	>200	BDL	ND	0.0000040980	0.0000163245	ND	0.0000017232	0.0000072602	0.0001009565	0.0000699183	0.0000639753	0.0000647558
	.5 Ni C Ef2 R	Root	0.5 mM Ni	0.0044	0.0003288458	0.0005799773	0.0002287340	0.0008405455	>200	BDL	ND	0.0000080826	0.0001020649	ND	0.0002771545	0.0000282222	0.0002231133	0.0001508815	0.0001370149	0.0001390027
	.5 Ni D Ef2 L	Leaf	0.5 mM Ni	0.0119	0.0001125466	0.0005051148	ND	>200	>200	BDL	ND	0.0000047853	BDL	ND	0.0000006969	0.0000085453	0.0000807943	0.0000102419	BDL	BDL
	.5 Ni D Ef2 R	Root	0.5 mM Ni	0.0045	0.0003962667	0.0002727037	ND	0.0005763419	BDL	BDL	ND	0.0000093543	0.0001668508	BDL	0.0003179378	0.0000325108	0.0002256793	BDL	BDL	BDL
	.4Cu A EA2 L	Leaf	0.4 mM Cu	0.0084	0.0001480870	0.0006313690	BDL	>200	>200	BDL	ND	0.0000040000	BDL	ND	BDL	0.0000195026	0.0001230256	0.0000367633	0.0000337783	0.0000340392
	.4Cu A E2 R	Root	0.4 mM Cu	0.0051	0.0002692651	0.0003503856	BDL	BDL	0.0005392941	BDL	ND	0.0000048856	0.0000775602	ND	0.0000038484	>200	>200	0.0000810101	0.0000742874	0.0000752803
	.4Cu CuB Ed2 L	Leaf	0.4 mM Cu	0.0096	0.0001158623	0.0004262604	ND	>200	0.0003590133	BDL	ND	0.0000034470	BDL	ND	BDL	0.0000222249	0.0001118269	BDL	BDL	BDL
	.4 CuB E2 R	Root	0.4 mM Cu	0.0006	0.0041442899	BDL	ND	BDL	BDL	BDL	ND	BDL	0.0002970000	ND	BDL	0.0013436825	0.0027587077	BDL	BDL	BDL
	.4Cu C E2 L	Leaf	0.4 mM Cu	0.0056	0.0002370311	0.0007743988	0.0001656508	>200	>200	BDL	ND	0.0000039740	BDL	ND	BDL	0.0000177415	0.0001720330	0.0001087489	0.0000987761	0.0001004307
	.4CuC E2R	Root	0.4 mM Cu	0.0022	0.0005375652	0.0004528485	BDL	BDL	0.0014002645	BDL	ND	0.0000249785	0.0001226558	ND	BDL	>200	>200	0.0001210358	0.0001093948	0.0001119679
	both A E2 L	Leaf	Both Metal	0.0193	0.0000855796	>200	ND	>200	>200	BDL	ND	0.0000035407	BDL	ND	0.0000100857	0.0000096633	0.0000550925	BDL	BDL	BDL
	both A E2 R	Root	Both Metal	0.0036	0.0006284831	0.0003422407	BDL	BDL	>200	BDL	ND	0.0000030586	0.0000955357	ND	0.0000725630	>200	>200	0.0001926364	0.0001742919	0.0001776111
	both B E2L	Leaf	Both Metal	0.0124	0.0001348387	>200	BDL	>200	>200	BDL	ND	0.0000035085	BDL	ND	0.0000274871	0.0000192852	0.0000885717	0.0000140528	0.0000128204	0.0000128539
	both B E2 R	Root	Both Metal	0.0015	0.0008612638	0.0008559333	BDL	ND	0.0020435152	BDL	ND	0.0000070982	0.0001121333	ND	0.0000355111	0.0006468233	0.0012054482	0.0002269737	0.0002089711	0.0002100078
	Both c E2 L	Leaf	Both Metal	0.0138	0.0001077832	>200	0.0000613570	>200	>200	BDL	ND	0.0000066129	BDL	ND	0.0000028338	0.0000075629	0.0000705186	0.0000601195	0.0000551270	0.0000554987
	both c E2 R	Root	Both Metal	0.006	0.0001828000	0.0001505500	ND	BDL	BDL	BDL	ND	0.0000027273	0.0000927071	ND	0.0000638911	>200	>200	BDL	BDL	BDL
1st Run	Cx 1 Leaf	Leaf	Control	0.0086	0.002670347	0.000864922	0.000839128	0.003508043	0.00427743			4.49615E-06	4.96983E-05		2.61203E-06	2.31732E-05		0.000169731		
	Cx 1 Root	Root	Control	0.009	0.002495366	0.000194294	0.000719426	0.000312026	0.003038372			2.52582E-06	3.96926E-05		2.41113E-06	9.99259E-06		0.000149209		
	Cx 2 Leaf	Leaf	Control	0.0261	0.000817847	7.75554E-05	0.000253217	0.000178651	0.001136292			9.38823E-07	1.44814E-05		1.11062E-06	3.15928E-06		5.51066E-05		
	Cx 2 Root	Root	Control	0.0143	0.001596416	0.000218469	0.000471012	0.00046039	0.00242922			1.93484E-06	2.75975E-05		2.13546E-06	7.46022E-06		0.000113068		
	Cx 3 Leaf	Leaf	Control	0.0391	0.000562066	0.000144657	0.000176442	0.000465652	0.000973841			8.66005E-07	1.08227E-05		8.04167E-07	2.19376E-06		4.06636E-05		
	Cx 3 Root	Root	Control	0.011	0.001910221	0.000215973	0.000582871	0.000396745	0.002453757			2.22928E-06	3.32599E-05		2.61353E-06	7.23335E-06		0.000124568		
	0.05 Ni 1 Leaf	Leaf	0.05 mM Ni	0.0543	0.000394756	2.72698E-05	4.89926E-05	6.91672E-05	0.000375366			4.46845E-07	5.83155E-06		5.23393E-07	1.39363E-05		2.23995E-05		
	0.05 Ni 1 Root	Root	0.05 mM Ni	0.0046	0.004308268	0.00025631	0.00036542	0.000179448	0.004314289			2.25445E-06	5.44354E-05		2.94061E-06	0.000103749		0.000250751		
	0.05 NI 2 Leaf	Leaf	0.05 mM Ni	0.0631	0.000201078	0.000137604	3.15676E-05	0.000282923	0.00064691			3.66882E-07	6.32967E-06		1.68177E-07	7.67643E-06		2.47362E-05		
	0.05 Ni 2 Root	Root	0.05 mM Ni	0.0093	0.000671338	0.000774581	0.000123691	0.001996021	0.001803939			1.09219E-06	1.99493E-05		1.23183E-06	5.13776E-05		8.88993E-05		
	0.5 Ni 1 Leaf	Leaf	0.5 mM Ni	0.056	0.00078537	0.000116213	6.005E-05	0.000340596	0.000718755			3.35514E-07	7.15244E-06		6.10571E-07	3.34291E-06		3.4938E-05		
	0.5 Ni 1 Root	Root	0.5 mM Ni	0.0011	0.019768086	0.003747594	0.006076715	0.007196288	0.026054189			2.22259E-05	0.00038397		3.37679E-05	8.31603E-05		0.001333334		
	0.5 Ni 2 Leaf	Leaf	0.5 mM Ni	0.0737	0.000261554	1.52359E-05	2.04576E-05	9.09568E-06	0.000225414			1.31728E-07	3.18786E-06		1.81771E-07	6.23058E-06		1.56058E-05		
	0.5 Ni 2 Roots	Root	0.5 mM Ni	0.0031	0.006505526	0.000393745	0.000511717	0.000306483	0.005911319			3.41677E-06	9.36261E-05		4.81209E-06	0.000161536		0.00038069		
	0.5 Ni 3 Leaf	Leaf	0.5 mM Ni	0.0914	0.000229861	0.000100679	1.67587E-05	0.000388821	0.000281671			1.87808E-07	4.01228E-06		2.17478E-07	5.18796E-06		1.32624E-05		
	0.5 Ni 3 Root	Root	0.5 mM Ni	0.0094	0.002274562	0.00028688	0.000152381	0.000720312	0.002091475			1.20621E-06	2.88346E-05		1.84708E-06	4.93962E-05		0.000123621		
	0.4 Cu 1 Leaf	Leaf	0.4 mM Cu	0.0464	0.000253572	0.000231272	1.77926E-05	0.001167635	0.000567564			6.29279E-07	5.91233E-06		2.37552E-07	4.81904E-06		2.00095E-05		
	0.4 Cu 1 Root	Root	0.4 mM Cu	0.0119	0.000930852	0.000611082	7.48138E-05	0.001548105	0.002075488			1.76688E-06	2.62378E-05		9.7851E-07	1.88202E-05		8.71093E-05		
	0.4 Cu 2 Leaf	Leaf	0.4 mM Cu	0.007	0.001653529	0.000838134	0.000132836	0.003562351	0.003254344			1.73604E-06	3.65837E-05		1.87968E-06	3.22907E-05		0.000167239		
	0.4 Cu 2 Root	Root	0.4 mM Cu	0.0138	0.000707981	0.000319156	7.34265E-05	0.001036795	0.001361551			6.02751E-07	2.02152E-05		6.69517E-07	1.60629E-05		6.67583E-05		
	Both 1 Leaf	Leaf	Both Metal	0.0062	0.003723559	0.002062374	0.000253394	0.011214446	0.005558475			7.99965E-06	5.14149E-05		3.01417E-06	7.71418E-05		0.000198866		
	Both 1 Root	Root	Both Metal	0.0077	0.002757874	0.000290672	0.000195212	0.000515656	0.002577875			2.08393E-06	4.04728E-05		2.18002E-06	6.16836E-05		0.000157695		
	Both 2 Leaf	Leaf	Both Metal	0.0041	0.002667452	0.000497744	0.000128079	0.001797803	0.001333629			9.42971E-07	6.05421E-05		2.14998E-06	3.47175E-05		0.000143277		
	Both 2 Root	Root	Both Metal	0.0039	0.002281806	0.000261926	8.60631E-05	0.000355773	0.001475966			7.10079E-07	5.87592E-05		1.76718E-06	3.54046E-05		0.000158812		

Table 1: N. tabacum Plant Matter ICP Readings

Sample Name	Ash weight (g) in 4 ml	Conditions	Plant Part	23 Na (mol/g)	24 Mg (mol/g)	27 Al (mol/g)	39 K (mol/g)	44 Ca (mol/g)	55 Mn (mol/g)	56 Fe (mol/g)	60 Ni (mol/g)	63 Cu (mol/g)	65 Cu (mol/g)	66 Zn (mol/g)	67 Zn (mol/g)	68 Zn (mol/g)
C+AL IP E1 IP-1 Matter	0.0332	Control	Leaf	0.000208507	>200	2.63382E-05	>200	>200	3.57809E-06	BDL	1.35743E-07	9.50622E-06	9.85616E-06	1.42307E-05	1.26042E-05	1.30011E-05
C+AR IPE1	0.0045	Control	Root	0.00089937	0.000304793	0.000225804	0.000644426	0.000152275	3.15152E-06	4.37841E-05	1.01037E-06	6.49284E-05	6.53128E-05	7.00848E-05	6.13439E-05	6.35373E-05
C+BL IP E1	0.013	Control	Leaf	>200	>200	6.10439E-05	>200	0.000123627	4.11748E-06	ND	3.41538E-07	2.18598E-05	2.22031E-05	1.7849E-05	1.52202E-05	1.59204E-05
C+ BR IP E1	0.0043	Control	Root	0.00092457	0.000210907	0.000188644	0.000332413	0.000150651	2.99704E-06	BDL	1.07907E-06	6.64393E-05	7.00308E-05	6.5105E-05	5.66137E-05	5.82052E-05
C+ CL IP E1	0.0122	Control	Leaf	>200	>200	9.41712E-05	>200	>200	4.707E-06	ND	3.80328E-07	2.23888E-05	2.35511E-05	2.41123E-05	2.14328E-05	2.1865E-05
C+ CR IP E1	0.0054	Control	Root	0.001024593	0.000261198	0.000175424	>200	0.00030502	2.3596E-06	BDL	8.32099E-07	5.46243E-05	5.77345E-05	3.62492E-05	3.08104E-05	3.22549E-05
.4 Na AL IP E1	0.0181	0.4 M NaCl	Leaf	>200	>200	4.64809E-05	>200	0.0001082	3.6894E-06	BDL	2.53407E-07	1.60014E-05	1.57722E-05	1.1994E-05	1.02198E-05	1.06422E-05
.4Na AR IP E1	0.0047	0.4 M NaCl	Root	>200	0.000122794	0.000194522	0.000130064	9.26306E-05	1.2472E-06	5.32644E-05	1.16312E-06	7.30321E-05	7.5344E-05	4.86009E-05	4.21493E-05	4.34443E-05
.4 Na BL IP E1	0.0184	0.4 M NaCl	Leaf	>200	>200	4.75072E-05	>200	>200	3.90198E-06	BDL	2.3913E-07	1.7011E-05	1.76274E-05	1.89756E-05	1.68436E-05	1.72826E-05
.4 Na BR IP E1	0.0047	0.4 M NaCl	Root	>200	0.000340518	0.000499026	0.000115976	>200	2.49439E-06	4.57599E-05	7.97163E-07	1.73212E-05	1.8692E-05	0.000256962	0.000233885	0.000236395
.4 Na CL IP E1	0.017	0.4 M NaCl	Leaf	>200	>200	4.64837E-05	>200	>200	3.37882E-06	BDL	2.73725E-07	1.66035E-05	1.75052E-05	2.36563E-05	2.09538E-05	2.15848E-05
.4 Na CR IP E1	0.0049	0.4 M NaCl	Root	>200	0.000127218	0.00021086	0.000112004	0.000128824	1.28534E-06	BDL	1.07755E-06	8.59994E-05	8.95749E-05	8.80297E-05	7.87402E-05	8.01224E-05
.05 Ni AL IP E1	0.0199	0.05 mM Ni	Leaf	>200	>200	8.06134E-05	>200	>200	4.5376E-06	BDL	1.67973E-06	1.63452E-05	1.6013E-05	1.17314E-05	1.02939E-05	1.05823E-05
.05 Ni AR IP E1	0.005	0.05 mM Ni	Root	0.00106391	0.000186787	0.000209458	0.000198101	0.000141204	1.89673E-06	6.39114E-05	0.00005192	9.45549E-05	9.89809E-05	5.2417E-05	4.65624E-05	4.75882E-05
.05 Ni BL IP E1	0.0154	0.05 mM Ni	Leaf	>200	>200	0.00010288	>200	>200	5.48383E-06	BDL	2.05108E-06	1.48522E-05	1.47844E-05	0.000105416	9.61993E-05	9.7194E-05
.05 Ni BR IP E1	0.0043	0.05 mM Ni	Root	0.001266847	0.000240659	0.000210164	0.00038733	0.000197577	2.22241E-06	5.48771E-05	7.5631E-05	0.000140908	0.000138496	8.54827E-05	7.51961E-05	7.72859E-05
.05 Ni CL IP E1	0.0211	0.05 mM Ni	Leaf	>200	>200	7.3042E-05	>200	>200	9.43662E-06	BDL	1.75545E-06	1.76947E-05	1.8335E-05	1.87706E-05	1.64504E-05	1.70951E-05
.05 Ni CR IP E1	0.0043	0.05 mM Ni	Root	0.00087107	0.000442341	0.000693754	0.000236098	>200	3.83256E-06	7.59037E-05	5.43225E-05	6.08579E-05	6.24916E-05	0.00042528	0.000368319	0.000372952
.5 Ni AR IP E1	0.0042	0.5 mM Ni	Root	0.001476232	1.10317E-06	0.000233693	ND	1.68095E-05	BDL	ND	1.01587E-06	7.04853E-05	7.40923E-05	8.93535E-05	7.90078E-05	8.07899E-05
.5Ni BL IP E1	0.0372	0.5 mM Ni	Leaf	0.000118133	2.65582E-05	3.1143E-05	2.21886E-05	>200	2.76833E-07	8.86175E-06	3.26047E-05	7.1275E-06	7.14574E-06	3.17964E-05	2.92053E-05	2.94032E-05
.5 Ni BR IP E1	0.0089	0.5 mM Ni	Root	>200	>200	0.000179572	>200	>200	2.29246E-05	1.76116E-05	3.22247E-05	3.39262E-05	3.57061E-05	3.97331E-05	3.51246E-05	3.62432E-05
.5 Ni LC IP E1	0.0239	0.5 mM Ni	Leaf	0.000248977	8.49442E-05	3.89016E-05	8.78352E-05	>200	8.81856E-07	2.40771E-05	>200	1.36681E-05	1.44649E-05	2.26048E-05	2.0267E-05	2.06503E-05
.5 Ni CR IP E1	0.0049	0.5 mM Ni	Root	>200	>200	0.000177373	>200	>200	2.77788E-05	BDL	5.48408E-05	6.46557E-05	6.65294E-05	5.01497E-05	4.28632E-05	4.5066E-05
.4 Cu AL IP E1	0.0124	0.4 mM Cu	Leaf	0.000352771	4.20081E-05	8.18399E-05	7.62647E-05	0.000132025	5.57185E-07	1.88882E-05	0.000133966	2.61813E-05	2.7733E-05	3.22688E-05	2.84612E-05	2.93416E-05
0.4Cu A IP1 L	0.0019	0.4 mM Cu	Leaf	0.000666746	ND	0.00030177	0.000525366	ND	8.26794E-07	ND	ND	6.75021E-07	5.05263E-07	8.35407E-05	6.94108E-05	7.3678E-05
0.4Cu A IP1 R	0.0008	0.4 mM Cu	Root	0.00129687	ND	0.000658148	ND	ND	BDL	ND	ND	0.000176603	0.000169892	6.28788E-05	3.51642E-05	4.55588E-05
0.4Cu B IP1 L	0.0023	0.4 mM Cu	Leaf	0.000508476	ND	0.000262892	0.000573851	ND	7.46245E-07	ND	ND	3.86473E-08	4.28094E-08	5.4303E-05	4.31097E-05	4.59284E-05
0.4Cu C IP1 R	0.0028	0.4 mM Cu	Root	0.000583851	ND	0.000318307	BDL	ND	BDL	BDL	ND	0.000146417	0.000134967	4.74242E-05	3.80426E-05	4.07521E-05
Both A IP1 R	0.0018	Both HM	Root	0.00061057	ND	0.000313679	ND	ND	ND	ND	6.88963E-05	0.000270801	0.000247255	5.16431E-05	3.83483E-05	4.25033E-05
Both B IP1 L	0.0083	Both HM	Leaf	0.000215417	0.000152257	6.98652E-05	0.00068608	ND	1.02344E-06	ND	1.84578E-06	2.79977E-07	2.44671E-07	1.37948E-05	1.05017E-05	1.14968E-05
Both B IP1 R	0.0016	Both HM	Root	0.000749457	ND	0.000404907	ND	ND	ND	ND	0.000051375	0.000195341	0.000187392	0.000139492	0.000117306	0.000124478
Both C IP1 L	0.0083	Both HM	Leaf	0.000244979	0.000155691	9.04346E-05	0.000739339	ND	1.08478E-06	ND	4.91566E-06	8.81239E-07	8.14087E-07	2.21205E-05	1.85923E-05	1.98044E-05
Both C IP1 R	0.0015	Both HM	Root	0.000723942	ND	0.000406578	BDL	ND	ND	ND	6.70044E-05	0.000210396	0.000200525	6.54949E-05	5.07144E-05	5.66431E-05
0.4Cu B IP1 R	0.0006	0.4 mM Cu	Root	0.001961159	ND	0.001021728	ND	ND	ND	ND	ND	0.000556106	0.000530605	0.000153414	0.000119741	0.000129922
0.4Cu C L IP1	0.0042	0.4 mM Cu	Leaf	0.000299246	BDL	0.000162187	0.000679653	ND	1.01818E-06	ND	ND	7.80045E-07	6.76923E-07	5.85599E-05	5.15849E-05	5.30056E-05
0.4Cu C L IP1	0.0057	0.4 mM Cu	Leaf	0.000254426	0.00017169	0.00013731	0.000603995	ND	1.07177E-06	ND	ND	9.22306E-07	8.70175E-07	1.6404E-05	1.26965E-05	1.37317E-05
Both A L(1) ip1	0.0038	Both HM	Leaf	0.000517236	BDL	0.000166651	0.00043186	ND	5.20574E-07	ND	6.77193E-07	6.08187E-07	5.11741E-07	3.93046E-05	3.16198E-05	3.43808E-05
Both A L(7) ip1	0.0064	Both HM	Leaf	0.000262136	BDL	9.18843E-05	0.000413154	ND	4.97727E-07	ND	5.45833E-07	3.09524E-07	3.09615E-07	1.56477E-05	1.22276E-05	1.32224E-05

Table 2: M. crystallinum ICP Plant Matter Readings Run 1.

Efflux Run	Sample Name	Ash weight (g) in 4 ml	Conditions	Plant Part	23 Na (mol/g)	24 Mg (mol/g)	39 K (mol/g)	44 Ca (mo	55 Mn (m	56 Fe (mol/g)	60 Ni (mol/g)	63 Cu (mol/g)	65 Cu (mol/g)	66 Zn (mol/g)	67 Zn (mol/g)	68 Zn (mol/g)
IP2	**Control A leaves**	0.003	Control	Leaf	BDL	0.001482333	>200	0.000283	BDL	5.75286E-05	BDL	2.28487E-05	2.29538E-05	4.31394E-05	3.55582E-05	9.551
	Control A roots	0.0025	Control	Root	BDL	0.000435053	BDL	7.51E-05	ND	BDL	ND	2.80076E-05	3.29009E-05	4.31127E-05	3.35618E-05	7.597
	Control B leaves	0.0146	Control	Leaf	0.000275259	>200	>200	>200	6.54E-06	BDL	ND	2.60144E-06	2.39831E-06	9.13408E-06	7.6238E-06	9.62
	Control B root	0.0064	Control	Root	BDL	0.000535062	>200	4.73E-05	BDL	3.34665E-05	ND	1.11329E-05	1.20231E-05	1.34167E-05	1.03843E-05	6.177
	Control B2 leaf	0.0072	Control	Leaf	BDL	0.000435588	>200	0.000118	BDL	BDL	ND	8.52028E-06	8.10256E-06	2.37542E-05	1.98441E-05	12.532
	Control A-2 Leaf	0.008	Control	Leaf	BDL	0.000415904	>200	0.000165	BDL	BDL	ND	8.82063E-06	0.0000098	2.68288E-05	2.31701E-05	16.06
	Control D leaves	0.0058	Control	Leaf	BDL	0.000460063	>200	0.000145	BDL	BDL	ND	7.82047E-06	8.43926E-06	1.95799E-05	1.6E-05	8.185
	,05mN Ni A leaves	0.0172	0.05 mM Ni	Leaf	0.000250506	0.000261124	>200	5.42E-05	BDL	BDL	5.40698E-06	3.83093E-06	3.32665E-06	6.16843E-06	4.98507E-06	7.527
	,05mN Ni A roots	0.003	0.05 mM Ni	Root	BDL	0.000159989	BDL	0.000126	ND	9.77095E-05	6.72711E-05	7.58899E-05	7.26113E-05	2.20404E-05	1.7202E-05	4.41
	,05mM Ni B leaves	0.005	0.05 mM Ni	Leaf	BDL	0.00039888	>200	7.48E-05	BDL	BDL	7.096E-06	1.2447E-05	1.42178E-05	5.17164E-05	4.54949E-05	19.299
	.05mM Ni B roots	0.0057	0.05 mM Ni	Root	BDL	0.000382234	0.000468844	8.58E-05	ND	0.000118637	8.92889E-05	9.97338E-05	9.41474E-05	3.66188E-06	1.25687E-06	0.78
	.05mM Ni B-2 Leaves	0.0093	0.05 mM Ni	Leaf	BDL	0.000201	>200	9.8E-05	BDL	BDL	3.73763E-06	7.43472E-06	6.41456E-06	8.73249E-06	6.85347E-06	5.518
	.5mM Ni A leaf	0.0626	0.5 mM Ni	Leaf	>200	>200	>200	>200	7.94E-06	2.68804E-06	0.000107721	5.08545E-07	5.21406E-07	1.88789E-06	1.53774E-06	8.529
	.5mM Ni A root	0.0037	0.5 mM Ni	Root	BDL	0.000198369	BDL	0.000304	ND	0.000105541	0.000257441	1.95418E-05	1.75601E-05	4.37707E-05	3.54143E-05	11.953
	.5mM Ni B leaf	0.0552	0.5 mM Ni	Leaf	>200	>200	>200	>200	5.52E-06	BDL	6.90716E-05	1.07591E-06	8.98774E-07	2.00834E-06	1.67056E-06	7.683
	.5mM Ni B root	0.0046	0.5 mM Ni	Root	BDL	0.000115652	ND	0.000111	ND	7.76988E-05	0.000279957	1.83354E-05	1.55559E-05	8.79051E-06	5.9987E-06	2.642
	.4M NaCl A leaves	0.0327	0.4 M NaCl	Leaf	>200	>200	>200	>200	3.76E-06	BDL	BDL	1.31023E-06	1.82169E-06	2.60254E-06	2.12698E-06	6.081
	.4M NaCl A roots	0.0043	0.4 M NaCl	Root	0.001221573	5.52248E-05	ND	5.46E-05	ND	4.94485E-05	ND	1.59764E-05	9.46547E-06	6.65088E-05	5.82242E-05	21.583
	.4M NaCl B leaves	0.0067	0.4 M NaCl	Leaf	>200	0.000709647	>200	>200	BDL	BDL	BDL	6.28856E-06	4.21401E-06	6.63718E-05	5.81599E-05	33.709
	.4M NaCl B roots	0.0037	0.4 M NaCl	Root	0.001303549	0.000104	ND	5.05E-05	ND	7.17645E-05	ND	1.74826E-05	1.6479E-05	1.56593E-05	1.19597E-05	3.898
	.4Cu A Leaves	0.0115	0.4 mM Cu	Leaf	0.000333217	>200	>200	8.32E-05	6.56E-06	BDL	BDL	3.20221E-06	3.96308E-06	5.59262E-06	4.09604E-06	4.463
	.4Cu A roots	0.0034	0.4 mM Cu	Root	BDL	0.000203206	BDL	0.000266	ND	5.28109E-05	ND	7.74665E-06	>200	2.77647E-05	2.12643E-05	6.727
	.4Cu B leaves	0.0141	0.4 mM Cu	Leaf	0.000429368	>200	>200	>200	9.44E-06	BDL	ND	1.59009E-05	1.52161E-05	6.78616E-06	5.42056E-06	6.762
	.4Cu B roots	0.0063	0.4 mM Cu	Root	BDL	0.000221074	BDL	>200	ND	7.35125E-05	BDL	0.000833751	>200	0.000160231	0.000144341	77.68
	Cu 5f2 AL	0.0082	0.4 mM Cu	Leaf	0.000427156	0.00029239	>200	0.000182	BDL	BDL	BDL	1.30685E-05	1.25163E-05	3.93437E-05	3.44478E-05	24.281
	0.4mM NaCl A2 leaves	0.0139	0.4 M NaCl	Leaf	>200	0.000390417	>200	0.00011	BDL	BDL	BDL	3.71269E-06	3.56657E-06	2.63344E-05	2.32063E-05	27.714
	Both A Leaf	0.0609	Both HM	Leaf	ND	5.44061E-07	ND	8.85E-07	ND	BDL	ND	9.13493E-07	1.12143E-06	9.43623E-07	6.38777E-07	3.642
	Both A roots	0.0132	Both HM	Root	BDL	6.38561E-05	BDL	>200	ND	2.04221E-05	0.00014856	5.08518E-05	>200	7.00184E-05	6.33315E-05	71.43
	Both B leaves	0.0101	Both HM	Leaf	>200	>200	>200	>200	4.05E-05	2.0232E-05	0.000248438	2.29414E-05	2.33018E-05	1.0471E-05	8.57455E-06	7.536
	Both B roots	0.056	Both HM	Root	BDL	1.35917E-05	BDL	6.16E-06	ND	9.83163E-06	2.0354E-05	3.44533E-05	379.46	1.23788E-06	9.60981E-07	4.624
IPT	**C1Le**	0.0054	Control	Leaf	0.000307002	9.56296E-05	>200	7.6E-05	2.65E-06	BDL	BDL	1.11534E-05	1.12499E-05	ND		ND
	C1R	0.00352	Control	Root	0.000124674	0.000128239	0.000840839	1.68E-05	4.1E-06	8.62541E-05	BDL	3.35642E-05	3.40152E-05	ND		ND
	C2Le	0.004	Control	Leaf	0.000348157	9.59667E-05	>200	7.3E-05	3.55E-06	BDL	BDL	1.6946E-05	1.69651E-05	ND		ND
	CR2root	0.0029	Control	Root	0.000103604	0.000457253	0.000955954	0.000119	7.77E-06	3.55172E-05	BDL	2.85495E-05	2.77176E-05	ND		ND
	C3Le	0.0066	Control	Leaf	0.00023766	0.000164111	>200	8.07E-05	3.18E-06	BDL	BDL	1.06686E-05	1.01145E-05	ND		ND
	C3R	0.004	Control	Root	0.000153504	0.000276142	>200	1.79E-05	4.37E-06	4.40571E-05	BDL	2.58635E-05	2.50635E-05	ND		ND
	N1 root	0.0037	0.05 mM Ni	Root	5.44019E-05	7.35135E-05	0.000692618	6.77E-05	5.47E-06	6.05714E-05	4.81441E-05	4.85148E-05	4.16336E-05	ND		ND
	N2Le	0.0062	0.05 mM Ni	Leaf	0.000246957	0.000179613	>200	8.2E-05	5.68E-06	BDL	3.74409E-06	1.16846E-05	1.12483E-05	ND		ND
	N2R	0.0027	0.05 mM Ni	Root	6.12947E-05	0.000101358	BDL	8.69E-05	1.46E-05	0.000103217	7.26321E-05	7.29547E-05	5.92075E-05	0.000392228		ND
	N3Le	0.0057	0.05 mM Ni	Leaf	0.00021528	0.000115088	>200	0.000129	3.38E-06	3.50677E-05	2.13333E-06	1.78134E-05	1.39504E-05	0.000657183		ND
	N3R	0.0037	0.05 mM Ni	Root	1.43455E-05	0.000214234	BDL	0.000516	1.05E-05	0.000162081	7.34486E-05	6.64882E-05	5.70227E-05	0.001103184		ND
	Cont Go Leaf	0.0083	Control	Leaf	0.000295962	0.000209253	>200	5.09E-05	4.83E-06	BDL	BDL	1.42957E-05	1.07187E-05	ND		ND
	Cont Go Root	0.0059	Control	Root	0.000120979	0.00017087	>200	5.84E-05	2.55E-06	9.86271E-05	1.58192E-06	6.7745E-05	6.1103E-05	0.000873423		ND
	Cont old Leaf	0.0092	Control	Leaf	0.000250242	0.000261837	>200	8.06E-05	3.49E-06	BDL	BDL	1.69179E-05	1.28792E-05	0.000279056		ND
	Cont old root	0.0032	Control	Root	0.000155804	6.56771E-05	BDL	5.83E-05	BDL	4.56786E-05	BDL	7.62421E-05	6.53016E-05	0.000333242		ND
	0.5 Go leaf	0.0948	0.5 mM Ni	Leaf	>200	>200	>200	>200	2.68E-06	7.61001E-07	0.000165725	1.88748E-06	1.54899E-06	0.000238523		ND
	0.5 Go root	0.0031	0.5 mM Ni	Root	2.2575E-05	ND	ND	0.000109	2.76E-05	0.000144249	0.000237422	9.80481E-05	8.4297E-05	0.000723728		ND

Table 3: M. crystallinum ICP Plant Matter Readings Run 2

Plant #	Media Condition	Na (uM)	Mg (uM)	K (uM)	44 Ca (ppb)	55 Mn (uM)	56 Fe (uM)	60 Ni (uM)	63 Cu (uM)	65 Cu (uM)	66 Zn (uM)	67 Zn (uM)	68 Zn (uM)
Control A Ef2 Tob A	Control	4.10	2.02	61.64	0.57	0.03	0.38	0.02	0.09	0.08	0.02	0.01	0.01
Control A Ef2 Tob B	Control	3.74	1.63	7.16	0.49	0.03	0.15	0.01	0.10	0.10	0.02	0.01	0.01
Control A Ef2 Tob C	Control	1.61	0.95	11.33	0.12	0.01	0.09	0.01	0.08	0.08	BDL	BDL	0.00
Control A Ef2 Tob D	Control	3.09	1.08	45.23	BDL	0.02	0.29	0.00	0.13	0.13	0.02	0.01	0.02
0.05 Ni TOB Ef2 A	0.05 mM Ni	2.16	3.93	17.88	0.41	0.03	0.05	0.49	0.15	0.15	BDL	0.02	0.01
0.05 Ni TOB Ef2 B	0.05 mM Ni	2.14	3.95	93.81	0.54	0.08	0.09	0.50	0.26	0.25	0.03	0.02	0.03
0.05 Ni TOB Ef2 C	0.05 mM Ni	1.21	10.71	30.59	2.62	0.05	0.06	1.64	0.26	0.25	0.02	0.02	0.02
0.05 Ni TOB Ef2 D	0.05 mM Ni	2.34	15.65	64.60	3.59	0.14	0.17	2.04	0.35	0.35	0.05	0.04	0.04
0.5 Ni TOB Ef2 A	0.5 mM Ni	2.36	7.47	57.81	1.17	0.23	0.17	7.44	BDL	ND	BDL	0.01	0.01
0.5 Ni TOB Ef2 B	0.5 mM Ni	4.77	7.19	62.51	0.94	0.14	0.15	6.53	0.90	0.88	0.03	0.02	0.03
0.5 Ni TOB Ef2 C	0.5 mM Ni	4.31	5.42	74.88	0.77	0.07	0.24	3.98	0.10	0.10	0.02	0.01	0.01
0.5 Ni TOB Ef2 D	0.5 mM Ni	2.59	1.11	4.45	0.13	0.02	0.14	1.24	0.17	0.17	BDL	BDL	0.01
0.4M Cu TOB Ef2 A	0.4 mM Cu	2.29	3.08	13.83	0.38	0.11	0.06	0.00	3.59	3.54	BDL	BDL	0.01
0.4M Cu TOB Ef2 B	0.4 mM Cu	2.88	2.26	18.39	0.42	0.04	0.07	0.01	7.67	7.47	0.05	0.04	0.04
0.4M Cu TOB Ef2 C	0.4 mM Cu	2.34	3.79	16.27	1.70	0.06	0.05	0.00	3.13	3.19	BDL	BDL	BDL
both TOB A	M Ni + 0.4 m	3.21	5.91	31.97	0.88	0.07	0.10	5.27	7.84	7.76	0.08	0.06	0.07
BOTH TOB B	M Ni + 0.4 m	1.34	2.61	10.51	0.76	0.06	0.04	2.39	2.48	2.36	0.02	0.01	0.02
BOTH TOB C	M Ni + 0.4 m	1.50	2.96	25.47	0.37	0.04	0.11	2.96	6.08	6.03	0.02	0.02	0.01
cx1	Control	4.20	0.68	22.42	ND	0.00	0.12	0.01	0.38	0.36	0.14	ND	0.13
cx2	Control	3.94	0.73	17.60	ND	0.00	0.16	0.00	0.35	0.33	0.13	ND	0.12
cx3	Control	2.13	0.94	10.02	ND	0.01	0.08	0.00	0.70	0.67	0.20	ND	0.17
.05 Ni 1	0.05 mM Ni	1.66	0.80	3.00	ND	0.01	0.10	0.31	0.69	0.68	0.18	ND	0.17
.05 Ni 2	0.05 mM Ni	0.89	1.57	9.36	ND	0.02	0.09	0.53	0.56	0.54	0.16	ND	0.15
.5 Ni 1	0.5 mM Ni	3.95	1.02	5.13	ND	0.04	0.53	2.55	0.70	0.66	0.17	ND	0.15
.5 Ni 2	0.5 mM Ni	3.36	2.53	12.47	ND	0.03	0.46	3.89	0.68	0.66	0.17	ND	0.15
.5 Ni 3	0.5 mM Ni	2.00	2.04	12.67	ND	0.04	0.13	3.68	0.66	0.63	0.15	ND	0.14
.4Cu 1	0.4 mM Cu	2.94	1.45	9.38	ND	0.02	0.02	0.01	4.51	4.37	0.15	ND	0.14
.4Cu 2	0.4 mM Cu	2.25	1.29	7.80	ND	0.01	0.05	0.00	5.63	5.41	0.15	ND	0.14
.5Ni + .4Cu 1	M Ni + 0.4 m	1.57	0.69	3.04	ND	0.01	0.03	1.73	2.49	2.38	0.16	ND	0.14
.5Ni + .4Cu 2	M Ni + 0.4 m	1.01	0.93	4.87	ND	0.01	0.04	2.49	3.10	2.94	0.17	ND	0.16

Table 4: N. tabacum Efflux Readings

Sample	Conditions	Na (uM)	Mg (uM)	K (uM)	Ca (uM)	Mn (uM)	Fe (uM)	Ni (uM)	63 Cu (uM)	65 Cu (uM)	66 Zn (uM)	67 Zn (uM)	68 Zn (uM)
Control A Ice Efflux 1	Control	0.75	2.97	4.33	0.61	0.01	0.06	BDL	BDL	BDL	ND	ND	ND
Control B Ice Eff 1	Control	1.57	2.40	7.00	0.32	0.01	0.11	0.01	0.08	0.08	ND	ND	ND
Control C Ice Eff 1	Control	1.03	3.31	4.90	0.69	0.02	0.15	ND	ND	ND	0.02	0.02	0.02
0.4mM Na Ice Eff1 A	0.4 mM Na	2585.94	0.89	6.07	0.48	0.01	0.10	BDL	BDL	BDL	0.06	0.06	0.06
0.4mM Na Ice Eff1 B	0.4 mM Na	675.15	0.62	2.40	0.49	0.00	0.05	BDL	ND	ND	0.06	0.06	0.05
0.4mM Na Ice Eff1 C	0.4 mM Na	2556.19	0.80	4.64	0.39	0.00	0.02	0.00	0.20	0.20	0.05	0.05	0.05
0.05 Ni Ice Ef1 A	0.05 mM Ni	3.20	2.03	4.32	0.77	0.01	0.05	0.42	0.12	0.12	0.02	0.03	0.02
0.05 Ni Ice Ef1 B	0.05 mM Ni	1.50	0.89	1.30	0.37	0.00	0.03	0.23	0.17	0.17	0.03	0.02	0.03
0.05 Ni Ice Ef1 C	0.05 mM Ni	1.68	0.86	1.44	0.54	0.00	0.04	0.22	0.18	0.18	0.04	0.04	0.04
0.5 Ni Ice Ef1 A	0.5 mM Ni	1.49	1.32	2.79	0.48	0.01	0.16	3.18	0.09	0.09	0.06	0.05	0.05
0.5 Ni Ice Ef1 B	0.5 mM Ni	2.24	1.39	2.05	0.37	0.01	0.05	3.11	0.09	0.08	0.04	0.02	0.03
0.5 Ni Ice Ef1 C	0.5 mM Ni	1.92	0.44	0.61	0.33	BDL	0.03	1.00	0.04	0.04	0.02	0.02	0.02
0.4M Cu Ice Ef1 A	0.4 mM Cu	2.63	1.00	1.99	0.33	0.00	0.01	ND	2.79	2.67	0.02	0.01	0.01
0.4M Cu Ice Ef1 B	0.4 mM Cu	2.47	0.74	1.28	0.31	0.00	0.02	ND	4.43	4.34	BDL	0.00	BDL
0.4M Cu Ice Ef1 C	0.4 mM Cu	2.29	0.56	0.80	0.26	0.00	0.05	ND	4.45	4.40	0.02	0.02	0.01
Both Ice Ef1 A	0.5 mM Ni + 0.4 mM Cu	1.70	0.42	0.35	0.19	BDL	ND	1.14	0.72	0.71	BDL	BDL	BDL
Both Ice Ef1 B	0.5 mM Ni + 0.4 mM Cu	2.70	0.85	1.41	0.36	0.01	0.04	2.91	6.70	6.55	0.02	0.02	0.02
Both Ice Ef1 C	0.5 mM Ni + 0.4 mM Cu	3.20	0.90	1.25	0.45	0.01	0.04	2.83	5.05	5.01	0.02	0.02	0.02
Control A Ice Ef2	Control	1.03	0.40	0.68	0.21	BDL	0.03	BDL	0.03	0.03	0.03	0.02	0.03
Control B Ice Ef2	Control	0.23	0.30	BDL	BDL	BDL	0.02	0.01	0.42	0.41	0.14	0.12	0.12
Control C Ice Ef2	Control	0.99	0.18	0.30	ND	BDL	0.01	BDL	0.55	0.54	0.05	0.04	0.04
Control D Ice Ef2	Control	0.79	0.21	0.45	BDL	BDL	0.02	ND	1.31	1.29	BDL	0.00	BDL
0.4mM Na Ice Eff2 A	0.4 mM Na	513.13	0.28	2.57	BDL	0.00	0.01	BDL	1.11	1.09	BDL	0.00	BDL
0.4mM Na Ice Eff2 B	0.4 mM Na	269.29	1.77	4.28	0.69	0.01	0.14	0.00	1.04	1.03	BDL	0.01	0.01
0.4mM Na Ice Eff2 C	0.4 mM Na	281.80	0.09	BDL	ND	BDL	0.10	BDL	0.91	0.89	ND	ND	ND
0.05 Ni Ice Ef2 A	0.05 mM Ni	1.72	1.97	3.09	0.28	0.01	0.08	0.39	1.05	1.04	BDL	0.01	0.01
0.05 Ni Ice Ef2 B	0.05 mM Ni	0.75	0.36	0.29	BDL	0.00	0.08	0.08	0.39	0.39	0.03	0.02	0.02
0.05 Ni Ice Ef2 C	0.05 mM Ni	1.11	0.51	0.84	BDL	0.01	0.06	0.11	0.78	0.77	BDL	0.01	BDL
0.5 Ni Ice Ef2 A	0.5 mM Ni	0.94	0.37	0.59	BDL	0.00	0.09	0.62	0.81	0.80	BDL	ND	ND
0.5 Ni Ice Ef2 B	0.5 mM Ni	0.70	0.35	0.30	BDL	0.00	0.10	0.69	0.75	0.74	BDL	ND	ND
0.5 Ni Ice Ef2 C	0.5 mM Ni	0.63	0.56	0.55	BDL	0.00	0.08	0.97	1.07	1.06	BDL	BDL	BDL
0.5 Ni Ice Ef1 D	0.5 mM Ni	0.57	0.31	BDL	BDL	0.01	0.35	0.62	1.24	1.22	BDL	BDL	0.01
0.4M Cu Ice Ef2 A	0.4 mM Cu	1.74	1.23	1.62	0.19	0.01	0.04	0.00	7.57	7.47	BDL	BDL	BDL
0.4M Cu Ice Ef2 B	0.4 mM Cu	1.13	0.56	0.28	BDL	0.01	BDL	ND	2.87	2.76	0.02	BDL	0.01
0.4M Cu Ice Ef2 C	0.4 mM Cu	0.81	0.50	BDL	BDL	0.00	0.01	ND	2.80	2.67	ND	ND	ND
Both Ice Ef2 A	0.5 mM Ni + 0.4 mM Cu	1.08	0.48	BDL	BDL	0.01	BDL	1.16	2.46	2.36	0.02	0.01	0.02
Both Ice Ef2 B	0.5 mM Ni + 0.4 mM Cu	0.99	0.62	0.27	BDL	0.01	0.02	1.42	1.39	1.37	0.02	0.01	0.01
Both Ice Ef2 C	0.5 mM Ni + 0.4 mM Cu	1.07	0.61	BDL	BDL	0.01	0.01	1.60	1.42	1.41	ND	ND	ND

Table 5: M. crystallinum Efflux Readings

N. tabacum Sample	Growth Conditions	Leaf MDA (nmol/g)	Root MDA (nmol/g)
Control 1	Control	5.1282	4.32692
Control 2	Control	8.173	4.647425
Control 3	Control	12.019	2.804475
0.05 mM Ni 1	0.05 mM Ni	5.2885	3.205125
0.05 mM Ni 2	0.05 mM Ni	13.942	3.84615
0.5 mM Ni 1	0.5 mM Ni	9.4551	1.7628205
0.5 mM Ni 2	0.5 mM Ni	5.7693	1.28205
0.5 mM Ni 3	0.5 mM Ni	10.4167	1.602564
0.4 Cu mM Cu 1	0.4 mM Cu	18.02875	6.730769
0.4 Cu mM Cu 2	0.4 mM Cu	12.9006	4.96795
Both 1	Both Metals	13.7019	40.0641026
Both 2	Both Metals	43.1891	43.26923
Control A	Control	8.2525	2.0833
Control B	Control	7.452	2.4038
Control C	Control	3.765	3.766
Control D	Control	7.0513	
0.05 mM Ni A	0.05 mM Ni	4.08654	2.4038
0.05 mM Ni B	0.05 mM Ni	9.936	2.3237
0.05 mM Ni C	0.05 mM Ni	10.81725	2.484
0.05 mM Ni D	0.05 mM Ni	7.1314	
0.5 mM Ni A	0.5 mM Ni	16.105	0.7212
0.5 mM Ni B	0.5 mM Ni	4.8076	1.2019
0.5 mM Ni C	0.5 mM Ni	6.891	2.5641
0.5 mM Ni D	0.5 mM Ni	10.81725	
0.4 mM Cu A	0.4 mM Cu	16.6667	0.9615
0.4 mM Cu B	0.4 mM Cu	5.84925	4.7276
0.4 mM Cu C	0.4 mM Cu	4.88775	3.125
Both A	Both Metals	14.7425	5.2083
Both B	Both Metals	13.54175	4.4872
Both C	Both Metals	23.4775641	3.3654

Table 6: N. tabacum MDA Readings

M. crystallinum Plant Sample	Leaf MDA (nmol/g)	Root MDA (nmol/g)
Control A	18.2692	1.8429
Control B	15.945	1.202
Control C	16.345	5.04807
Control A	3.9263	2.0833
Control B	0.88141	1.84295
Control C	4.40705	2.72436
Control D	6.730769	2.1634615
0.4 M NaCl A	7.2917	0.07211
0.4 M NaCl B	6.97115	5.92949
0.4 M NaCl C	6.16987	6.41026
0.4 M NaCl A	4.4075	1.6827
0.4 M NaCl B	6.97115	5.048
0.4 M NaCl C	7.445	6.33013
0.05 mM Ni B	14.2625	3.0448
0.05 mM Ni C	6.41	10.256
0.05 mM Ni A	20.9936	3.9263
0.05 mM Ni B	2.00321	1.28205
0.05 mM Ni C	19.39103	9.935897
0.5 mM Ni A	42.0675	0.5607
0.5 mM Ni B	41.5875	3.2852
0.5 mM Ni C	51.8425	4.24679
0.5 mM Ni A	79.0064	6.6506
0.5 mM Ni B	88.78205	0.48077
0.5 mM Ni C	102.5641	3.6859
0.5 mM Ni D	59.134615	4.647436
0.4 mM Cu A	16.1859	2.9647
0.4 mM Cu B	12.04044	4.24679
0.4 mM Cu C	6.89103	4.64744
0.4 mM Cu A	8.895	1.6828
0.4 mM Cu B	23.4775	1.7628
0.4 mM Cu C	41.6675	2.16346
Both HMs A	33.9	0.4008
Both HMs B	74.44	1.7628
Both HMs C	84.695	2.8846
Both HMs A	83.3333	4.7276
Both HMs B	87.66026	1.60256
Both HMs C	52.72436	5.1282

Table 7: M. crystallinum MDA Readings

Bibliography

Abdel-Ghany, S. E., Müller-Moulé, P., Niyogi, K. K., Pilon, M., & Shikanai, T. (2005). Two P-type ATPases are Required for Copper Delivery in *Arabidopsis thaliana* chloroplasts. *Plant Cell*, *17*(4), 1233–1251. https://doi.org/10.1105/tpc.104.030452

Adams, P., Nelson, D. E., Yamada, S., Chmara, W., Jensen, R. G., Bohnert, H. J., & Griffiths, H. (1998). Growth and development of *Mesembryanthemum crystallinum* (Aizoaceae). *New Phytologist*, *138*(2), 171–190. https://doi.org/10.1046/J.1469-8137.1998.00111.X

Adams, P., Thomas, J. C., Vernon, D. M., Bohnert, H. J., & Jensen, R. G. (1992). Distinct Cellular and Organismic Responses to Salt Stress. *Plant and Cell Physiology*, *33*(8), 1215–1223. https://doi.org/10.1093/oxfordjournals.pcp.a078376

Ahmad M.S., & Ashraf M. (2011) Essential Roles and Hazardous Effects of Nickel in Plants. Rev Environ Contam Toxicol 214:125-167. https://doi.org/10.1007/978-1-4614-0668-6_6

Alberts, B., Johnson, A., Lewis, J., Morgan, D., Raff, M., Roberts, K., & Walter, P. (2015). *Molecular Biology of The Cell* (S. G. Lewis & E. Zayatz, Eds.; 6th ed.). Garland Science, and Taylor & Francis Group. https://doi.org/10.3390/ijms161226074

Aldrich, M. V., Gardea-Torresdey, J. L., Peralta-Videa, J. R., & Parsons, J. G. (2003). Uptake and Reduction of Cr(VI) to Cr(III) by Mesquite (Prosopis spp.): Chromate-Plant Interaction in Hydroponics and Solid Media Studied using XAS. *Environmental Science and Technology*, *37*(9), 1859–1864. https://doi.org/10.1021/es0208916

Amari T, Ghnaya T, Debez A, Taamali M, Youssef NB et al., (2014). Comparative Ni Tolerance and Accumulation Potentials between *Mesembryanthemum crystallinum* (halophyte) and *Brassica juncea*: metal accumulation, nutrient status and photosynthetic activity. J. *Plant Physiol. 171*, 1634-1644. https://doi.org/10.1016/j.jplph.2014.06.020

Amari T, Ghnaya T, Sghaier S, Porrini M, Lucchini G, Sacchi G, Abdelly C (2016). Evaluation of the Ni^{+2} Phytoextraction Potential in Mesembryanthemum crystallinum (Halophyte) and Brassica juncea. *Journal of Bioremediation & Biodegradation*, *7*(2), 7:336. 10.4172/2155-6199.1000336

Antón, J. (2011). Compatible Solute. In: *et al.* Encyclopedia of Astrobiology. Springer, Berlin,

Heidelberg. https://doi.org/10.1007/978-3-642-11274-4_336

Antonio, C., Singh, V. P., Prasad, S. M., Singh, S., Parihar, P., & Singh, R. (2016). Heavy Metal Tolerance in Plants: Role of Transcriptomics, Proteomics, Metabolomics, and Ionomics. *Frontiers in Plant Science*, *6*. https://doi.org/10.3389/fpls.2015.01143

Arnold, B. J., Lahner, B., Dacosta, J. M., Weisman, C. M., Hollister, J. D., & Salt, D. E. (2016). Borrowed Alleles and Convergence in Serpentine Adaptation. *Proceedings of the National Academy of Sciences of the United States of America*, *113*(29), 1–6. https://doi.org/10.1073/pnas.1600405113

Baker, A. J. M. (1981). Accumulators and Excluders - Strategies in the Response of Plants to Heavy Metals. *Journal of Plant Nutrition*, *3* (1–4), 643–654. DOI: https://doi.org/10.1080/01904168109362867

Bani, A., Echevarria, G., Zhang, X., Benizri, E., Laubie, B., Morel, J.L., Simonnot, M.O., (2015). The effect of plant density in nickel-phytomining field experiments with A*lyssum murale* in Albania. Aust. J. Bot. 63, 72–77 https://doi.org/10.1016/j.scitotenv.2018.02.229

Barberon, M., Dubeaux, G., Kolb, C., Isono, E., Zelazny, E., & Vert, G. (2014). Polarization of IRON-REGULATED TRANSPORTER 1 (IRT1) to the Plant-Soil Interface Plays a Crucial Role in Metal Homeostasis. *Proceedings of the National Academy of Sciences of the United States of America*, *111*(22), 8293–8298. https://doi.org/10.1073/pnas.1402262111

Barkla, B. J., Vera-Estrella, R., & Raymond, C. (2016). Single-Cell-Type Quantitative Proteomic and Ionomic Analysis of Epidermal Bladder Cells from the Halophyte Model Plant *Mesembryanthemum crystallinum* to Identify Salt-Responsive Proteins. *BMC Plant Biology*, *16*(1), 1–16. https://doi.org/10.1186/s12870-016-0797-1

Bernier, F. & Berna, A. (2001). Germins and germin-like proteins: Plant do-all proteins. But what do they do exactly? *Plant Physiology and Biochemistry, 39* (7-8), 545-554. https://doi.org/10.1016/S0981-9428(01)01285-2

Blanchard, R. K., and Cousings, R. J. (1997) The Role of Metals in Gene Expression. Carlson-Newberry S. J., and Costello R. B., *Emerging Technologies for Nutrition Research: Potential for Assessing Military Performance Capability.* Washington (DC): National Academies Press (US). 363-374. https://www.ncbi.nlm.nih.gov/books/NBK233783/

Bohnert, H. I., Ostrem, J. A., Cushman, J. C., Michalowski, C. B., Rickers, J., Meyer, G., Jay, E., Vernon, D. M., Krueger, M., Vazquez-Moreno, L., Velten, J., Hoefner, R., & Schmitt, J. M. (1988). *Mesembryanthemum crystallinum*, a Higher Plant Model for the Study of Environmentally Induced Changes in Gene Expression.*Plant Molecular Biology Reporter*, *6*(1), 10–28. https://doi.org/10.1007/BF02675305

Britto, D. T., & Kronzucker, H. J. (2006). Futile Cycling at the Plasma Membrane: A Hallmark of Low-Affinity Nutrient Transport. *Trends in Plant Science*, *11*(11), 529–534. https://doi.org/10.1016/j.tplants.2006.09.011

Britto D.T., & Kronzucker H.J. (2015). Sodium Efflux in Plant Roots: What do we Really Know? *Journal of Plant Physiology*, *186-187*, 1-12. https://doi.org/10.1016/j.jplph.2015.08.002

Callahan, D. L., Baker, A. J. M., Kolev, S. D., & Wedd, A. G. (2006). Metal Ion Ligands in Hyperaccumulating Plants. *Journal of Biological Inorganic Chemistry*, *11*(1), 2–12. https://doi.org/10.1007/s00775-005-0056-7

Cataldo D.A., Garland T.R., and Wildung R.E. (1978). Nickel in Plants. I. Uptake Kinetics using Intact Soybean Seedlings. *Plant Physiol*. *62*, 563-565. https://doi.org/10.1104/pp.62.4.563

Chivers, P. T., & Sauer, R. T. (1999). NikR is a ribbon-helix-helix DNA-binding protein. *Protein Science, 8*(11), 2494–2500. https://doi.org/10.1110/ps.8.11.2494

Choudhuri, S., & Klaassen, C. (2006). Structure, function, expression, genomic organization, and single nucleotide polymorphisms of human ABCB1 (MDR1), ABCC (MRP), and ABCG2 (BCRP) efflux transporters. *International Journal of Toxicology*, *25*(4), 231–259. https://doi.org/10.1080/10915810600746023

Cobbett CS (2000) Phytochelatins and their roles in heavy metal detoxification. *Plant Physiology 123*, 825-832. https://doi.org/10.1104/pp.123.3.825

Cockburn, W., Whitelam, G. C., Broad, A., & Smith, J. (1996). The Participation of Phyto-chrome in the Signal Transduction Pathway of Salt Stress responses in Mesembryanthe-mum crystallinum L. *Journal of Experimental Botany, 47*(298), 647-653. https://academic.oup.com/jxb/article/47/5/647/514361

Conte, S. S., & Walker, E. L. (2011). Transporters contributing to iron trafficking in plants. In *Molecular Plant 4*(3), 464–476. Oxford University Press. https://doi.org/10.1093/mp/ssr015

Coogan, T. P., Latta, D. M., Snow, E. T., Costa, M., &; Lawrence, A. (1989). Toxicity and Carcinogenicity of Nickel Compounds. *Critical Reviews in Toxicology*, *19*(4), 341–384. https://doi.org/10.3109/10408448909029327

Cousins, R. J. (1994). Metal Elements and Gene Expression. *Annual Review of Nutrition*, *14*(1), 449–469. www.annualreviews.org

Crooke, W. M., & Inkson, R. H. E. (1955). The Relationship Between Nickel, Toxicity and Major Nutrient Supply. *Plant and Soil*, *VI* (1), 1–15. https://doi.org/10.1007/BF01393752

Cushman, J.C., Michalowski, C.B., & Bohnert, H.J. (1990). Developmental control of crassulacean Acid metabolism inducibility by salt stress in the common ice plant. *Plant Physiol. 94*(3), 1137-1142. https://doi.org/10.1104/pp.94.3.1137

Demidchik, V., Shabala, S. N., Coutts, K. B., Tester, M. A., & Davies, J. M. (2003). Free oxygen radicals regulate plasma membrane Ca^{2+}- and K^{+}-permeable channels in plant root cells. *Journal of Cell Science*, *116*(1), 81–88. https://doi.org/10.1242/JCS.00201

Demidchik, V. (2014). Mechanisms and physiological roles of K+ efflux from root cells. *Journal of Plant Physiology*, *171*(9), 696–707. https://doi.org/10.1016/j.jplph.2014.01.015

Dodd, A.N., Borland, A.M., Haslam R.P., Griffiths, H., & Maxwell, K. (2002). Crassulacean metabolism: plastic, fantastic. *Journal of Experimental Botany, 53*(369): 569-580 10.1093/jexbot/53.369.569

Drouillard, K. G., Lafontaine, J., Grgicak-Mannion, A., McPhedran, K., & Szalinska, E. (2020). Spatial and Temporal Trends of Metal and Organic Contaminants in the Huron-Erie Corridor: 1999–2014. In O. Hutzinger, J. Crossman, & C. Weisener (Eds.), *The Handbook of Environmental Chemistry, 101*, 49–83. Springer Nature Switzerland. https://doi.org/https://doi.org/10.1007/978-3-030-57874-9

Dutta, S., Mitra, M., Agarwal, P., Mahapatra, K., De, S., Sett, U., & Roy, S. (2018). Oxidative and Genotoxic Damages in Plants in Response to Heavy Metal Stress and Maintenance of Genome Stability. *Plant Signaling & Behavior*, *13*(8). https://doi.org/10.1080/15592324.2018.1460048

Ellison, R., Noffke, S., Drouillard, K. G., & Hartig, J. (2022). Contaminated Sediment Remediation in the U.S. Side of the Detroit River and the Path Forward on Remaining Sites. Presentation. University of Windsor. US Environmental Protection Agency – Great Lakes National Program Office. https://www.uwindsor.ca/glier/456/media-and-reports

Fabiano, C.C., Tezotto T., Favarin J.L., Polacco J.C., & Mazzafera, P. (2015). Essentiality of nickel in plants: a role in plant stresses. *Front. Plant Sci., 6*. https://doi.org/10.3389/fpls.2015.00754

Fennessey, J. (2021). *Halophyte Resilience to Roadside Salinity in Urban Southeastern Michigan*. Master's Thesis. University of Michigan. 1-85. https://dx.doi.org/10.7302/2327

Fernández M, Marín R, Proverbio F, Ruette F. (2021). Effect of magnesium sulfate in oxidized lipid bilayers properties by using molecular dynamics. *Biochem Biophys Rep*. *26*:100998, 1-13. https://doi.org/10.1016/j.bbrep.2021.100998

Forsthoefel, N. R., Cushman, M. A. F., Ostrem, J. A., & Cushman, J. C. (1998). Induction of a cysteine protease cDNA from Mesembryanthemum crystallinum leaves by environmental stress and plant growth regulators. *Plant Science*, *136*(2), 195–206. https://doi.org/10.1016/S0168-9452(98)00096-X

Frankel, E. N., Neff, W. E., Brooks, D. D. and Fujimoto, K., 1987. Fluorescence formation from the interaction of DNA with lipid oxidation degradation products. *Biochim. et Biophys. Acta*, *919*, 239-244. https://doi.org/10.1016/0005-2760(83)90141-8

Fukada, T., & Kambe, T. (2011). Molecular and genetic features of zinc transporters in Physiology and pathogenesis. *Metallomics*, *3*(7), 662–674. https://doi.org/10.1039/C1MT00011J

Gao C., Zhao, Q, Jiang L. (2015). Vacuoles protect plants from high magnesium stress. *Proc Nat Acad Sci 112* (10) 2931-2932. https://doi.org/10.1073/pnas.1501318112

Gajweska E. & Skłodowska M. (2007). Effect of Nickel on ROS Content and Antioxidative Enzyme Activities in Wheat Leaves. *Biometals*, *20* (1), 27-36. https://doi.org/10.1007/s10534-006-9011-5

Gaweł S, Wardas M, Niedworok E, Wardas P. (2004). Dialdehyd malonowy (MDA) jako wskaźnik procesów peroksydacji lipidów w organizmie [Malondialdehyde (MDA) as a lipid peroxidation marker]. Wiadomosci lekarskie (Warsaw, Poland: 1960), 57(9-10) 453-455. PMID: 15765761.gaj

Gerstein, A. C., Ono, J., Lo, D. S., Campbell, M. L., Kuzmin, A., & Otto, S. P. (2014). Too much of a good thing: The unique and repeated paths toward copper adaptation. *Genetics*, 199 (2), 555–571. https://doi.org/10.1534/genetics.114.171124

Guerinot ML, & Yi Y. (1994). Iron: nutritious, noxious, and not readily available. *Plant Physiol. 104*: 815-820. doi: 10.1104/pp.104.3.815

Guerinot M.L. (2000) The ZIP Family of Metal Transporters. *Biochim Biophys Acta, 1465*,190–198. https://doi.org/10.1016/S0005-2736(00)00138-3

Gupta, N., Ram, H., & Kumar, B. (2016). Mechanism of Zinc absorption in plants: uptake, transport, translocation and accumulation. *Reviews in Environmental Science and Bio/Technology*, *15*, 89–109. https://doi.org/10.1007/s11157-016-9390-1

Halliwell, B., Gutteridge, J.M., (1984) Oxygen toxicity, oxygen radicals, transition metals and disease. *Biochem J, 219*(1), 1-14. https://doi.org/10.1042/bj2190001.

Hassan, M. U., Chattha, M. U., Khan, I., Chattha, M. B., Aamer, M., Nawaz, M., Ali, A., Aman, M., Khan, U., Tahir, &, & Khan, A. (2019). Nickel toxicity in plants: reasons, toxic effects, tolerance mechanisms, and remediation possibilities-a review. *Environmental*

Science and Pollution Research, *26*, 12673–12688. https://doi.org/10.1007/s11356-019-04892-x

Hoagland, D. R., & Arnon, D. I. (1950). Preparing the nutrient solution. *The Water-Culture Method for Growing Plants without Soil*, *347*, 29–31. https://archive.org/details/watercultureme3450hoag

Höfner, R., Vazquez-Moreno, L., Winter, K., Bohnert, H. J., & Schmitt, J. M. (1987). Induction of Crassulacean Acid Metabolism in Mesembryanthemum crystallinum by High Salinity: Mass Increase and de Novo Synthesis of PEP-Carboxylase. *Plant Physiology*, *83*(4), 915–919. https://doi.org/10.1104/pp.83.4.915

Homa, J., Stürzenbaum, S. R., & Kolaczkowska, E. (2016). Metallothionein 2 and Heat Shock Protein 72 Protect *Allolobophora chlorotica* from Cadmium but not Nickel or Copper Exposure: Body Malformation and Coelomocyte Functioning. In *Archives of Environmental Contamination and Toxicology, 71*(2), 267–277. https://doi.org/10.1007/s00244-016-0276-6

Hussain, D., Haydon, M. J., Wang, Y., Wong, E., Sherson, S. M., Young, J., Camakaris, J., Harper, J. F., & Cobbett, C. S. (2004). P-type ATPase heavy metal transporters with roles in essential zinc homeostasis in Arabidopsis. *Plant Cell*, *16*(5), 1327–1339. https://doi.org/10.1105/tpc.020487

Ishfaq, M., Wang, Y., Yan, M., Wang, Z., Wu, L., Li, C., & Li, X. (2022). Physiological Essence of Magnesium in Plants and Its Widespread Deficiency in the Farming System of China. *Frontiers in Plant Science*, *13*. https://doi.org/10.3389/fpls.2022.802274

Jalmi, S. K., Bhagat, P. K., Verma, D., Noryang, S., Tayyeba, S., Singh, K., Sharma, D., & Sinha, A. K. (2018). Traversing the Links between Heavy Metal Stress and Plant Signaling. *Frontiers in Plant Science*, *9*(February), 1–21. https://doi.org/10.3389/fpls.2018.00012

Javed, M. T., Tanwir, K., Akram, M. S., Shahid, M., Niazi, N. K., & Lindberg, S. (2018). Phytoremediation of Cadmium-Polluted Water/Sediment by Aquatic Macrophytes: Role of Plant-Induced pH Changes. In *Cadmium Toxicity and Tolerance in Plants: From Physiology to Remediation* (495–529). https://doi.org/10.1016/B978-0-12-814864-8.00020-6

Jordan, F. L., Robin-Abbott, M., Maier, R. M., & Glenn, E. P. (2002). A Comparison of Chelator-Facilitated Metal Uptake by a Halophyte and a Glycophyte. *Environmental Toxicology and Chemistry, 21*(12). https://doi.org/10.1002/etc.5620211224

Karley, A. J., & White, P. J. (2009). Moving cationic minerals to edible tissues: potassium, magnesium, calcium. *Current Opinion in Plant Biology*, *12*(3), 291–298. https://doi.org/10.1016/J.PBI.2009.04.013

Kehrer, J. P. (2000). The Haber-Weiss Reaction and Mechanisms of Toxicity. *Toxicology*,

149(1), 43–50. https://doi.org/10.1016/S0300-483X(00)00231-6

Larsen, F., & Postma, D. (1997). Nickel mobilization in a groundwater well field: Release by pyrite oxidation and desorption from manganese oxides. *Environmental Science & Technology*, *31*(9), 2589–2595. https://doi.org/10.1021/ES9610794

Li, L., Tutone, A. F., Drummond, R. S. M., Gardner, R. C., & Luan, S. (2001). A Novel Family of Magnesium Transport Genes in Arabidopsis. *The Plant Cell*, *13*(12), 2761–2775. https://doi.org/10.1105/tpc.010352

Liu, W., Zhang, X., Liang, L., Chen, C., Wei, S., Zhou, O. (2015). Phytochelatin and oxi-dative stress under heavy metal stress tolerance in plants. In: Gupta, D., Palma, J., Corpas, F. (Eds.), Reactive Oxygen Species and Oxidative Damage in Plants under Stress. 191–217. Springer, Cham. https://doi.org/10.1007/978-3-319-20421-5_8

Medda, R., Padiglia, A., & Floris, G. (1995). Plant copper-amine oxidases. *Phytochemistry*, *39*(1), 1–9. https://doi.org/10.1016/0031-9422(94)00756-J

Meyerstein, D. (2021). Re-examining Fenton and Fenton-like Reactions. *Nature Reviews Chemistry*, *5*, 595–597. https://doi.org/10.1038/s41570-021-00310-4

Michalowski, C. B., & Bohnert H. J. (1992). Nucleotide Sequence of a Root-Specific Transcript Encoding a Germin-Like Protein from the Halophyte *Mesembryanthemum crystallinum*, *Plant Physiology*, *100*(1), 537–538, https://doi.org/10.1104/pp.100.1.537

Mittler, R. (2002). Oxidative Stress, Antioxidants and Stress Tolerance. *Trends in Plant Sciences*, *7*(9), 405–410. https://doi.org/https://doi.org/10.1016/S1360-1385(02)02312-9

Moffat A. S. (2002). Finding new ways to protect drought-stricken plants. *Science 296*(5571)*:* 1226 –1229. Retrieved from https://www.proquest.com/scholarly-journals/finding-new-ways-protect-drought-stricken-plants/docview/213576924/se-2?accountid=14578

Mohammed A.S., Kapri A., Goel R. (2011). Heavy Metal Pollution: Source, Impact, and Remedies. In: Khan M., Zaidi A., Goel R., Musarrat J. (eds) Biomanagement of Metal-Contaminated Soils. *Environmental Pollution*, *20*. 1-28 Springer, Dordrecht. https://doi.org/10.1007/978-94-007-1914-9_1

Mosulén, S., José Domínguez, M., Vigara, J., Vílchez, C., Guiraum, A., & Vega, J. M. (2003). Metal toxicity in *Chlamydomonas reinhardti*. Effect on sulfate and nitrate assimilation. *Biomolecular Engineering*, *20*, 199–203. https://doi.org/10.1016/S1389-0344(03)00053-4

Munakata, M., Matsui, M., Tabushi, M., & Shigematsu, T. (1970). Selectivity in the Metal-Complex-Catalyzed Decarboxylation of Oxaloacetic Acid and a Role of Metal Ion in an Enzyme System. *Bulletin of the Chemical Society of Japan*, *43*(1), 114–118. https://doi.org/10.1246/BCSJ.43.114

Munkhtsetseg T., Shun-Chung Y., Der-Chuen L., Kuo-Chen Y. (2014). Root-Secreted Nicotinamide from *Arabidopsis halleri* Facilitates Zinc Hypertolerance by Regulating Zinc Bioavailability. *Plant Physiology*, *166*. 839-852. 10.1104/pp.114.241224

Nishida S., Tsuzuki C., Kato A., Aisu A., Yoshida J., & Mizuno T. (2011). AtIRT1, the Primary Iron Uptake Transporter in the Root, Mediates Excess Nickel Accumulation in *Arabidopsis thaliana*. *Plant and Cell Physiology*, *52*(8), 1433–1442. https://doi.org/10.1093/pcp/pcr089

Page V. and Feller U. (2015). Heavy Metals in Crop Plants: Transport and Redistribution Processes on the Whole Plant Level. *Agronomy*, *5*, 447-463. 10.3390/agronomy5030447

Pandey, N., & Sharma, C. P. (2002). Effect of heavy metals Co^{2+}, Ni^{2+} and Cd^{2+} on growth and metabolism of cabbage. *Plant Science*, *163*, 753-758. https://doi.org/10.1016/S0168-9452(02)00210-8

Pardo T, Rodríguez-Garrido, Saad RF, Soto-Vázquez JL, Loureiro-Viñas M, Prieto-Fernández Á, Guillaume Echevarria b, Emil Benizri E, Kidd PS. (2018) Assessing the agromining potential of Mediterranean nickel-hyperaccumulating plant species at field-scale in ultramafic soils under humid-temperate climate. *Science of the Total Environment*, *630*, 275-286. https://doi.org/10.1016/j.scitotenv.2018.02.229

Pianelli K, Mari S., Marques L., Lebrun M., & Czernic P. (2005). Nicotianamine Over-accumulation Confers Resistance to Nickel in *Arabidopsis thaliana*. *Transgenic Research, 14*, 739-748. 10.1007/s11248-005-7159-3

Pilon, M., Ravet, K., & Tapken, W. (2011). The Biogenesis and Physiological Function of Chloroplast Superoxide Dismutases. *Biochimica et Biophysica Acta - Bioenergetics*, *1807*(8), 989–998. https://doi.org/10.1016/j.bbabio.2010.11.002

Pietrini, F., Carnevale, M., Beni, C., Zacchini, M., Gallucci, F., & Santangelo, E. (2019). Effect of Different Copper levels on growth and morpho-physiological parameters in giant reed (Arundo donax L.) in semi-hydroponic mesocosm experiment. *Water*, *11*(9), 1–19. https://doi.org/10.3390/w11091837

Proctor, J., & McGowan, I. D. (1976). Influence of Magnesium on Nickel Toxicity. *Nature*, *260*(134), 407. https://doi.org/10.1038/260134a0

Rensing, C., Ghosh, M., & Rosen, B. P. (1999). Families of Soft-Metal-Ion-Transporting ATPases. *Journal of Bacteriology*, *181*(19), 5891–5897. 10.1128/JB.181.19.5891-5897.1999

Rivers-Auty, J., & Brough, D. (2015). Potassium efflux fires the canon: Potassium efflux as a common trigger for canonical and noncanonical NLRP3 pathways. *European Journal of Immunology*, *45*(10), 2758–2761. https://doi.org/10.1002/EJI.201545958

Rosen, B. P. (1999). Families of arsenic transporters. *Trends in Microbiology*, *7*(5), 207–212. https://doi.org/10.1016/S0966-842X(99)01494-8

Rubio M.I., Escrig I., Martinez-Cortina C., Lopez-Benet F.J., & Sanz A. (1994). Cadmium and Nickel Accumulation in Rice Plants. Effects on Mineral Nutrition and Possible Interactions of Abscisic and Gibberellic Acids. *Plant Growth Regulation 14*, 151-157. https://doi.org/10.1007/BF00025217

Schropp, W. and Arenz, B. (1942), Über die Wirkung der A-Z-Lösungen nach Hoagland und einiger ihrer Bestandteile auf das Pflanzenwachstum. Bodenk., *Pflanzenernaehr., 26*: 198-246. https://doi.org/10.1002/jpln.19420260403

Schulze, L. M. (2014). *Na^+ Transport and Toxicity in Plants*. Ph. D. Thesis. University of Toronto. 1-161. https://hdl.handle.net/1807/94552

Seregin, I. V., & Ivanov, V. B. (2001). Physiological aspects of cadmium and lead toxic effects on higher plants. *Russian Journal of Plant Physiology*, *48*(4), 523–544. https://doi.org/10.1023/A:1016719901147

Shi H, Lee BH, Wu SJ, and Zhu JK. (2003). Overexpression of a plasma membrane Na/H antiporter gene improves salt tolerance in *Arabidopsis thaliana*. *Nat Biotechnol 21*: 81– 85. https://doi.org/10.1038/nbt766

Smirnoff, N., & Cumbes, Q. (1989). Hydroxyl Radical Scavenging Activity of Compatible Solutes. *Phytochemistry*, *28*(4), 1057–1060. 10.1016/0031-9422(89)80182-7

Stitt, M., & Zeeman, S. C. (2012). Starch Turnover: Pathways, Regulation and Role in Growth. *Current Opinion in Plant Biology*, *15*(3), 282–292. https://doi.org/10.1016/j.pbi.2012.03.016

Sze, H., Li, X., & Palmgren, M. G. (1999). Energization of Plant Cell Membranes by H^+ - Pumping ATPases: Regulation and Biosynthesis. *The Plant Cell*, *11*(April), 677–689. https://doi.org/10.1105/tpc.11.4.677

Thomas, J. C., Malick, F. K., Endreszl, C., Davies, E. C., & Murray, K. S. (1998). Distinct Responses to Copper Stress in the Halophyte *Mesembryanthemum crystallinum*. *Physiologia Plantarum*, *102*(3), 360–368. https://doi.org/https://doi.org/10.1034/j.1399-3054.1998.1020304.x

Thomas J.C., Perron M., & Davies E.C. (2004). Genetic Responsiveness to Copper in the Ice Plant *Mesembryanthemum crystallinum*. *Plant Science, 167*, 259-266. https://doi.org/10.1016/j.plantsci.2004.03.022

Thomas, J. C., Perron, M., LaRosa, P. C., & Smigocki, A. C. (2005). Cytokinin and the Regulation of a Tobacco Metallothionein-like Gene during Copper Stress. *Physiologia Plantarum*, *123*(3), 262–271. https://doi.org/10.1111/j.1399-3054.2005.00440.x

Tilstone G.H. and Macnair M.R. (1997). Nickel tolerance and copper – Nickel Co – Tolerance in *Mimulus guttatus* from Copper Mine and Serpentine Habitats. *Plant and Soil 191*, 173-180. 10.1023/A:1004234604143

Tränkner, M., & Jamali Jaghdani, S. (2019). Minimum magnesium concentrations for photosynthetic efficiency in wheat and sunflower seedlings. *Plant Physiology and Biochemistry*, *144*, 234–243. https://doi.org/10.1016/j.plaphy.2019.09.040

Tsvetkov, P., Coy, S., Petrova, B., Dreishpoon, M., Verma, A., Abdusamad, M., Rossen, J., Joesch-Cohen, L., Humeidi, R., Spangler, R. D., Eaton, J. K., Frenkel, E., Kocak, M., Corsello, S. M., Lutsenko, S., Kanarek, N., Santagata, S., & Golub, T. R. (2022). Copper induces cell death by targeting lipoylated TCA cycle proteins. *Science (New York, N.Y.)*, *375*(6586), 1254–1261. https://doi.org/10.1126/science.abf0529

Valko, M., & Cronin, H. M. and M. T. D. (2005). Metals, Toxicity and Oxidative Stress. *Current Medicinal Chemistry*, *12*(10), 1161–1208. https://doi.org/http://dx.doi.org/10.2174/0929867053764635

Van de Mortel JE, Almar Villanueva L, Schat H, Kwekkeboom J, Coughlan S, Moerland PD, Loren Ver, Van Themaat E, Koornneef M, Aarts MG (2006). Large Expression Differences in Genes for Iron and Zinc Homeostasis, Stress Response, and Lignin Biosynthesis Distinguish Roots of *Arabidopsis thaliana* and the Related Metal Hyperaccumulator *Thlaspi caerulescens*. *Plant Physiology*, *142*, 1127–1147. https://doi.org/10.1104/pp.106.082073

Vera-Estrella R., Gomez-Mendez F., Amezcua-Romero J., Barkla B.J., Rosas-Santiago P., Pantoja O. (2017). Cadmium and Zinc Activate Adaptative Mechanisms in Nicotiana tabacum Similar to those Observed in Metal Tolerant Plants. *Planta*. *246*(3), 433-451. 10.1007/s00425-017-2700-1

Vernon, D. M., Ostrem, J. A., Schmitt, J. M., & Bohnert, H. J. (1988). PEPCase Transcript Levels in Mesembryanthemum crystallinum Decline Rapidly upon Relief from Salt Stress. *Plant Physiology*, *86*(4), 1002–1004. https://doi.org/10.1104/pp.86.4.1002

Verret, F., Gravot, A., Auroy, P., Preveral, S., Forestier, C., Vavasseur, A., & Richaud, P. (2005). Heavy metal transport by AtHMA4 involves the N-terminal degenerated metal binding domain and the C-terminal His11 stretch. *FEBS Letters*, *579*(6), 1515–1522. https://doi.org/10.1016/j.febslet.2005.01.065

Vert, G., Grotz, N., Dédaldéchamp, F., Gaymard, F., Guerinot, M.L., Briat, J-F., & Curie, C.C. (2002) IRT1, an Arabidopsis transporter essential for iron uptake from the soil and for

Plant Growth. *The Plant Cell, 14*, 1223-1233. www.plantcell.org/cgi/doi/10.1105/tpc.001388

Wang, Z., Hong, C., Xing, Y., Wang, K., Li, Y., Feng, L., & Ma, S. (2018). Spatial distribution and sources of heavy metals in natural pasture soil around copper-molybdenum mine in Northeast China. *Ecotoxicology and Environmental Safety*, *154*(February), 329–336. https://doi.org/10.1016/j.ecoenv.2018.02.048

Warren, L. (1959). The Thiobarbituric Acid Assay of Sialic Acids. *The Journal of Biological Chemistry*, *234*(8), 1971–1975. https://doi.org/10.1016/s0021-9258(18)69851-5

Watt, R. K., & Ludden, P. W. (1999). Nickel-binding proteins. *CMLS, Cell. Mol. Life Sci*, *56*, 604–625. https://doi.org/10.1007/s000180050456

Webb, M. (1970). Interrelationships Between the Utilization of Magnesium and the Uptake of other Bivalent Cations by Bacteria. *Biochimica et Biophysica Acta*, *222*(2), 428–239. https://doi.org/10.1016/0304-4165(70)90133-9

Wilkinson, S.R. and Welch, R.M. and Mayland, H.F. and Grunes, D.L. (1990) Magnesium in plants: uptake, distribution, function, and utilization by man and animals. *Metal Ions in Biological Systems, 26,* 33-56. Siegel, Helmut, (ed.) Marcel Dekker, Inc., New York and Basel, Switzerland. https://api.semanticscholar.org/CorpusID:82055093

Witte, C. P., Tiller, S. A., Taylor, M. A., & Davies, H. V. (2002). Addition of nickel to Murashige and Skoog medium in plant tissue culture activates urease and may reduce metabolic stress. *Plant Cell, Tissue and Organ Culture*, *68*(1), 103–104. https://doi.org/10.1023/A:1012966218478

White, P. J., & Brown, P. H. (2010). Plant nutrition for sustainable development and global health. *Annals of Botany*, *105* (7), 1073–1080. https://doi.org/10.1093/aob/mcq085

Woo, E.-J., Dunwell, J. M., Goodenough, P. W., Marvier, A. C., & Pickersgill, R. W. (2000). Germin is a manganese containing homohexamer with oxalate oxidase and superoxide dismutase activities. *Nature Structural Biology*, *7*, 1036–1040 https://doi.org/10.1038/80954

Yan, Y.-W., Mao, D.-D., Yang, L., Qi, J.-L., Zhang, X.-X., Tang, Q.-L., Li, Y.-P., Tang, R.-J., & Luan, S. (2018). Magnesium Transporter MGT6 plays an essential role in maintaining magnesium homeostasis and regulating high magnesium tolerance in Arabidopsis. *Frontiers in Plant Science*, *9*(274), 1–13. https://doi.org/10.3389/fpls.2018.00274

Yang, L. T., Zhou, Y. F., Wang, Y. Y., Wu, Y. M., Ye, X., Guo, J. X. et al. (2019). Magnesium deficiency induced global transcriptome change in C*itrus sinensis* leaves revealed by RNA-Seq. *Int. J. Mol. Sci*. *20*, 3129. https://doi.org/10.3390/ijms20133129

Yruela, I. (2005). Copper in Plants: Acquisition, Transport, and Interactions. *Brazilian Journal of Plant Physiology*, *36* (March 2005), 409–430. https://doi.org/10.1590/S1677-

04202005000100012

Yusuf, M., Fariduddin, Q., Hayat, S., & Ahmad, A. (2011). Nickel: An Overview of Uptake, Essentiality and Toxicity in Plants. *Bulletin of Environmental Contamination and Toxicology*, *86*(1), 1–17. https://doi.org/10.1007/s00128-010-0171-1

Zhao, H., Zhou, Q., Zhou, M., Li, C., Gong, X., Liu, C., Qu, C., Wang, L., Si, W., & Hong, F. (2021). Magnesium Deficiency Results in Damage of Nitrogen and Carbon Cross-talk of Maize and Improvement by Cerium Addition. *Biological Trace Element Research*, *148*, 102–109. https://doi.org/10.1007/s12011-012-9340-x